# New Rotes to Quantum Dots and Other Materials with Critical Dimensions of the Order of Nanometres


**Paul O'Brien**

**The School of Chemistry**

**and The Manchester Materials Science Centre**

IUPAC Workshop on Advanced Materials III 5th Sept 2005 Stellenbosch

# Structure of Talk

- Looking at some nanodimensional objects by way of introduction
- Synthetic approaches zinc oxide and band gap engineering
- How nanoparticles grow and
- Rods
- Assemblies of Nanoparticles and mesoscopic objects
- Closing remarks

# Structure of Talk

- **Looking at some nanodimensional objects by way of introduction**
- Synthetic approaches zinc oxide and doping
- How nanoparticles grow and
- Rods
- Assemblies of Nanoparticles and mesoscopic objects
- Closing remarks


# What are lost dimensions?

## Industrial Development and a History of Precise Size Control

1980


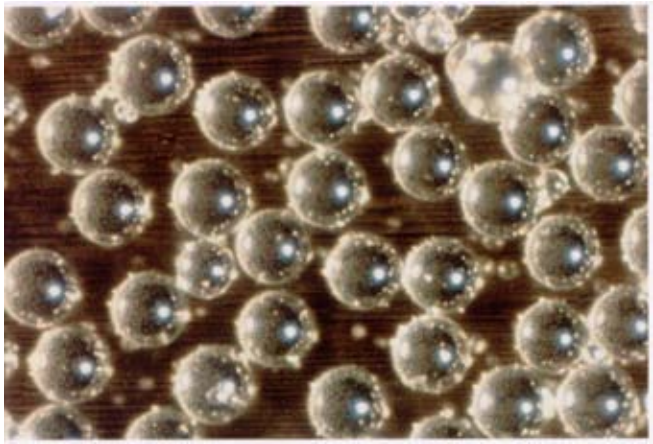

2004

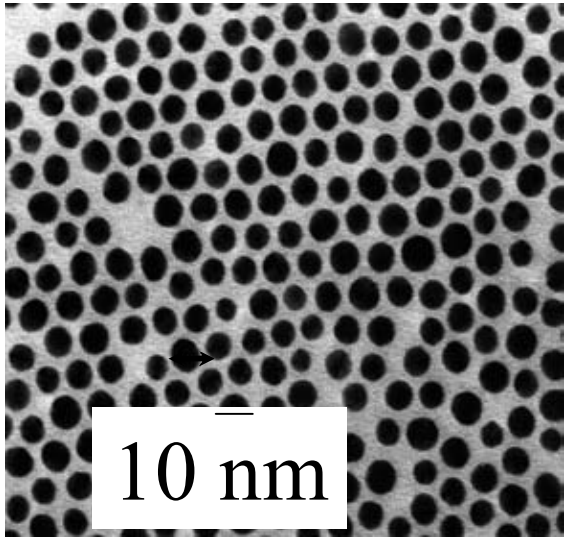


## Ball Bearings for the 21st Century!

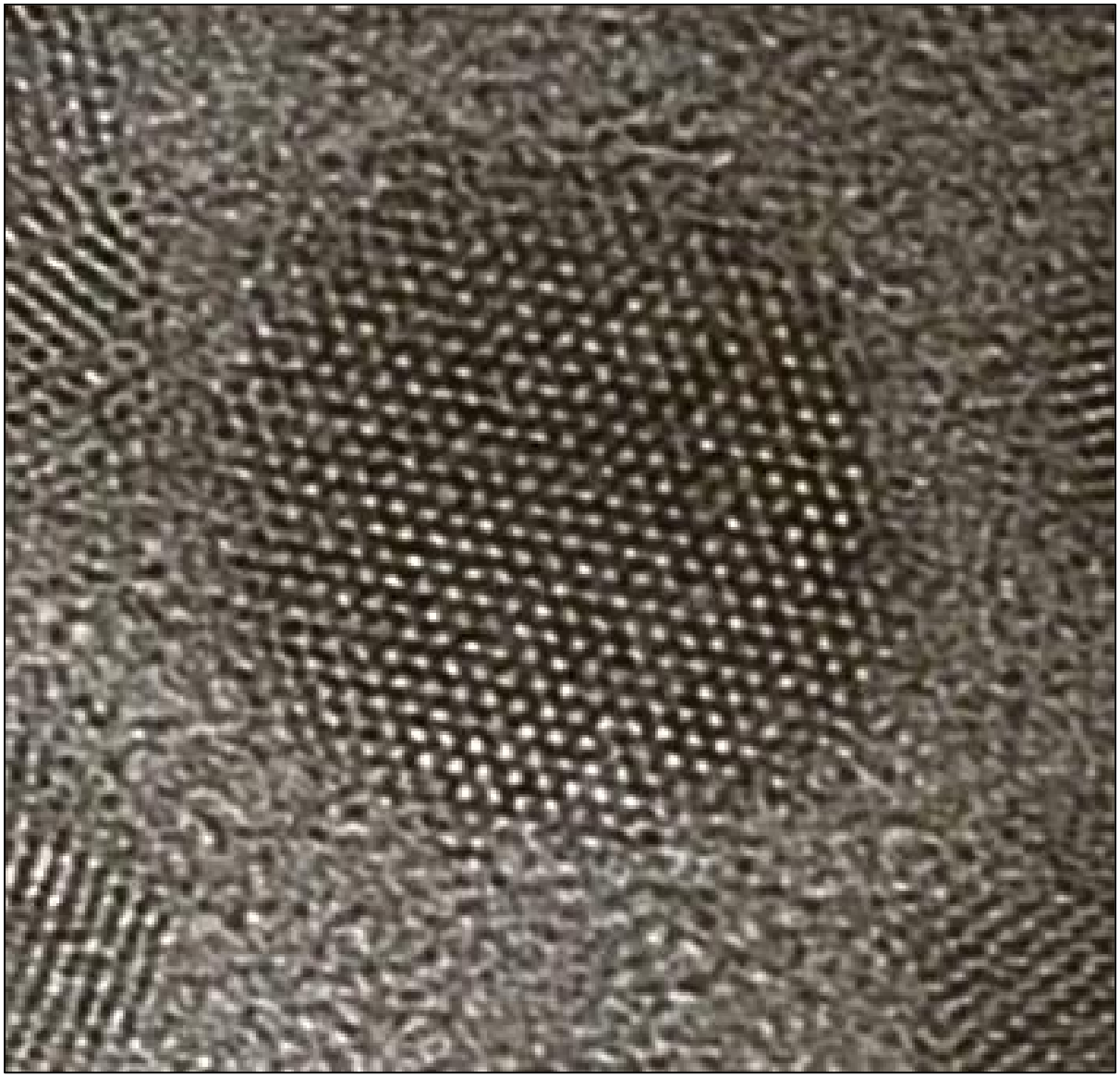

Chem Commun., 1999, 1573-1574

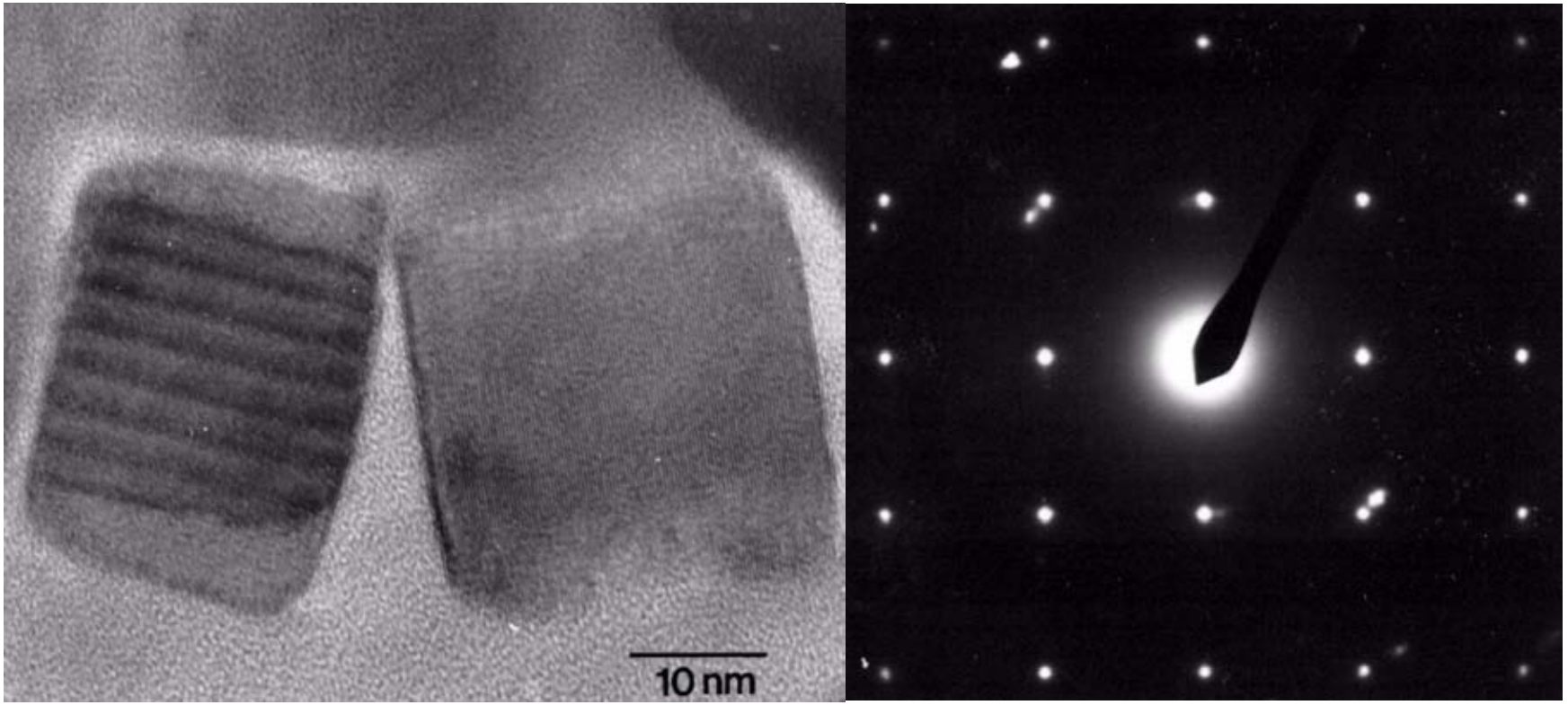


# Sample of PbS Coated with TOPO

J. Materials Chemistry, 1997, 7, 1011

# Quantum Dot Structures I

**Crystalline core e.g CdS**

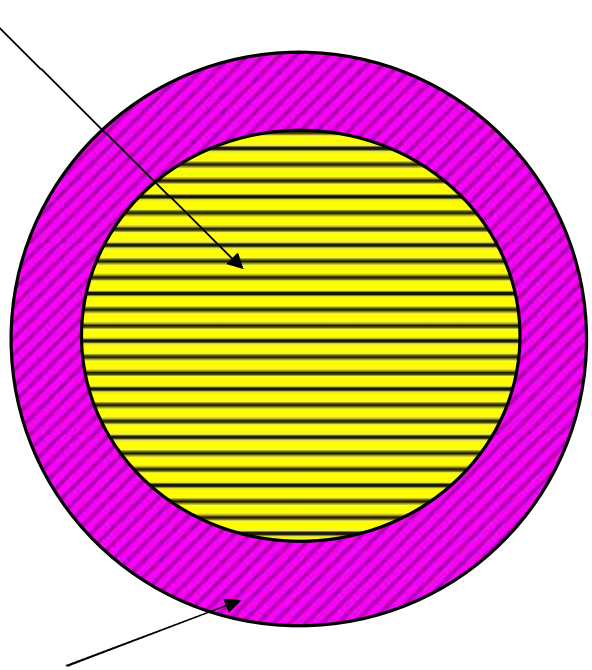

**Organic Capping Agent**

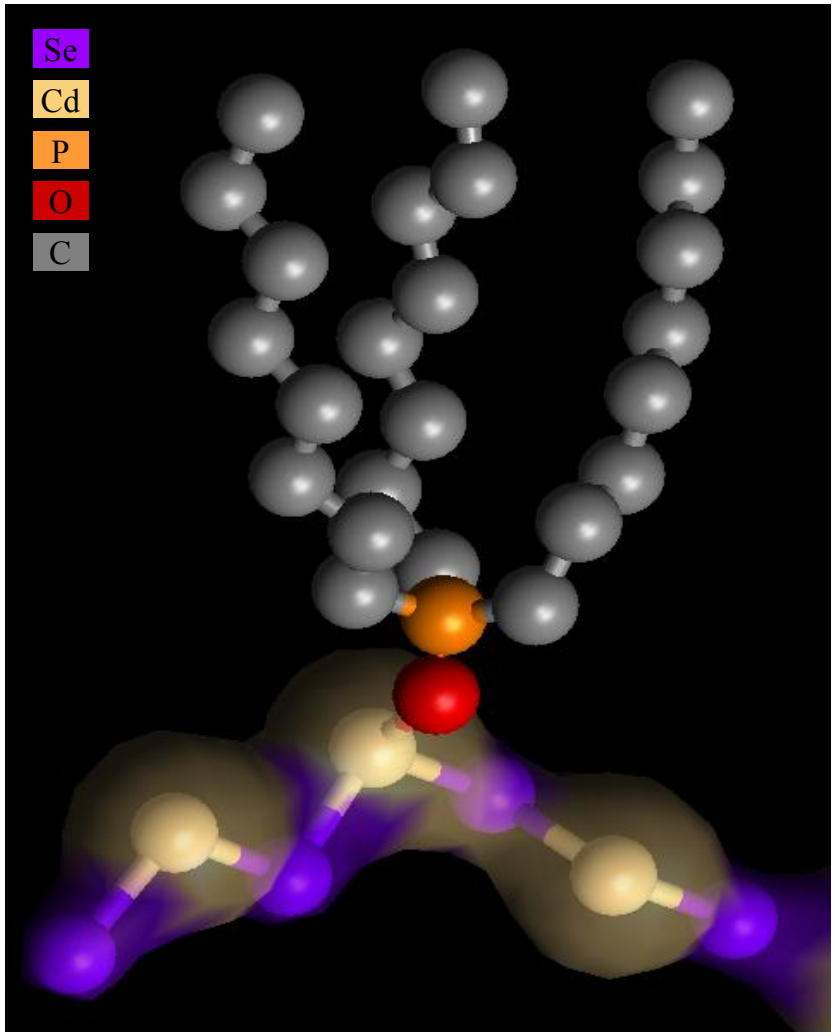


**‘Metal Organic Dot’**

# Quantum Dots II

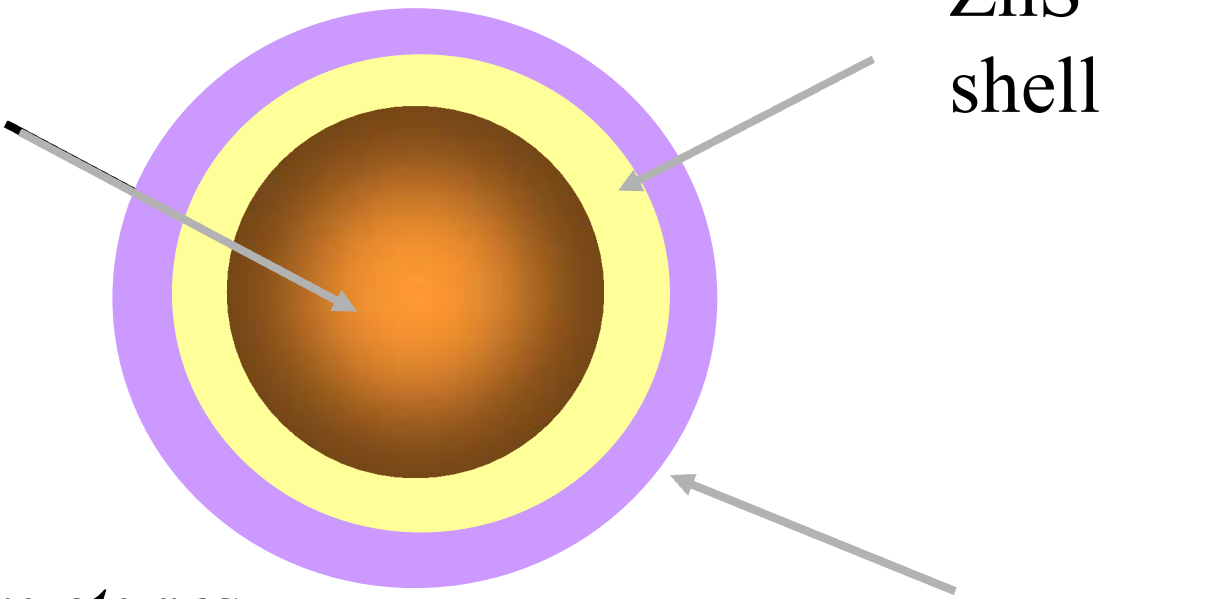


## *Core Shell Structures*

- Broadband excitation
- Narrow bandwidth emission
- Emit light of high intensity
- Available in many colours
- Resistant to quenching
- Photochemically stable

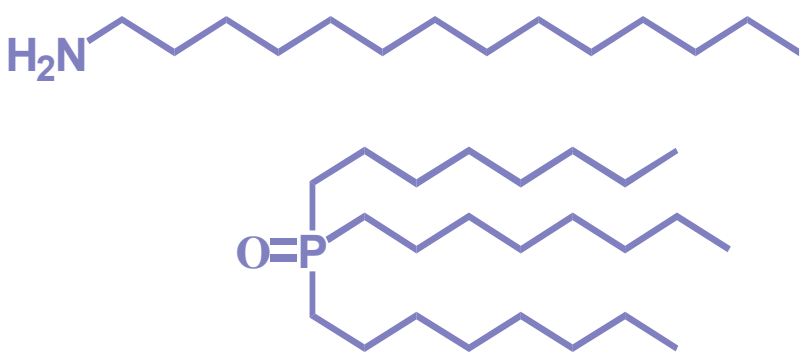

# Structure of Talk

- Looking at some nanodimensional objects by way of introduction
- **Synthetic approaches zinc oxide and band gap engineering**
- How nanoparticles grow and
- Rods
- Assemblies of Nanoparticles and mesoscopic objects
- Closing remarks

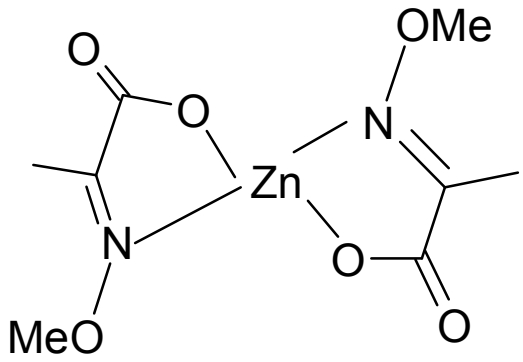


Zinc ketoacidoximate

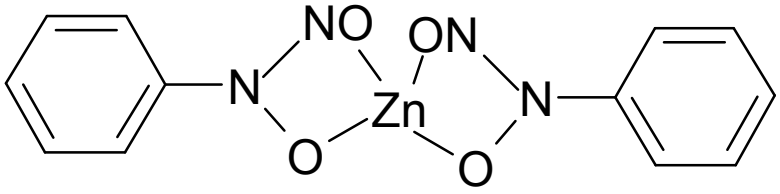


Zinc cupferrate

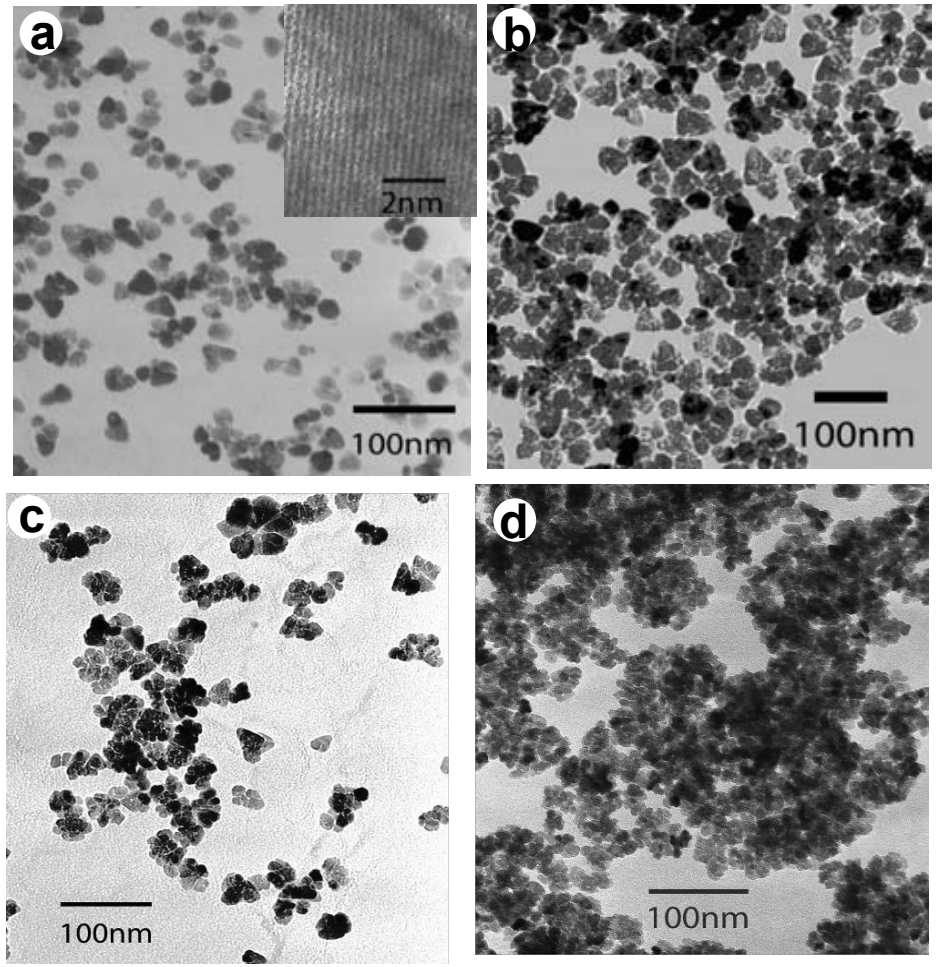


TEM images of ZnO nanocrystallites grown by thermal decomposition of cupferrate at (a)245 °C (b)230 °C (c)200 °C (d)180 °C. The estimated diameters are 12, 13, 8.5 and 7 nm respectively. In trioctylamine/octylamine 1:5 v/v

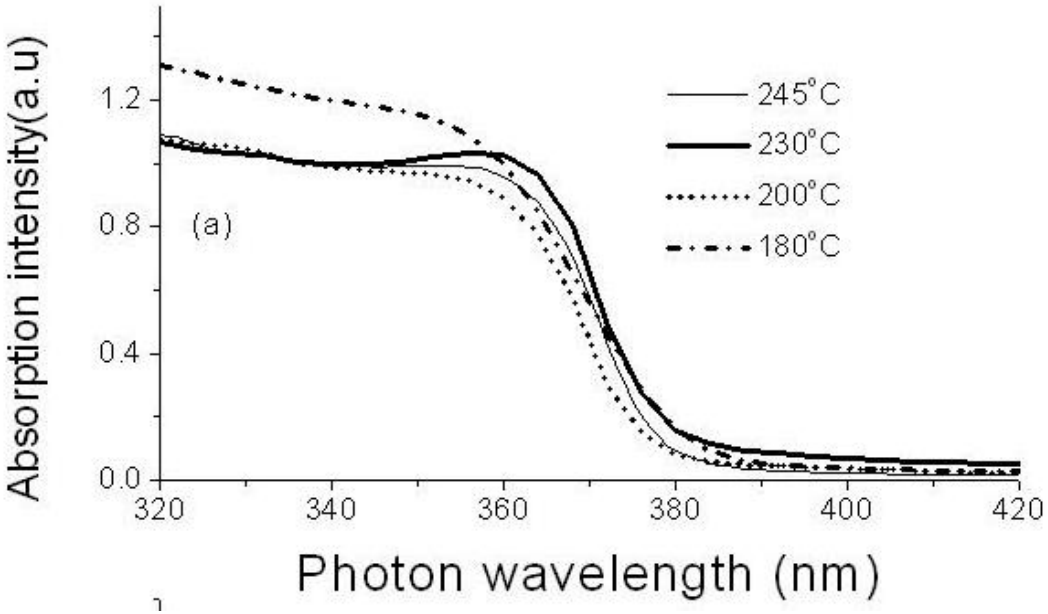


Absorption and emission spectra of ZnO nanocrystals synthesized by decomposition of cupferrate.

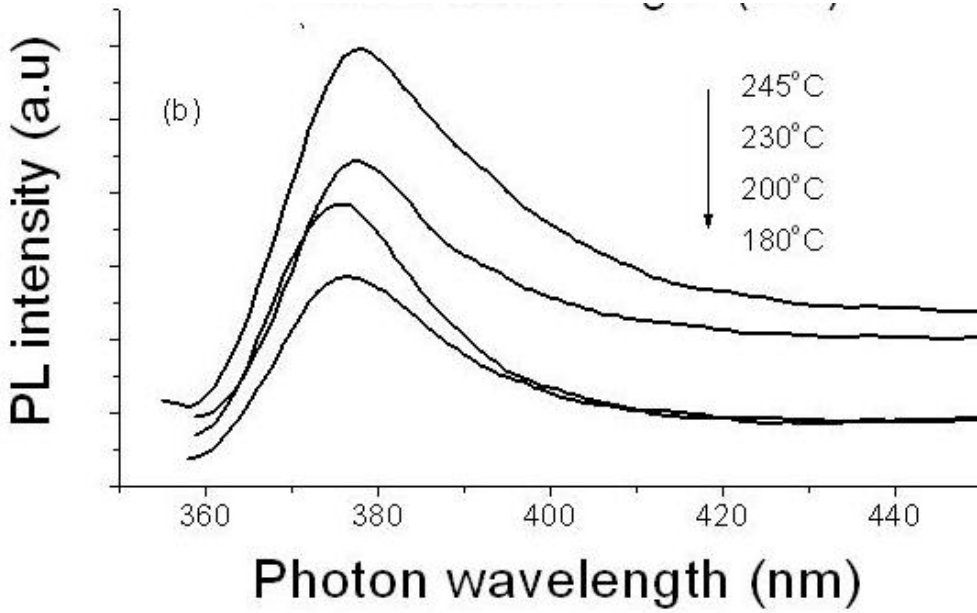

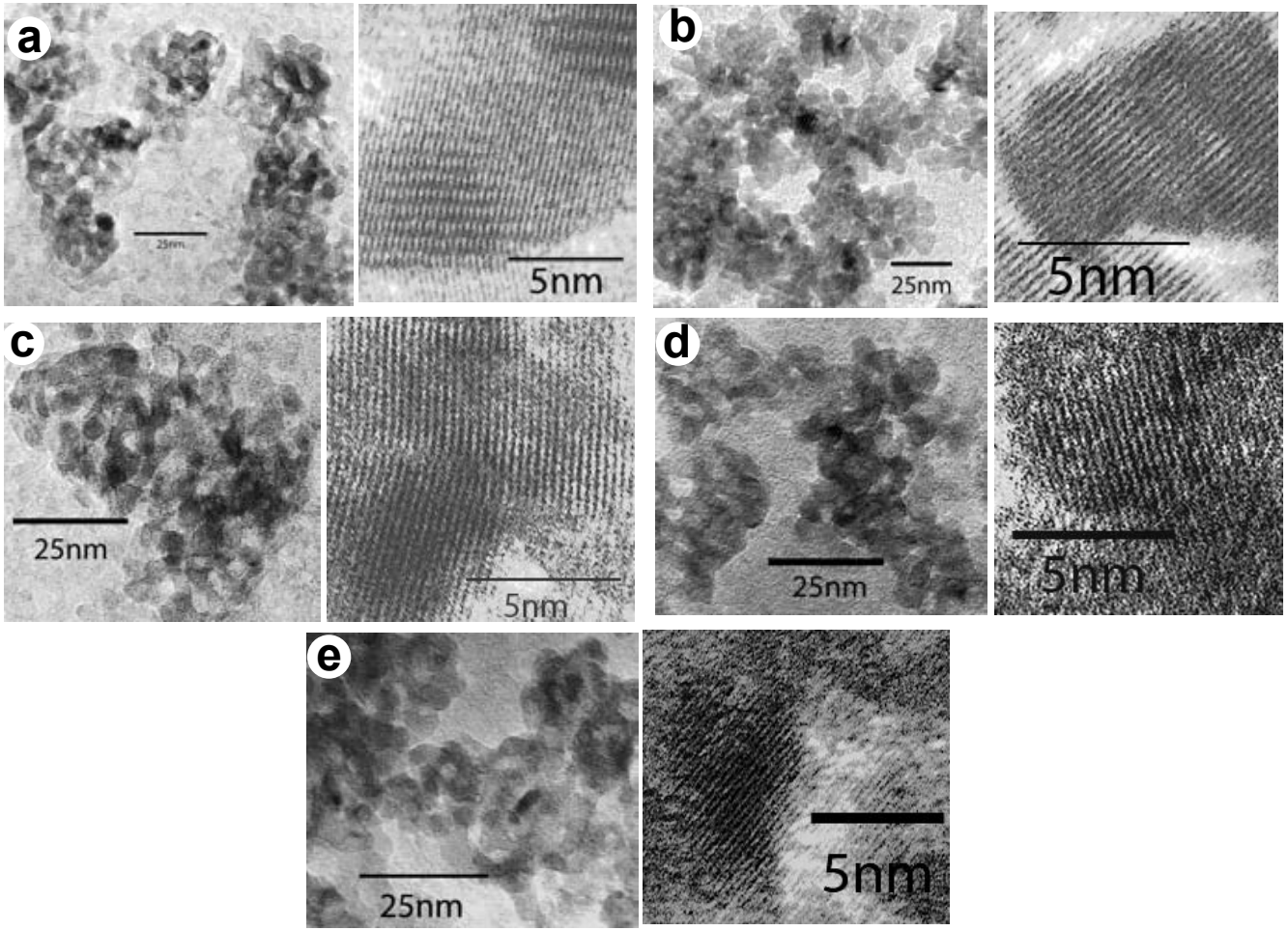


TEM and HRTEM images of ZnO nanocrystallites grown by thermal decomposition of ketoacidoximate at (a) 200 °C (b) 180 °C (c) 160 °C (d) 130 °C (e) 110 °C. The estimated diameters are 3.9, 4.7, 5.3, 6, 6.4 nm respectively.

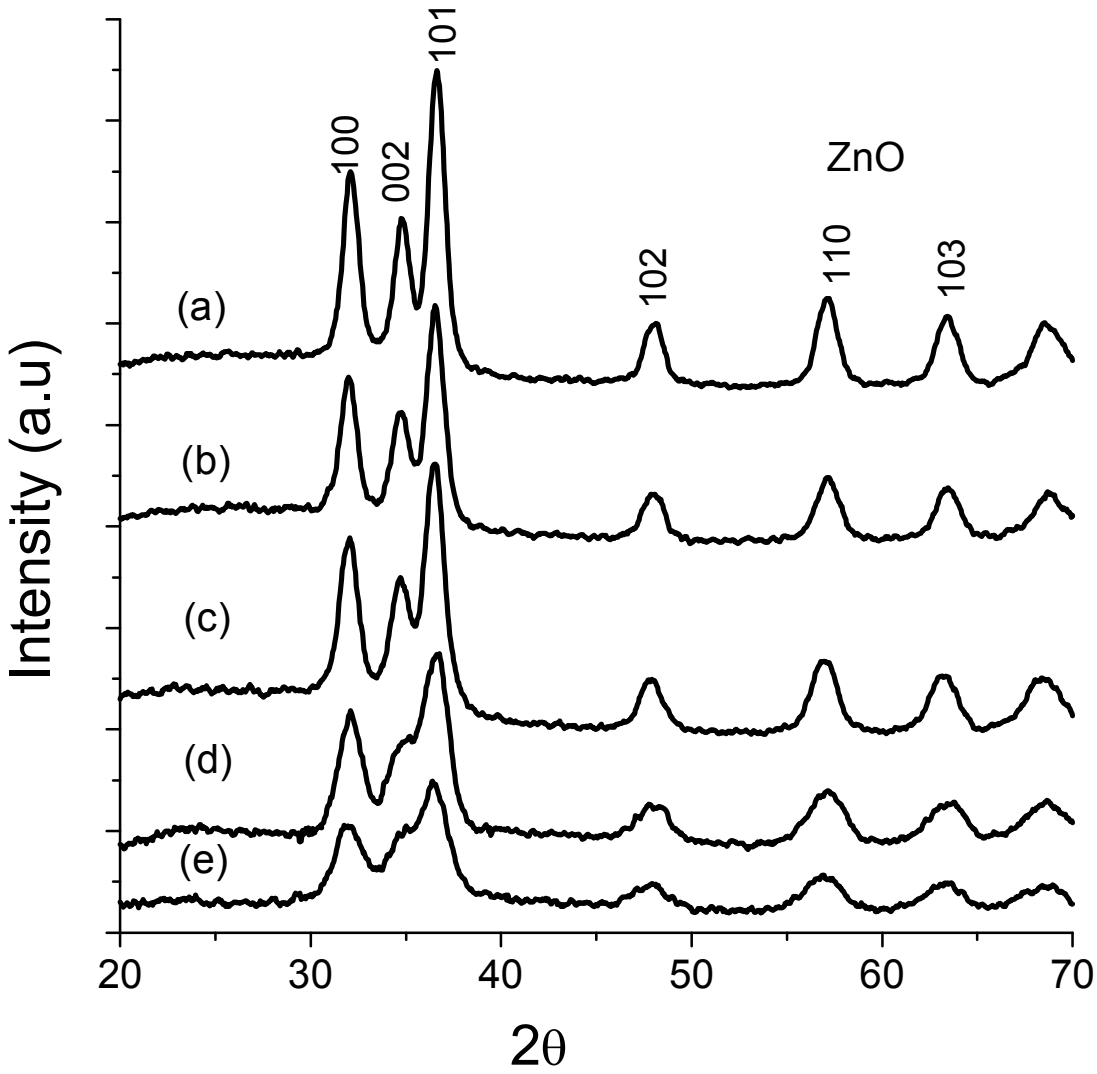


XRD patterns of ZnO nanocrystallites grown at (a)200 °C (b)180 °C (c)160 °C (d)130 °C (e)110 °C. from ketoacidoximate

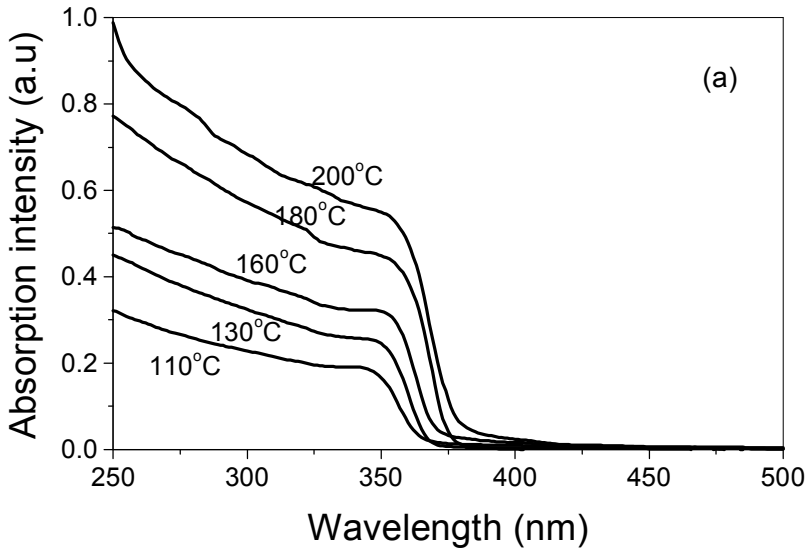


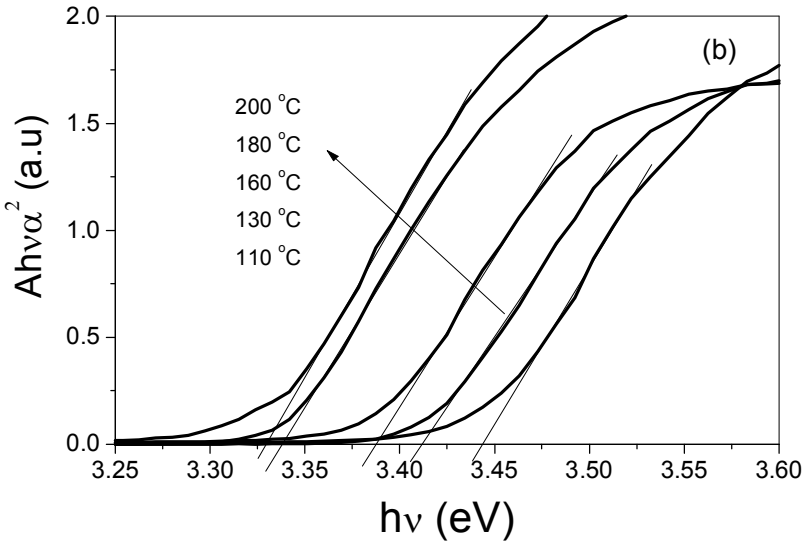


Absorption spectra and plots of $Ah\nu\alpha^2$ versus photon energy for ZnO nanocrystals grown at different temperatures (ketoacidoximate). (A is arbitrary constant)

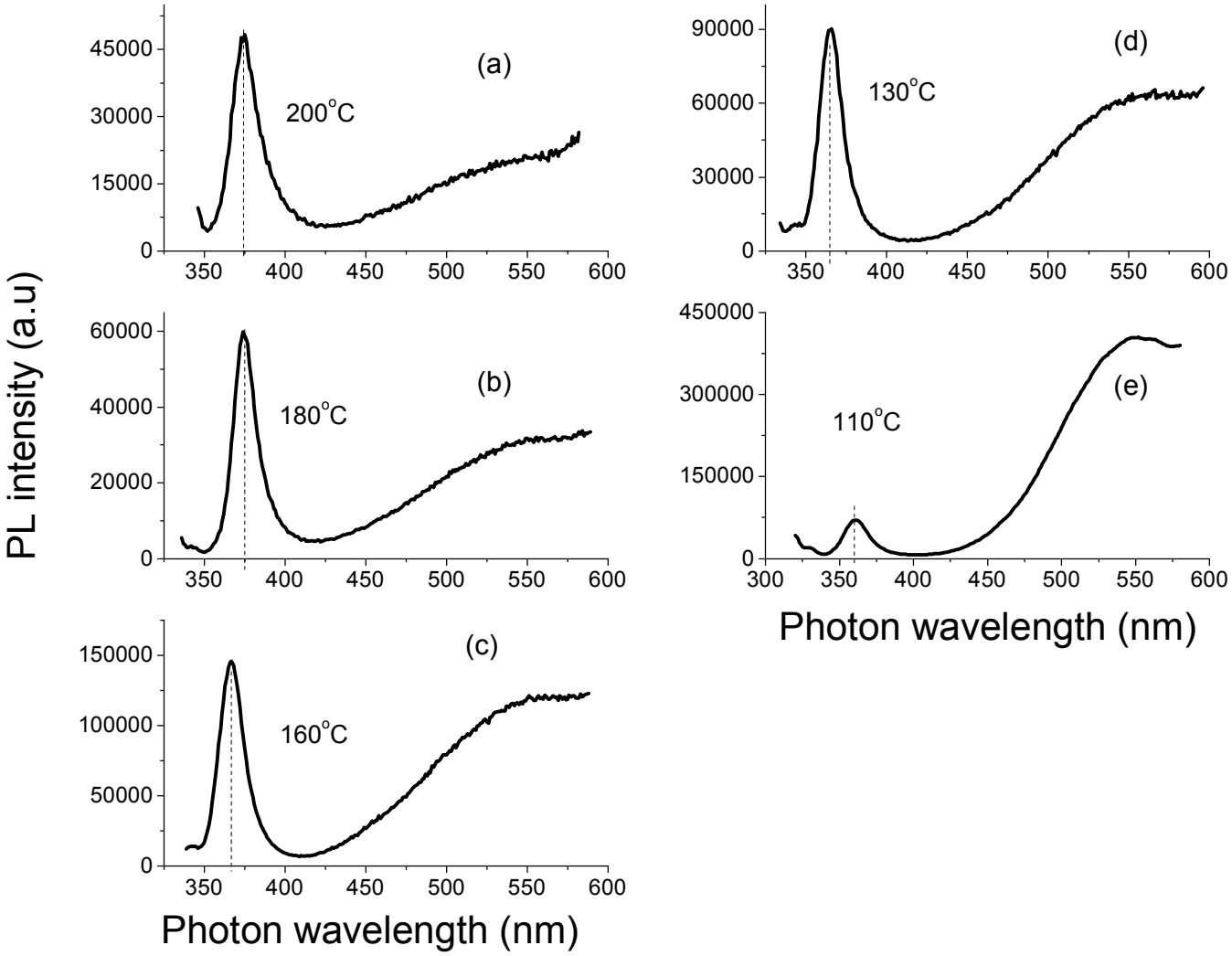


Emission spectra of ZnO nanocrystals grown from zinc ketoacidoximate at different temperatures (a)200 °C (b)180 °C (c)160 °C (d)130 °C (e)110 °C.

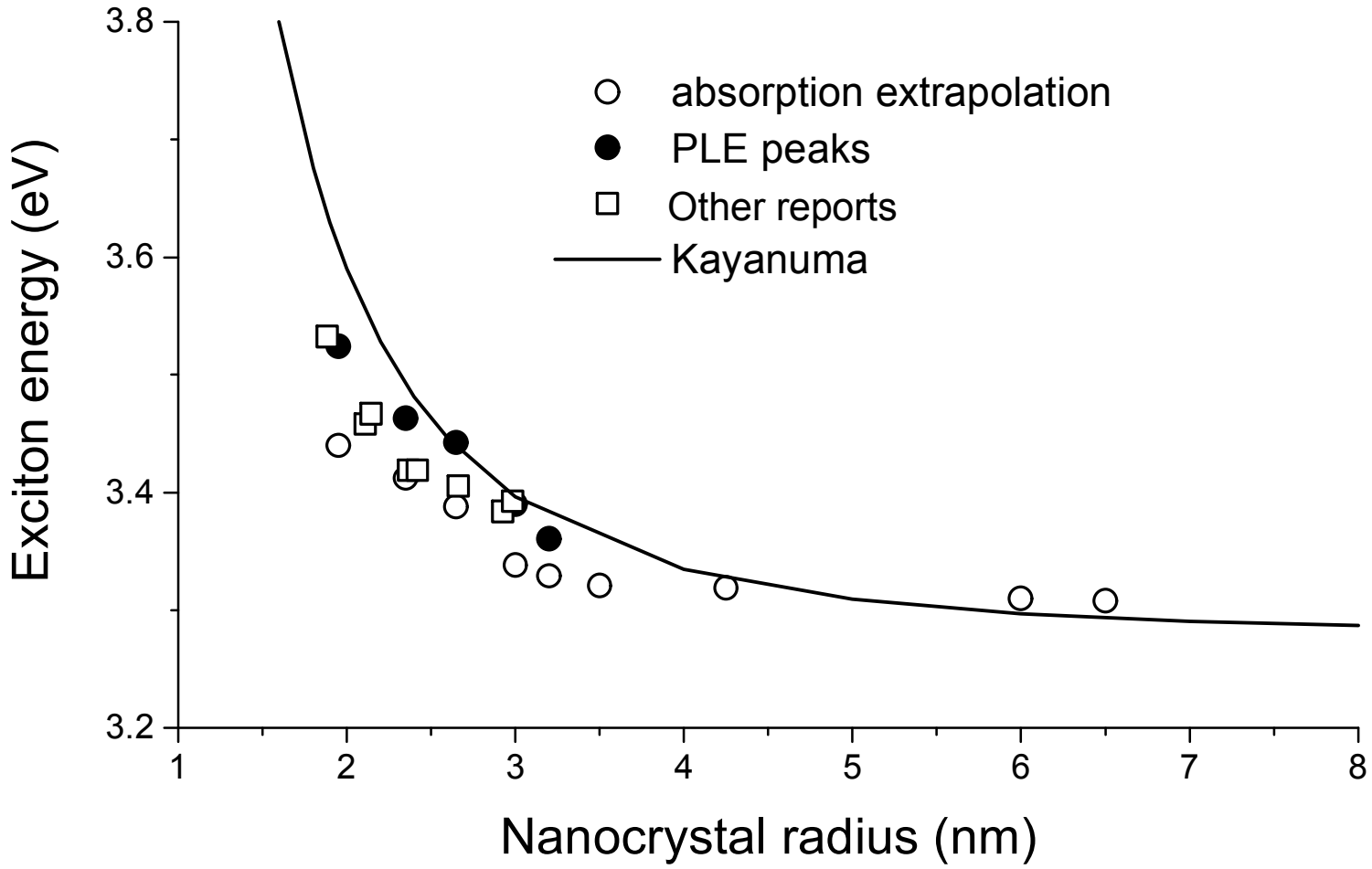
absorption extrapolation
PLE peaks
Other reports
Kayanuma
Exciton energy (eV)
Nanocrystal radius (nm)
3.8
3.6
3.4
3.2
1
2
3
4
5
6
7
8

# Bandgap Engineering in Zinc Oxide Nanoparticles

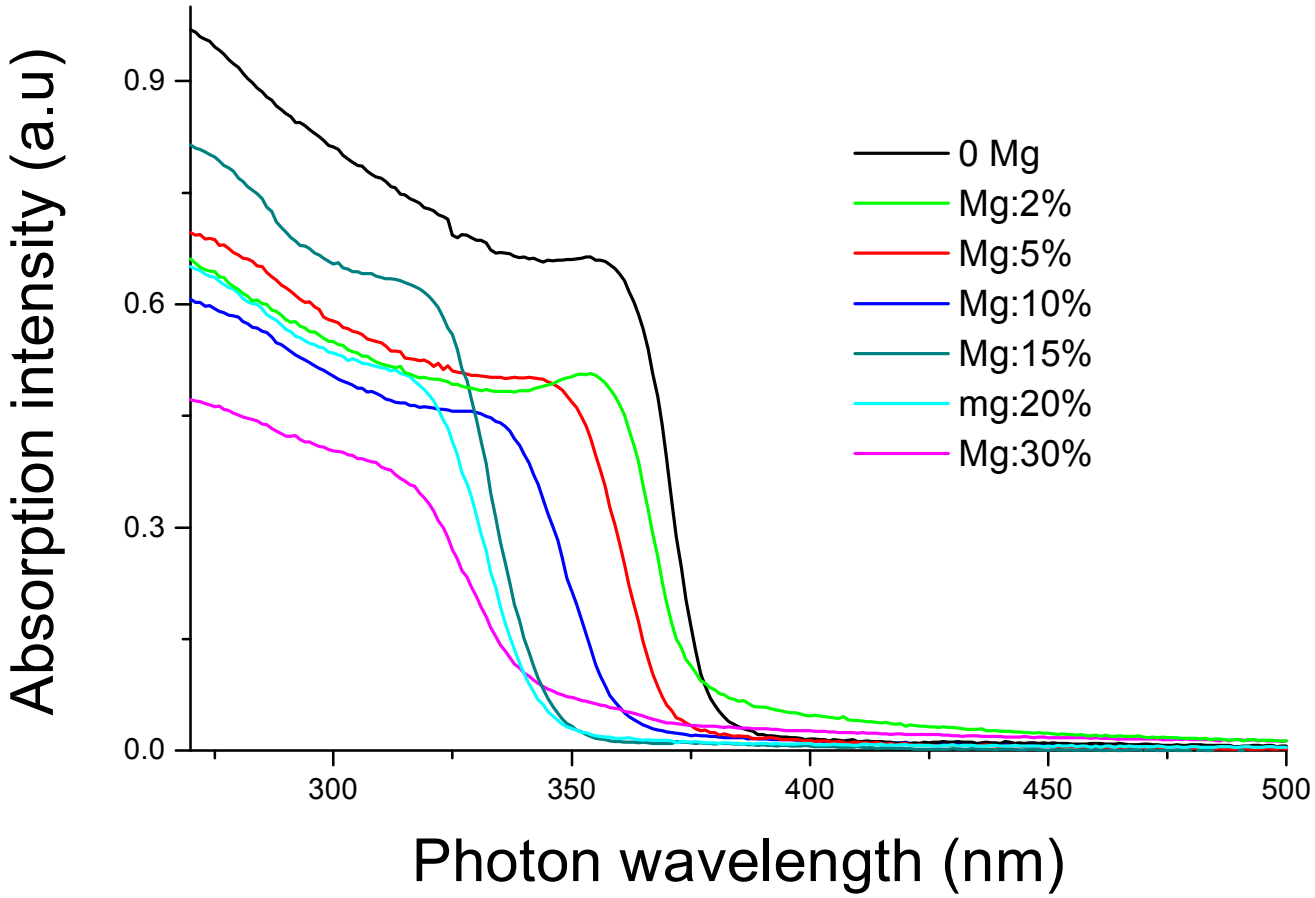


All doping was carried out at 180 ºC employing the cupferrate precursors.

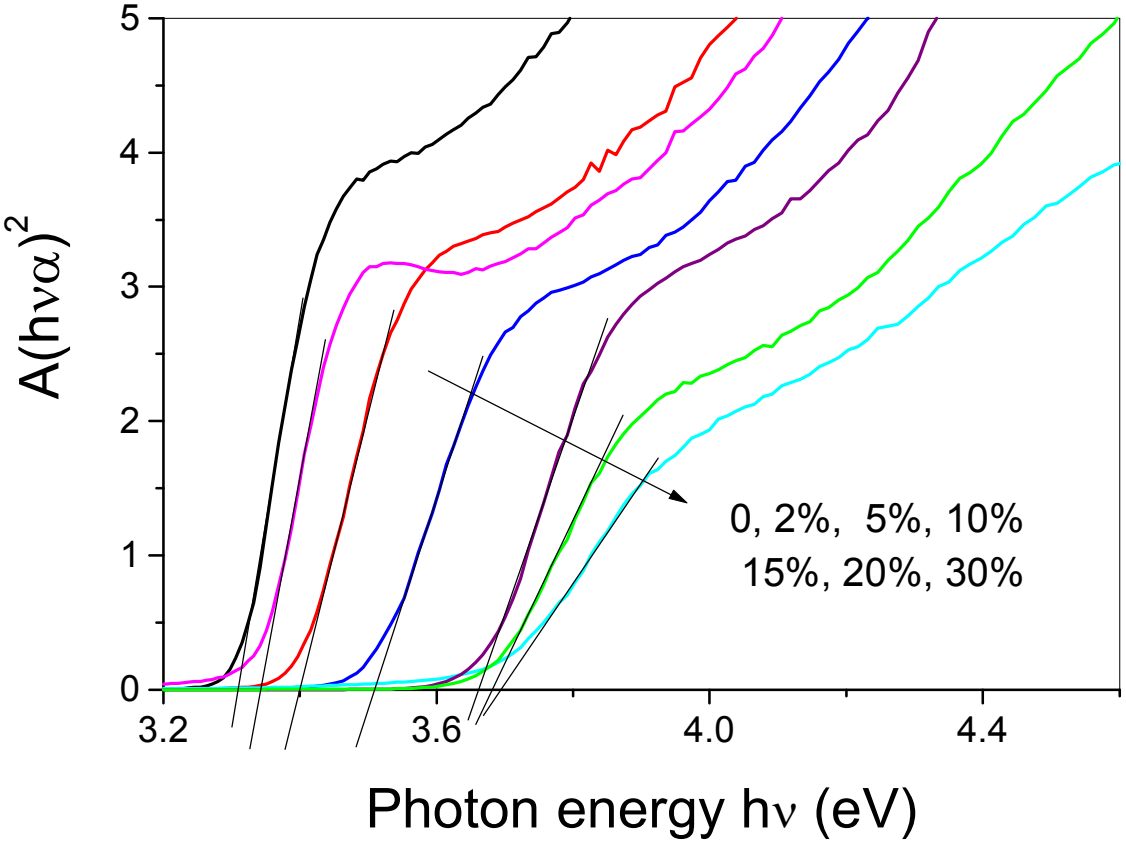


| Mg(%) | Eg(eV) |
|---|---|
| 0 | 3.31 |
| 2 | 3.34 |
| 5 | 3.40 |
| 10 | 3.50 |
| 15 | 3.66 |
| 20 | 3.68 |
| 30 | 3.69 |

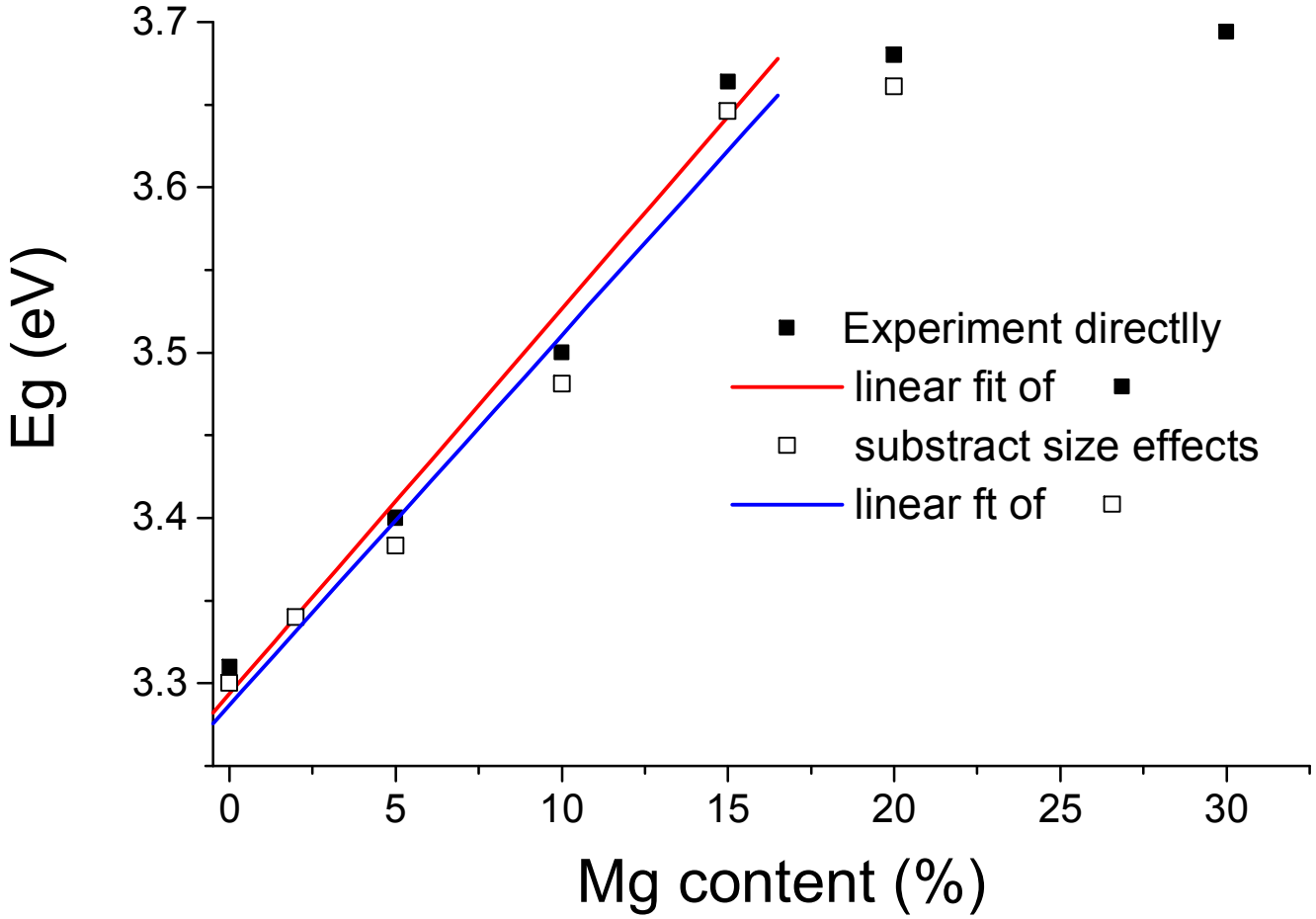
Eg (eV)
3.7
3.6
3.5
3.4
3.3
0
5
10
15
20
25
30
Mg content (%)
Experiment directlly
linear fit of
substract size effects
linear ft of

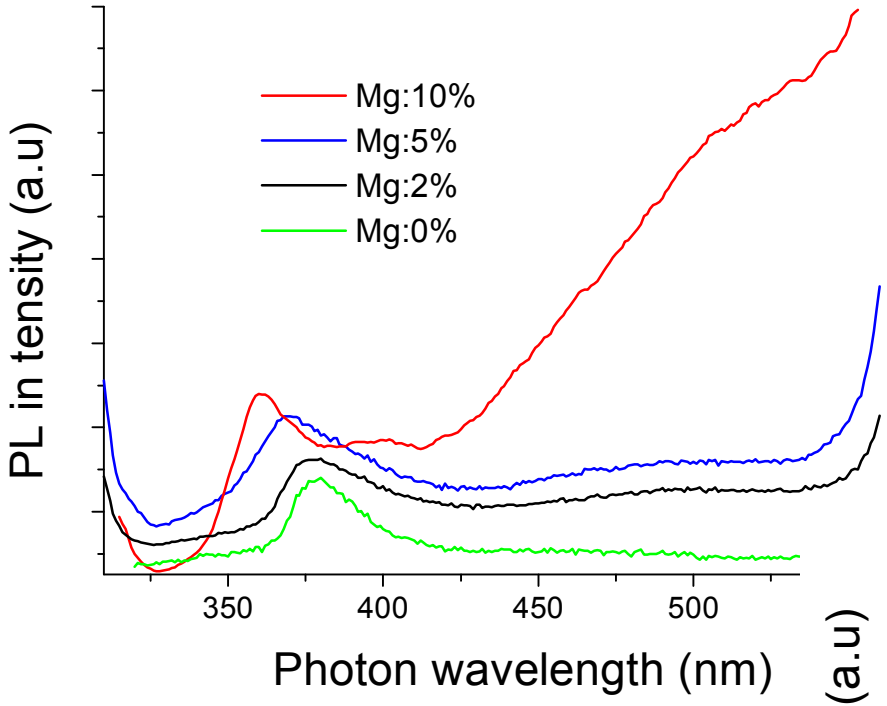
Mg:10%
Mg:5%
Mg:2%
Mg:0%
PL in tensity (a.u)
350
400
450
500
Photon wavelength (nm)

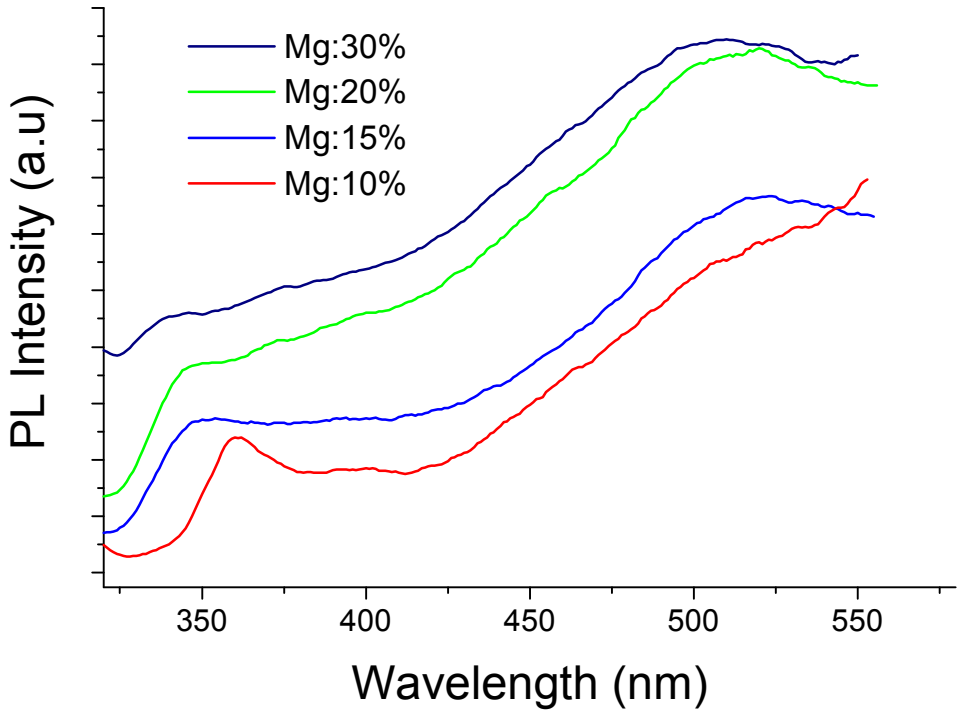
Mg:30%
Mg:20%
Mg:15%
Mg:10%
PL Intensity (a.u)
350
400
450
500
550
Wavelength (nm)

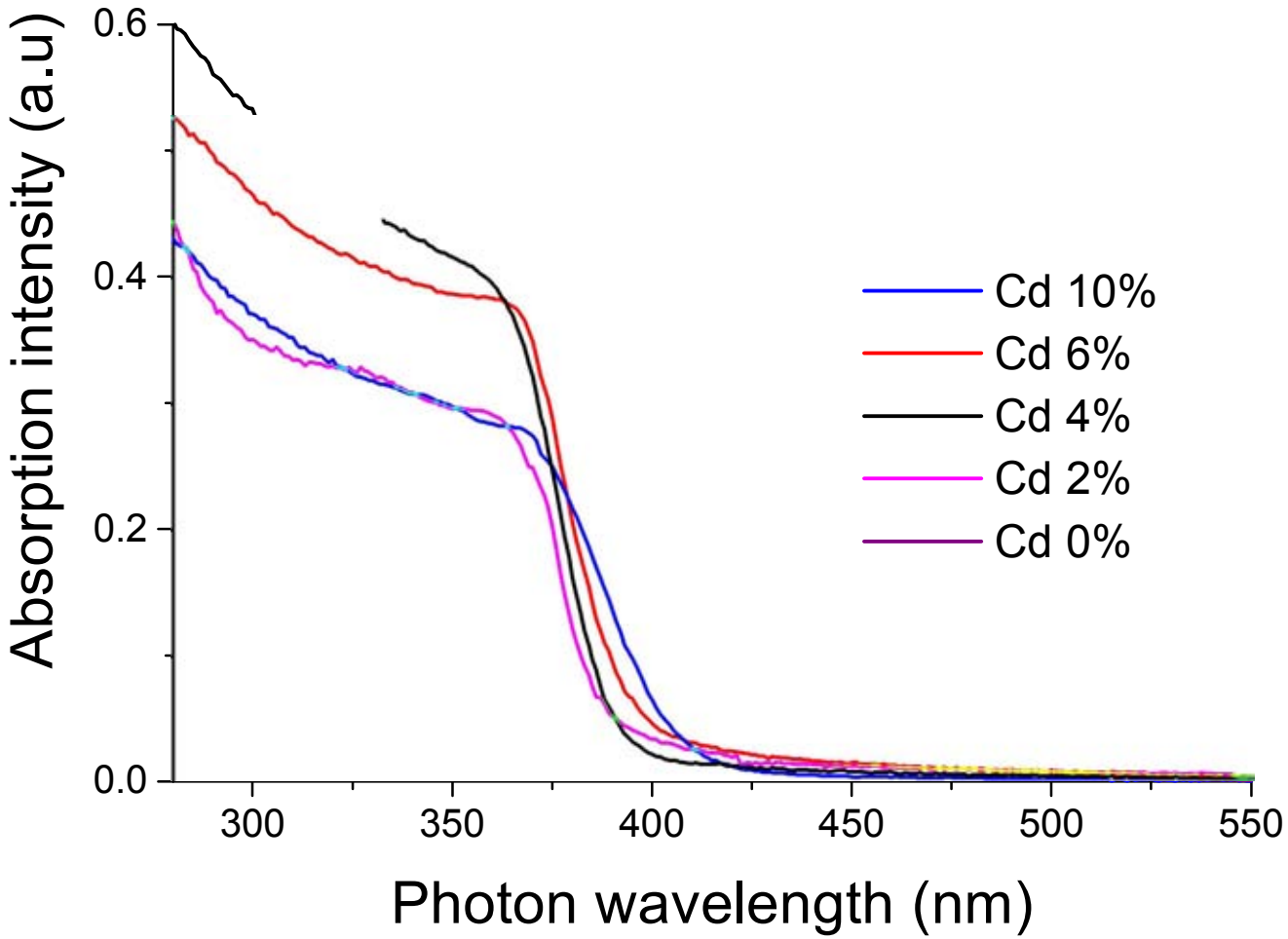


Cadmium Doping using cupferate

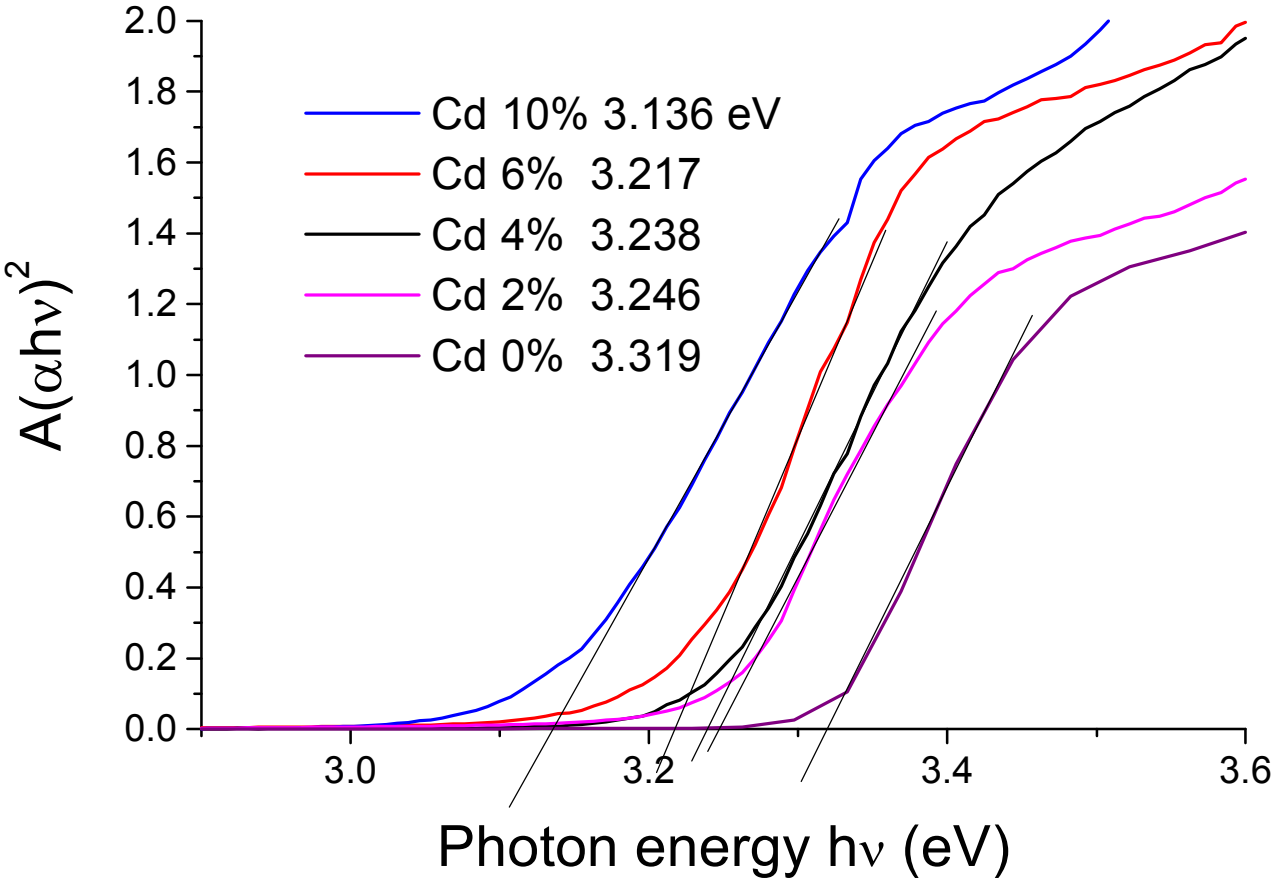
Cd 10% 3.136 eV
Cd 6% 3.217
Cd 4% 3.238
Cd 2% 3.246
Cd 0% 3.319
A(αhν)²
Photon energy hν (eV)
0.0
0.2
0.4
0.6
0.8
1.0
1.2
1.4
1.6
1.8
2.0
3.0
3.2
3.4
3.6

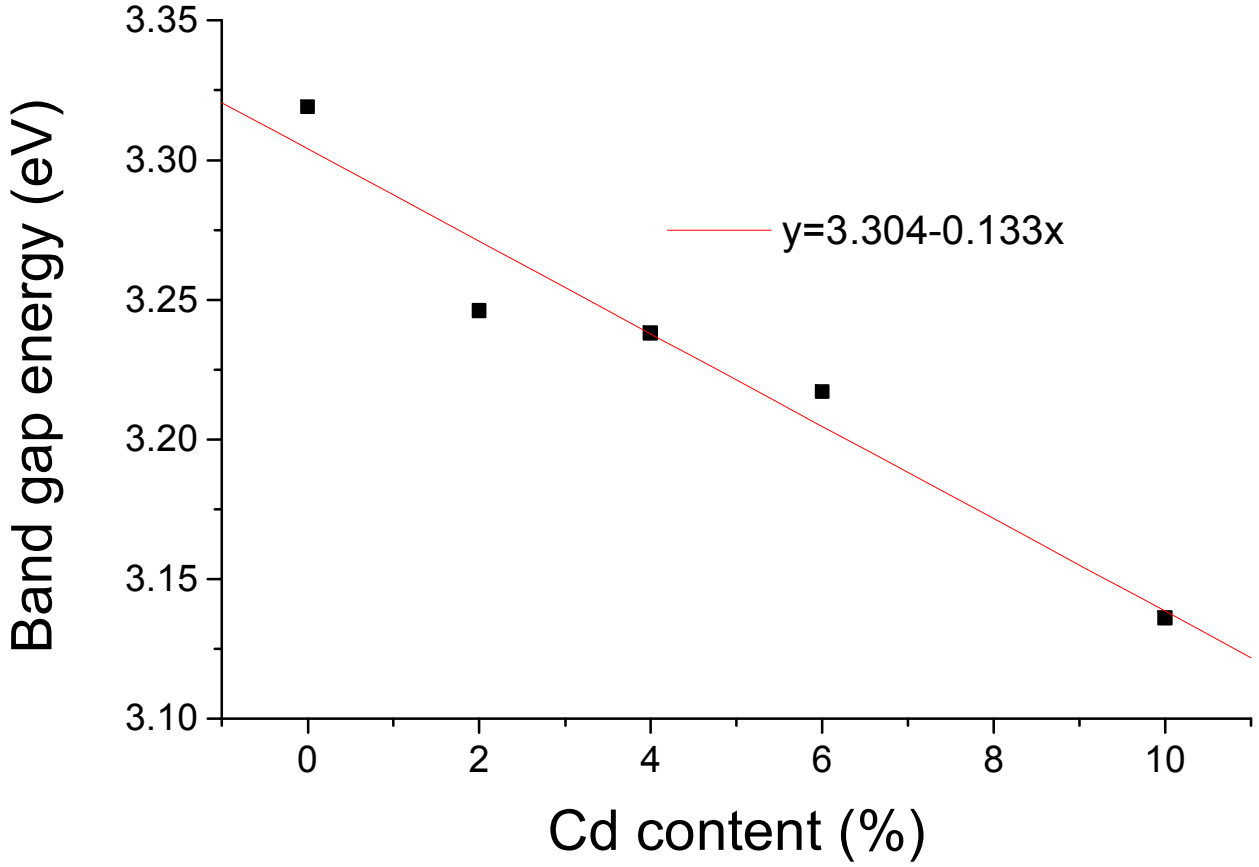
Band gap energy (eV)
3.35
3.30
3.25
3.20
3.15
3.10
0
2
4
6
8
10
Cd content (%)
y=3.304-0.133x

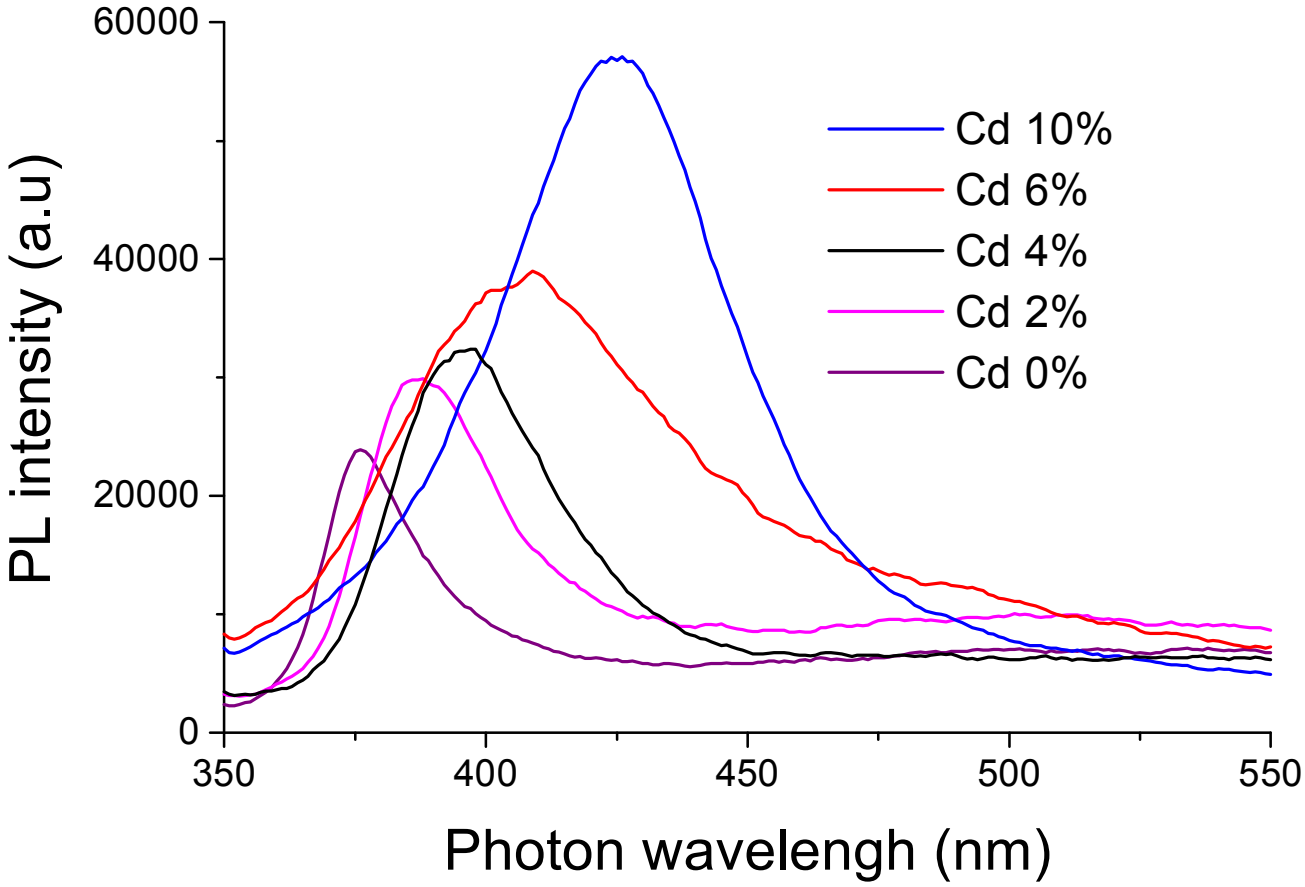
60000
40000
20000
0
PL intensity (a.u)
350
400
450
500
550
Photon wavelengh (nm)
Cd 10%
Cd 6%
Cd 4%
Cd 2%
Cd 0%

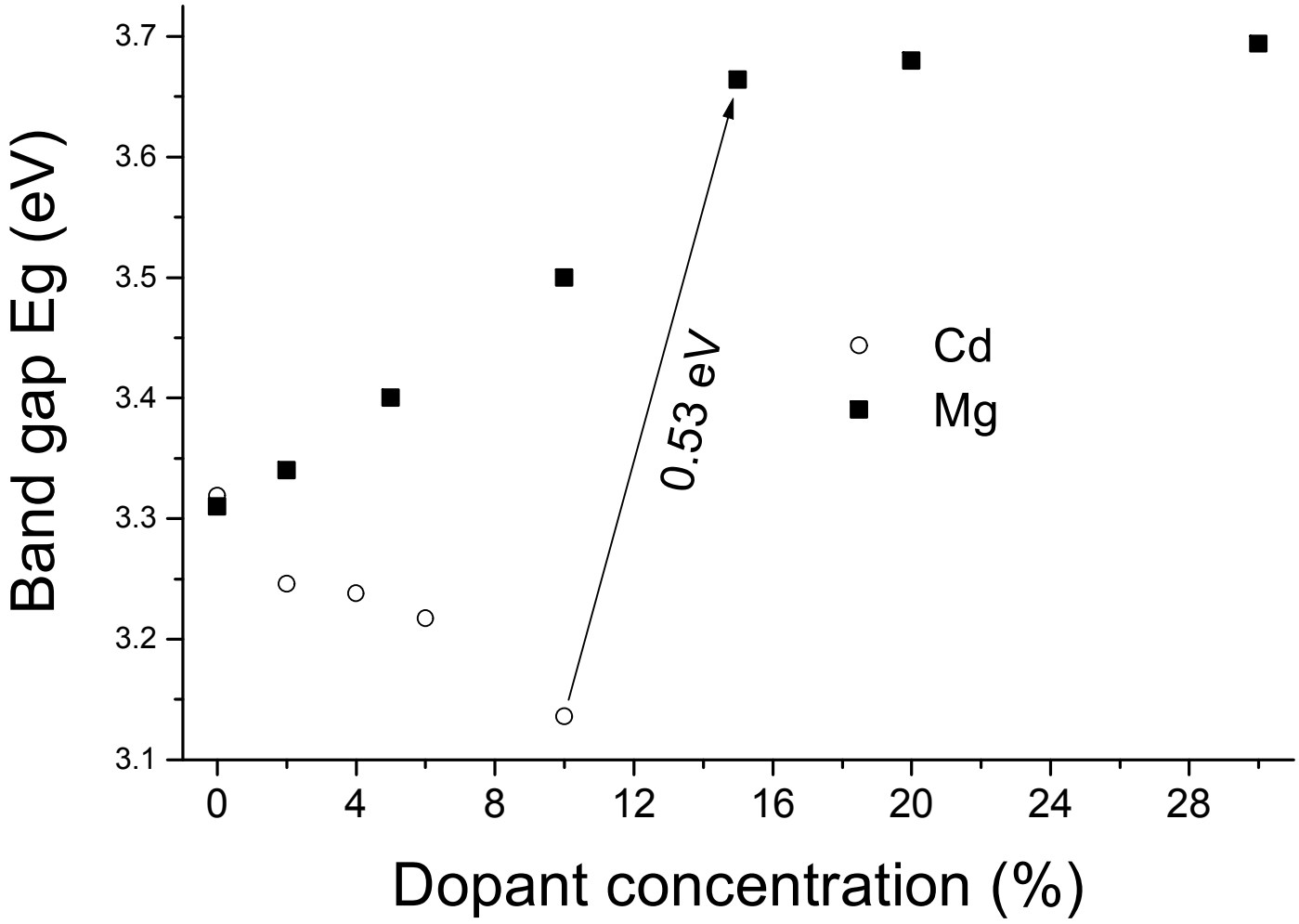
Band gap Eg (eV)
3.7
3.6
3.5
3.4
3.3
3.2
3.1
0
4
8
12
16
20
24
28
Dopant concentration (%)
0.53 eV
Cd
Mg

# Structure of Talk

- Looking at some nanodimensional objects
- Synthetic approaches zinc oxide and doping
- **How nanoparticles grow and**
- **Rods**
- Assemblies of nanoparticles and mesoscopic objects
- Closing remarks

JOURNAL

# Controlled synthesis of CdS nanorods and hexagonal nanocrystals

Yunchao Li,† Xiaohong Li,† Chunhe Yang and Yongfang Li*

*Key Laboratory of Organic Solids, Center for Molecular Science, Institute of Chemistry, Chinese Academy of Sciences, Beijing, China 100080. E-mail: liyf@iccas.ac.cn*

*Received 3rd July 2003, Accepted 27th August 2003*
*First published as an Advance Article on the web 3rd September 2003*

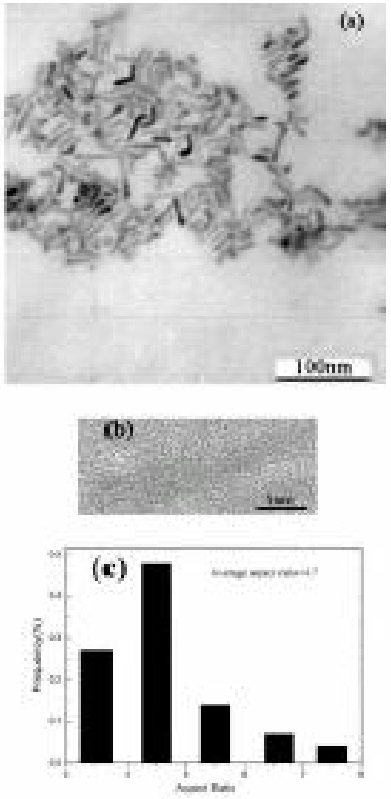


Fig. 7 (a) TEM image of CdS nanorods synthesized at 180 °C for 3 h with a reaction solution of 0.1 g $Cd(C_2H_5OCS_2)_2$ in 4 g HDA. (b) High resolution TEM image of a representative nanorod. (c) Aspect ratio histogram of the nanocrystals.

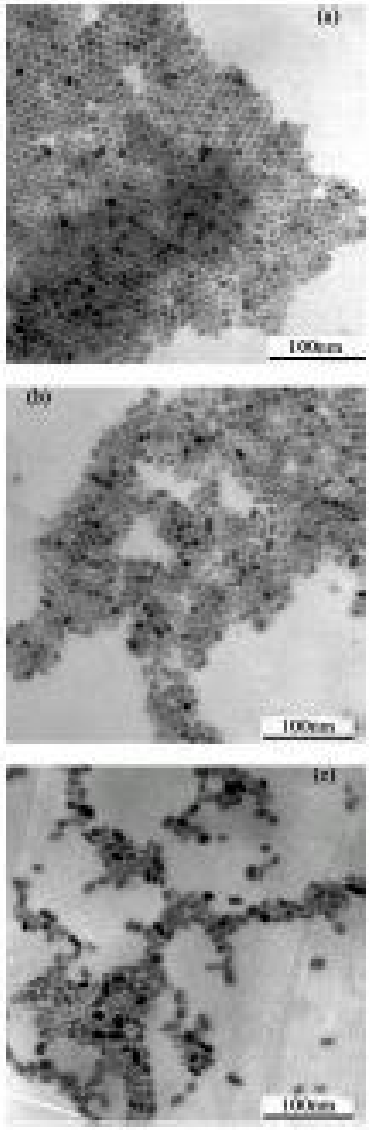


Fig. 8 TEM images of CdS nanocrystals prepared at 260 °C for 3 h, from solutions of (a) 0.1 g, (b) 0.2 g, (c) 0.4 g $Cd(C_2H_5OCS_2)_2$ in 4 g HDA and 2 ml TOP.

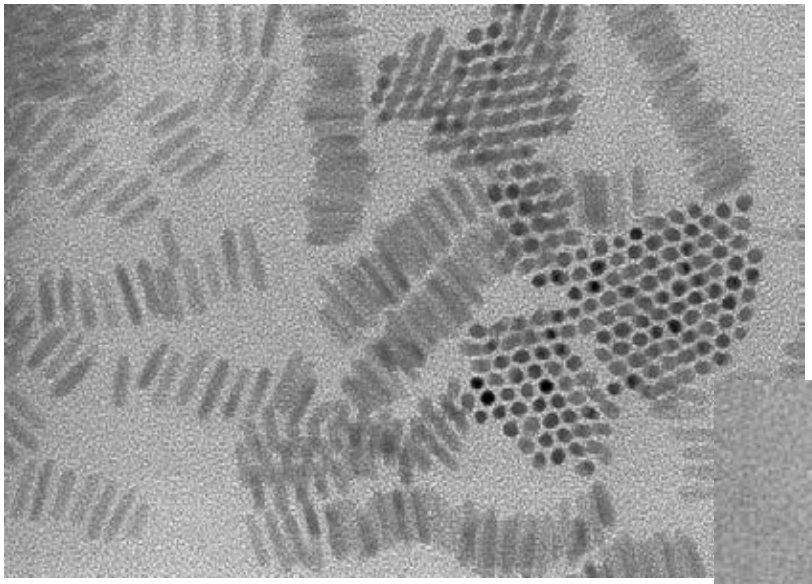

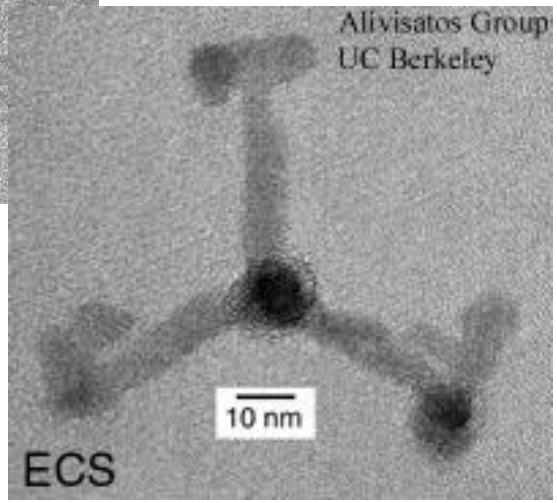
Alivisatos Group
UC Berkeley
10 nm
ECS

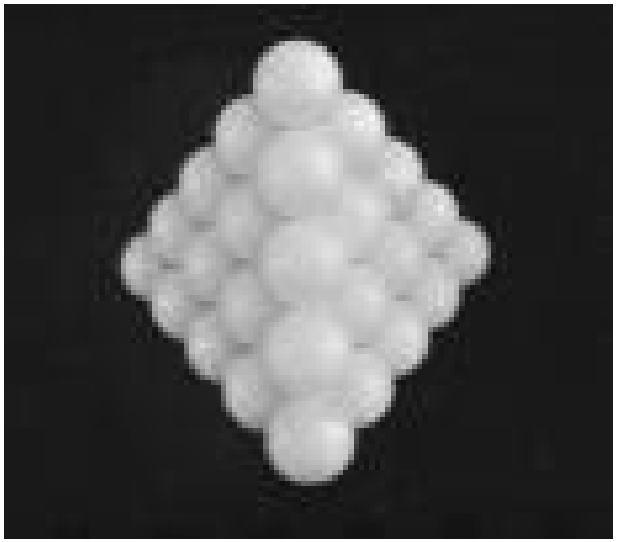

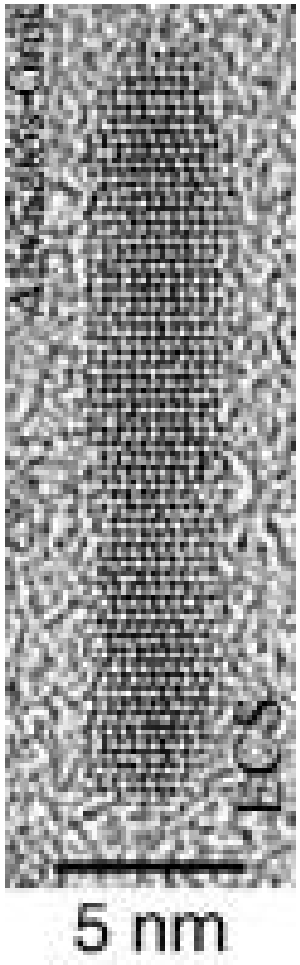
5 nm

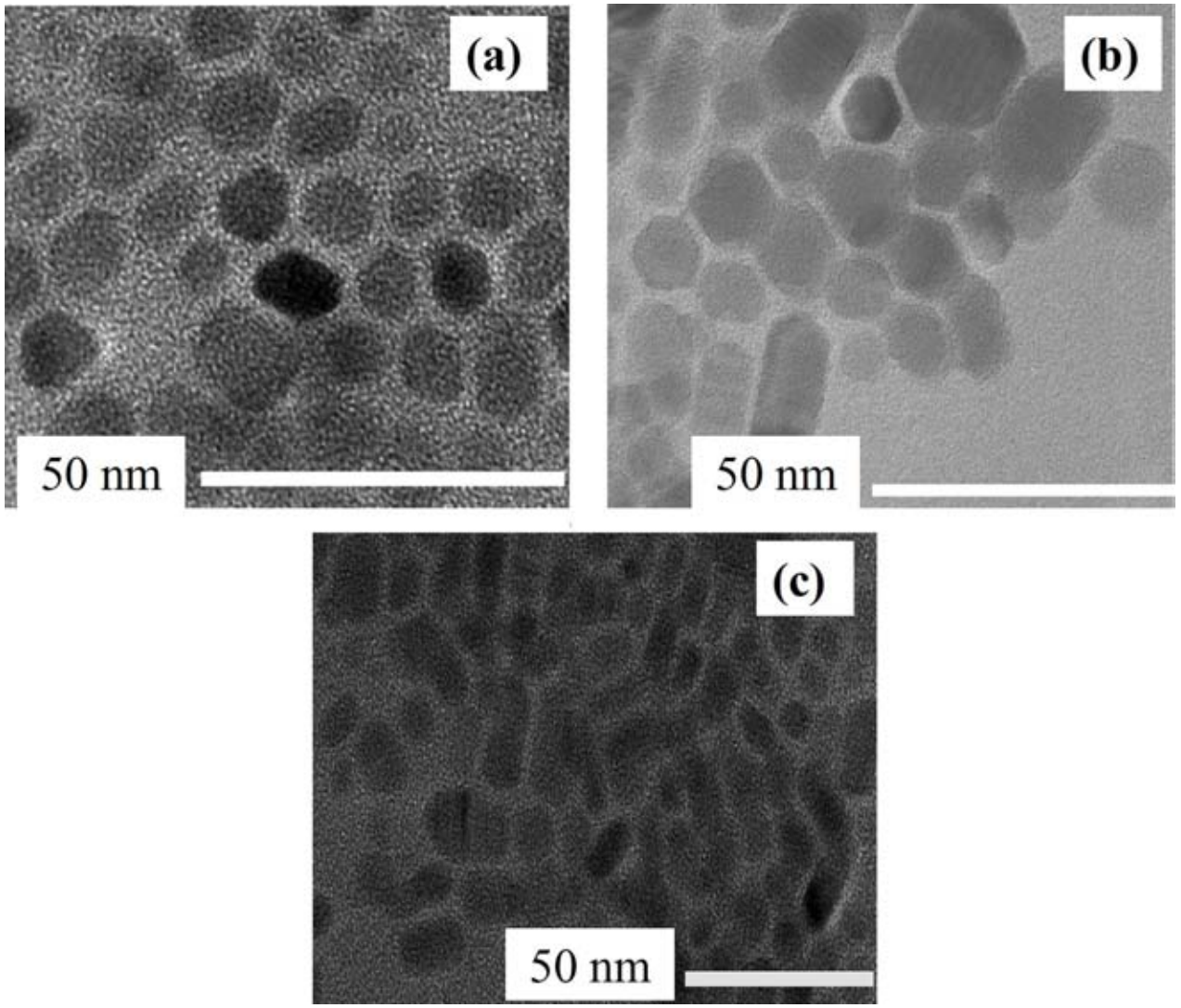


EM images of CdS particles using
(a) 1.5g, (b) 2.5g and (c) 3.5g of precursor.

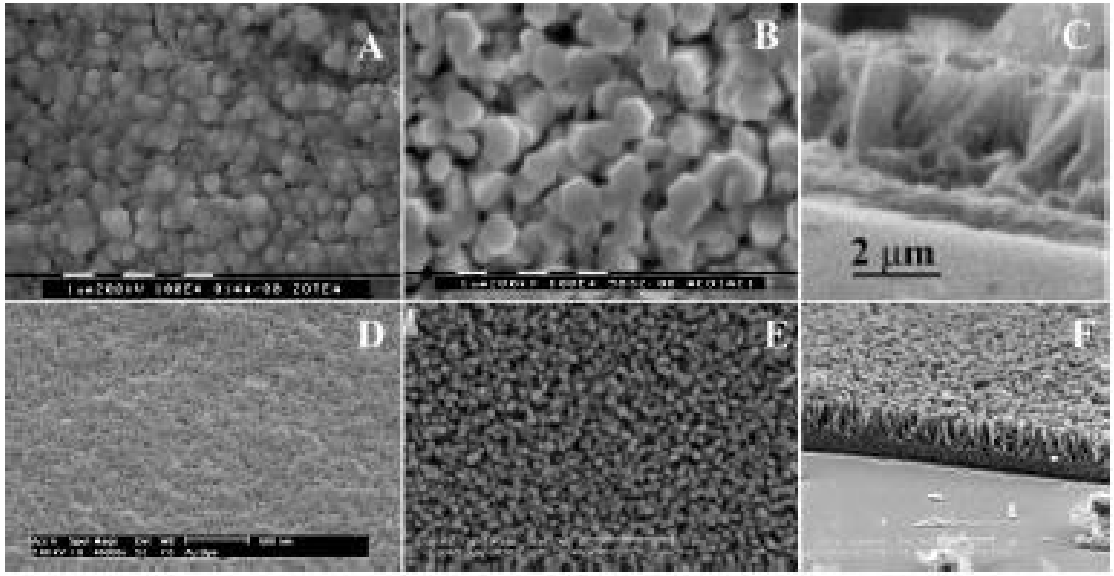


Fig. 17 A. CBD-ZnO microcrystalline templates on TO(F) glass comprising nodular grains (deposited from TEA-systems); B,C. ZnO microcolumns grown on CBD-ZnO templates from HMT-system ([Zn] = 0.025 mol dm$^{-3}$, [HMT] = 0.025 mol dm$^{-3}$, pH 5, 90 °C); D. nanocrystalline ZnO templates on glass microscope slides (prepared by sol gel (SG) method); E,F. ZnO nanocolumns grown on SG-ZnO templates from HMT-system.

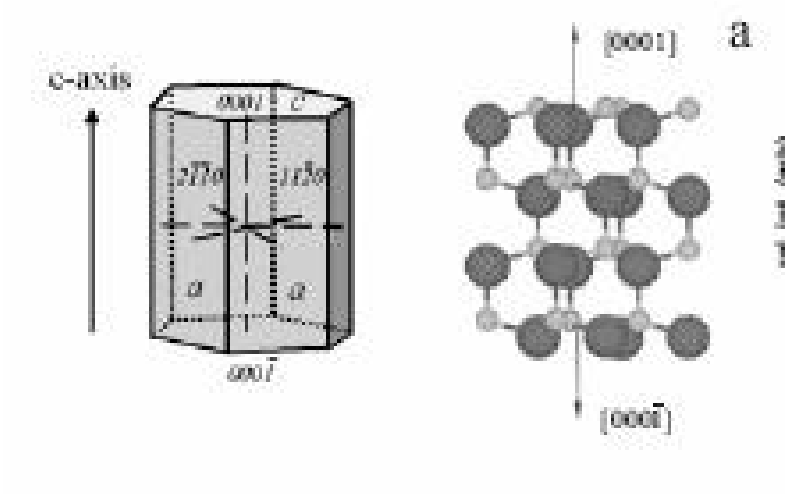

## Tetrahedron

**N = 2**

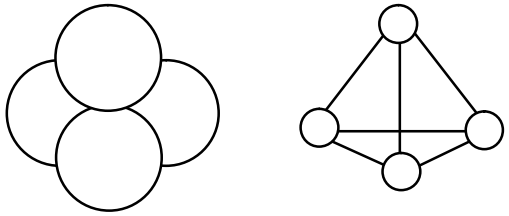

Total atoms = 4
Surface atoms = 4

**N = 3**

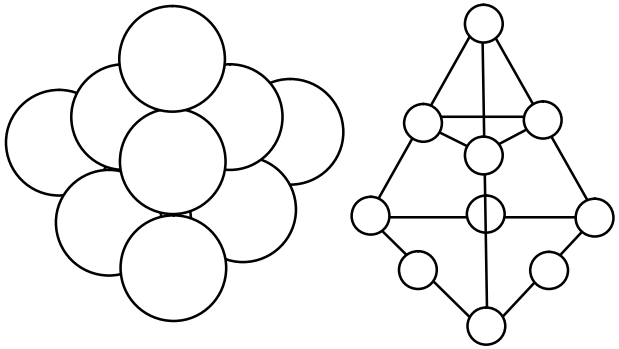

Total atoms = 10
Surface atoms = 10

## Cube

**N = 2**

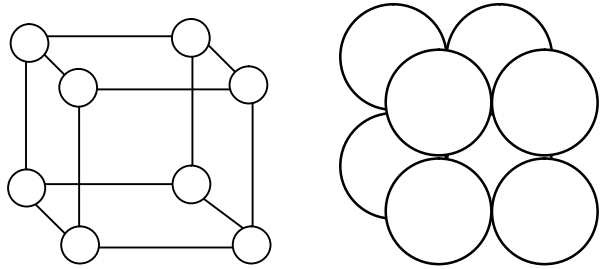

Total atoms = 8
Surface atoms = 8

**N = 3**

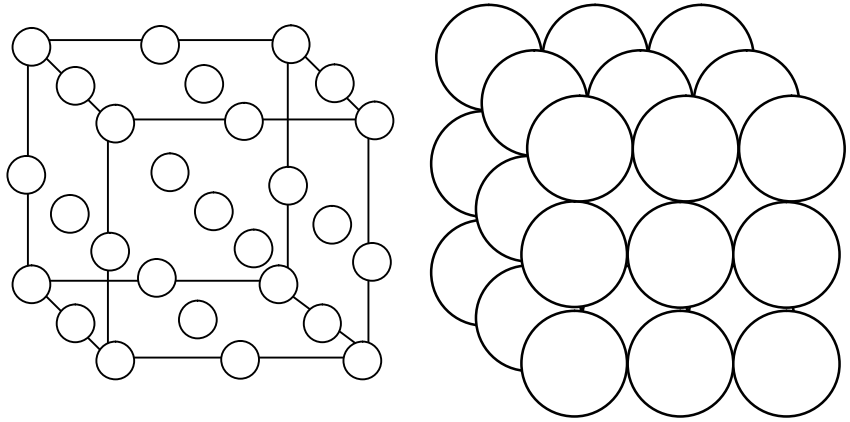

Total atoms = 27
Surface atoms = 26

| Shape | Total atoms | Surface atoms |
|---|---|---|
| **Cube** Bcc packing | $(N+1)^3+N^3$ | $6N^2+2$ |
| **Cube** Fcc packing | $4N^3+6N^2+3N+1$ | $12N^2+2$ |
| **Octahedron** Fcc packing | $\frac{2N^3}{3}+\frac{N}{3}$ | $4N^2-8N+6$ |
| **Tetrahedron** Fcc packing | $\frac{N^3}{6}+\frac{N^2}{2}+\frac{N}{3}$ | $2N^2-4N+4$ |
| **Cuboctahedron** triangular faces, fcc packing | $\frac{10N^3}{3}-5N^2+\frac{11N}{3}-1$ | $10N^2-20N+12$ |

**Relationship between the number of shells N and the total number of atoms and surface atoms for different shapes**

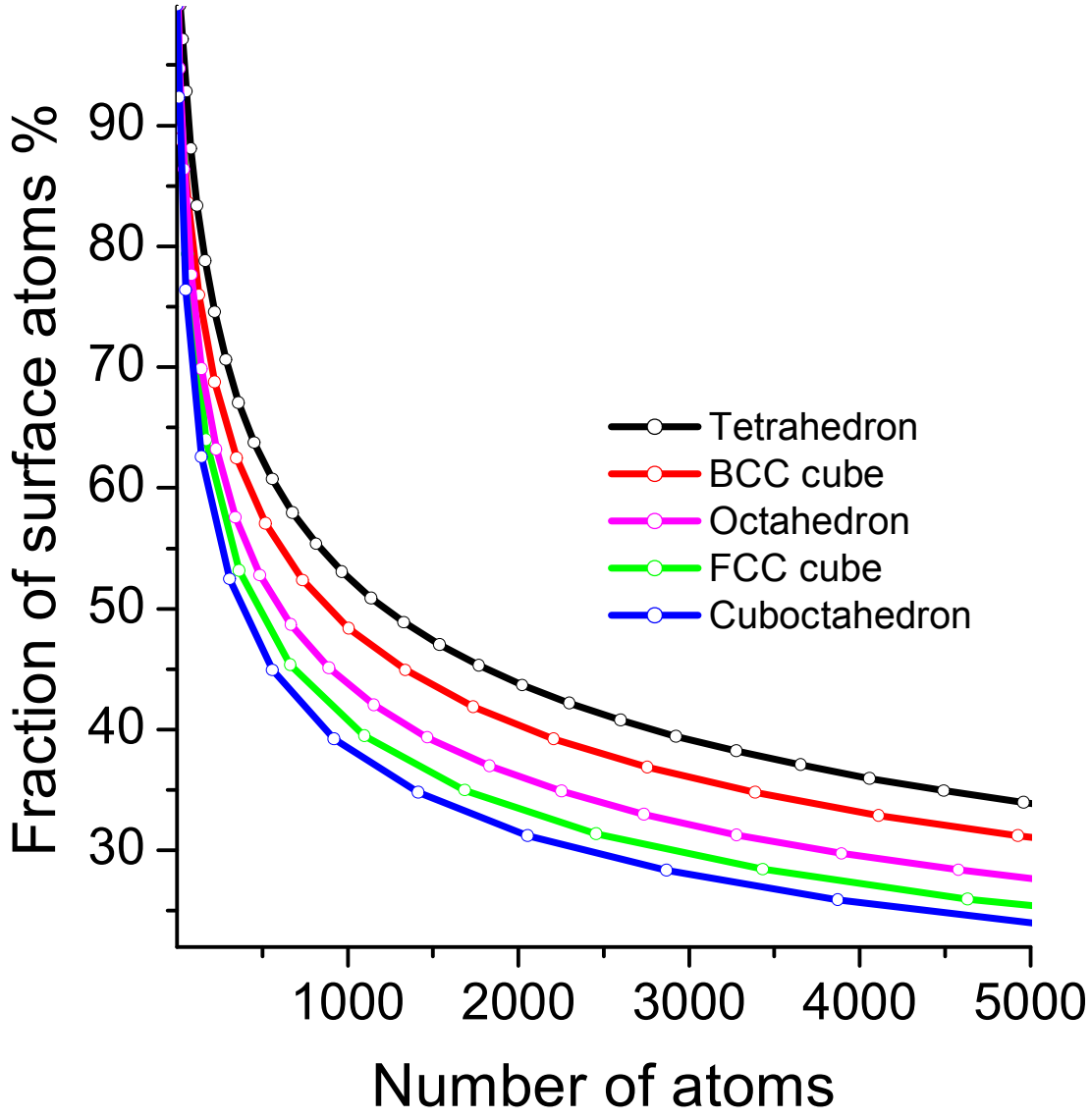
Fraction of surface atoms %
90
80
70
60
50
40
30
1000
2000
3000
4000
5000
Number of atoms
Tetrahedron
BCC cube
Octahedron
FCC cube
Cuboctahedron

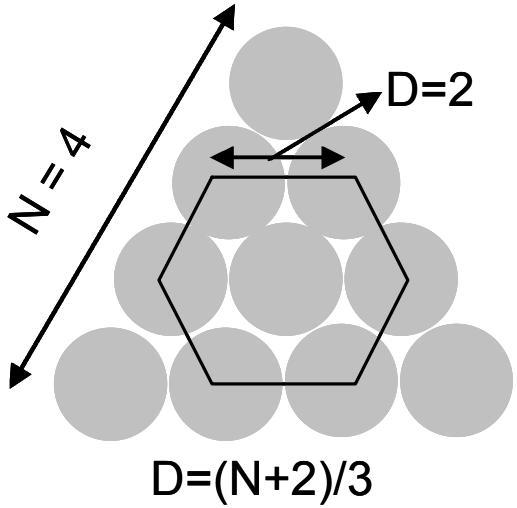
N=4
D=2
D=(N+2)/3

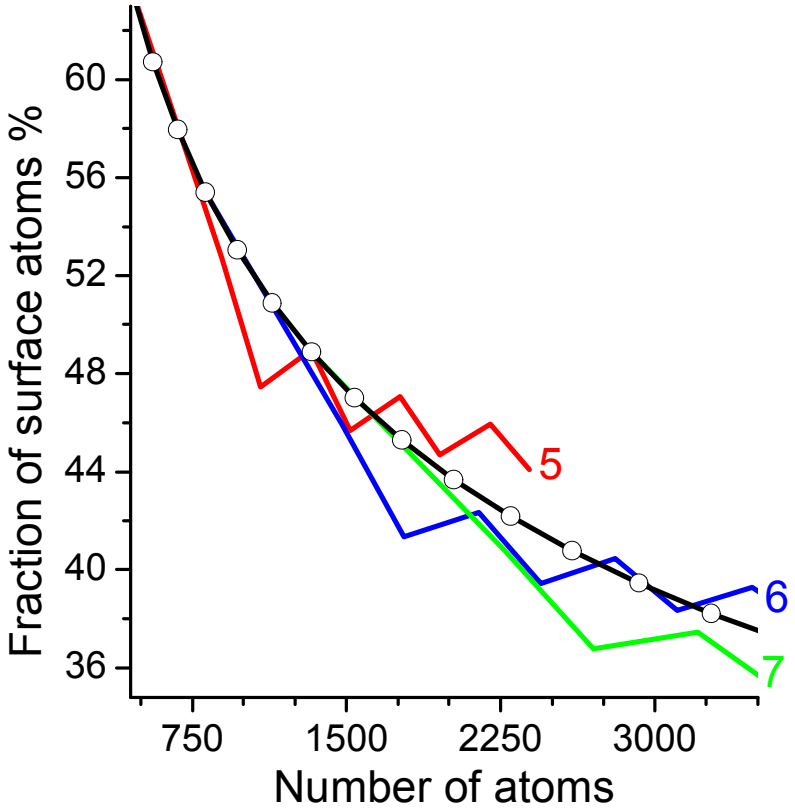
Fraction of surface atoms %
60
56
52
48
44
40
36
750
1500
2250
3000
Number of atoms
5
6
7

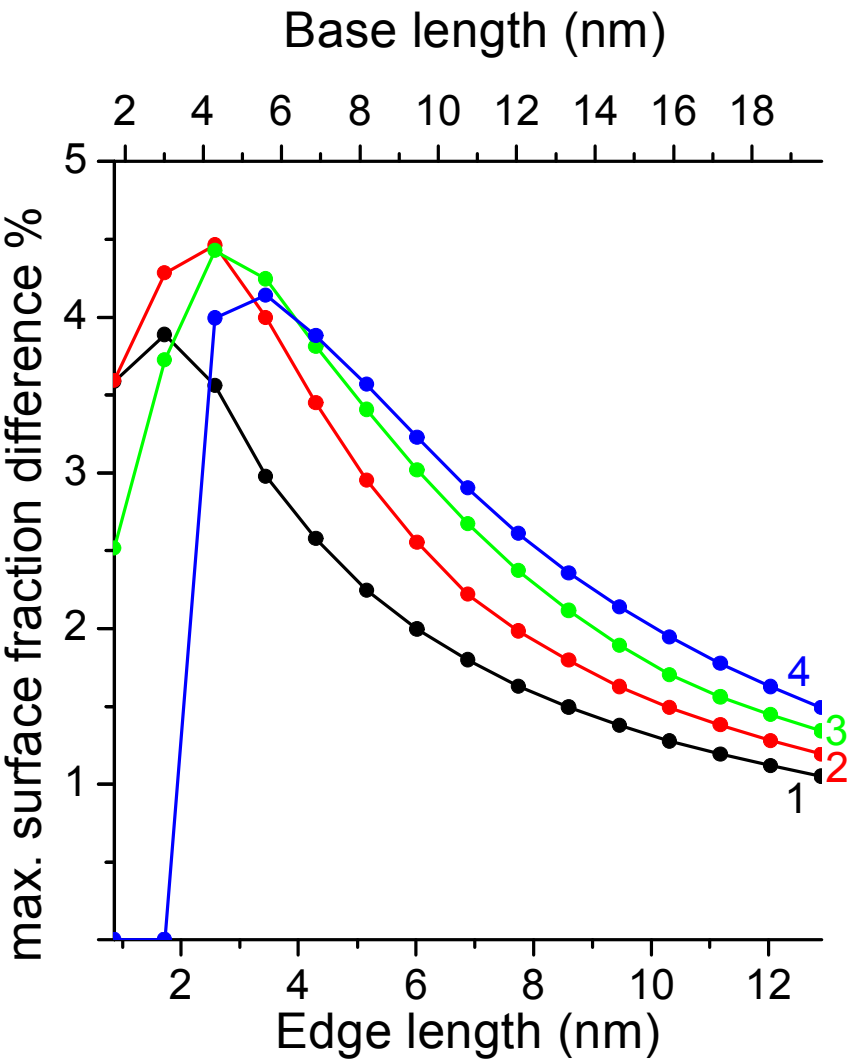
Base length (nm)
2
4
6
8
10
12
14
16
18
max. surface fraction difference %
5
4
3
2
1
2
4
6
8
10
12
Edge length (nm)
4
3
2
1

## Triangular face

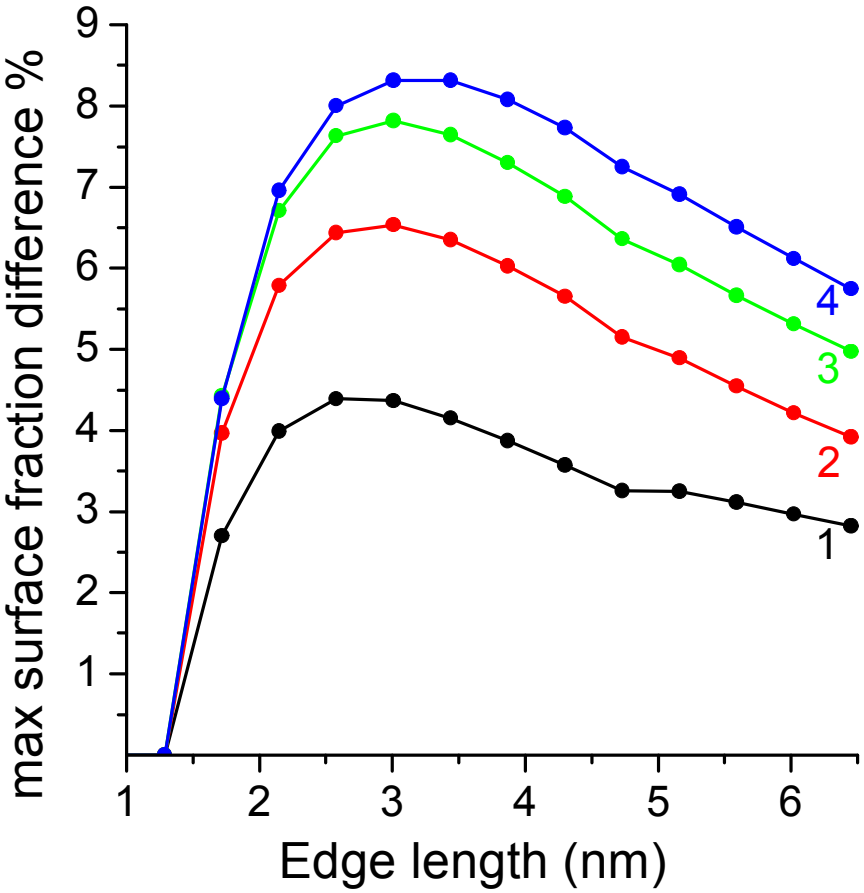

# Structure of Talk

- Looking at some nanodimensional objects
- Synthetic approaches zinc oxide and doping
- How nanoparticles grow and
- **Rods**
- Assemblies of nanoparticles and mesoscopic objects
- Closing remarks

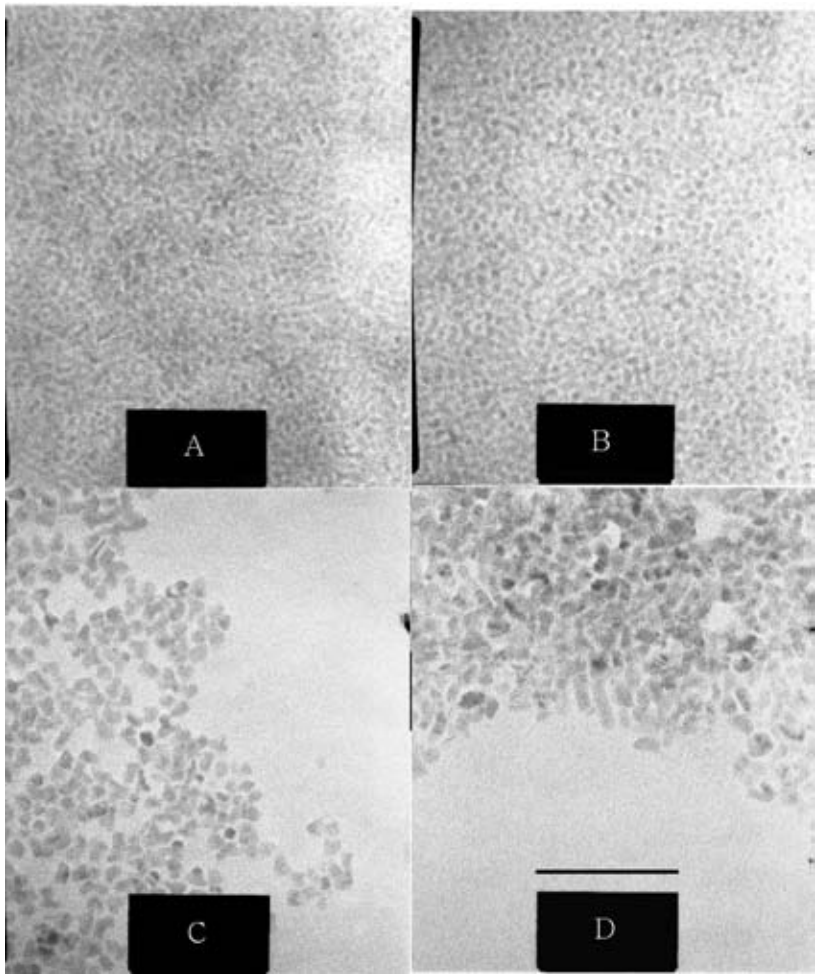


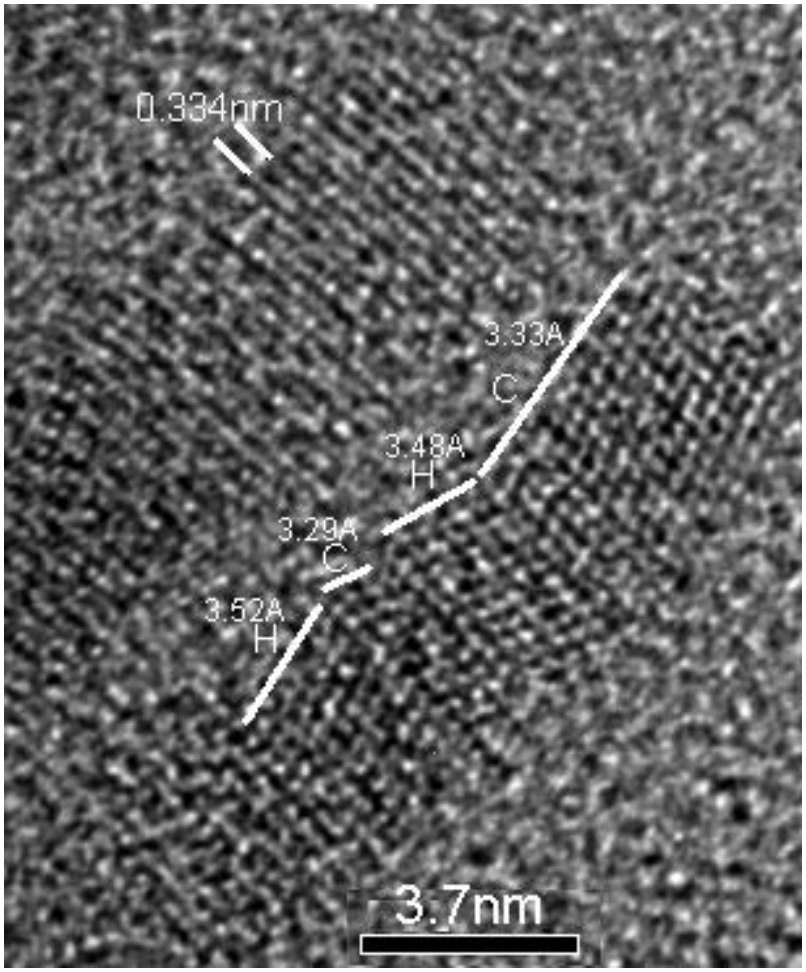


| Sample | mmol $CdAc_2$ | Final Molarity | $\lambda_{em}$ (nm) | % rods | Diam** (nm) (std) |
|---|---|---|---|---|---|
| A | 1.3 | 0.011 | 465 | <5 | 3.5 (0.7) |
| B | 2.2 | 0.018 | 489 | <5 | 4.0 (1) |
| C | 21.7 | 0.181 | 499 | ~15 | 6.5 (1) |
| D | 31.6* | 0.198 | 504 | 72 | 7.0 (1) |

Chem Comm

May 2005

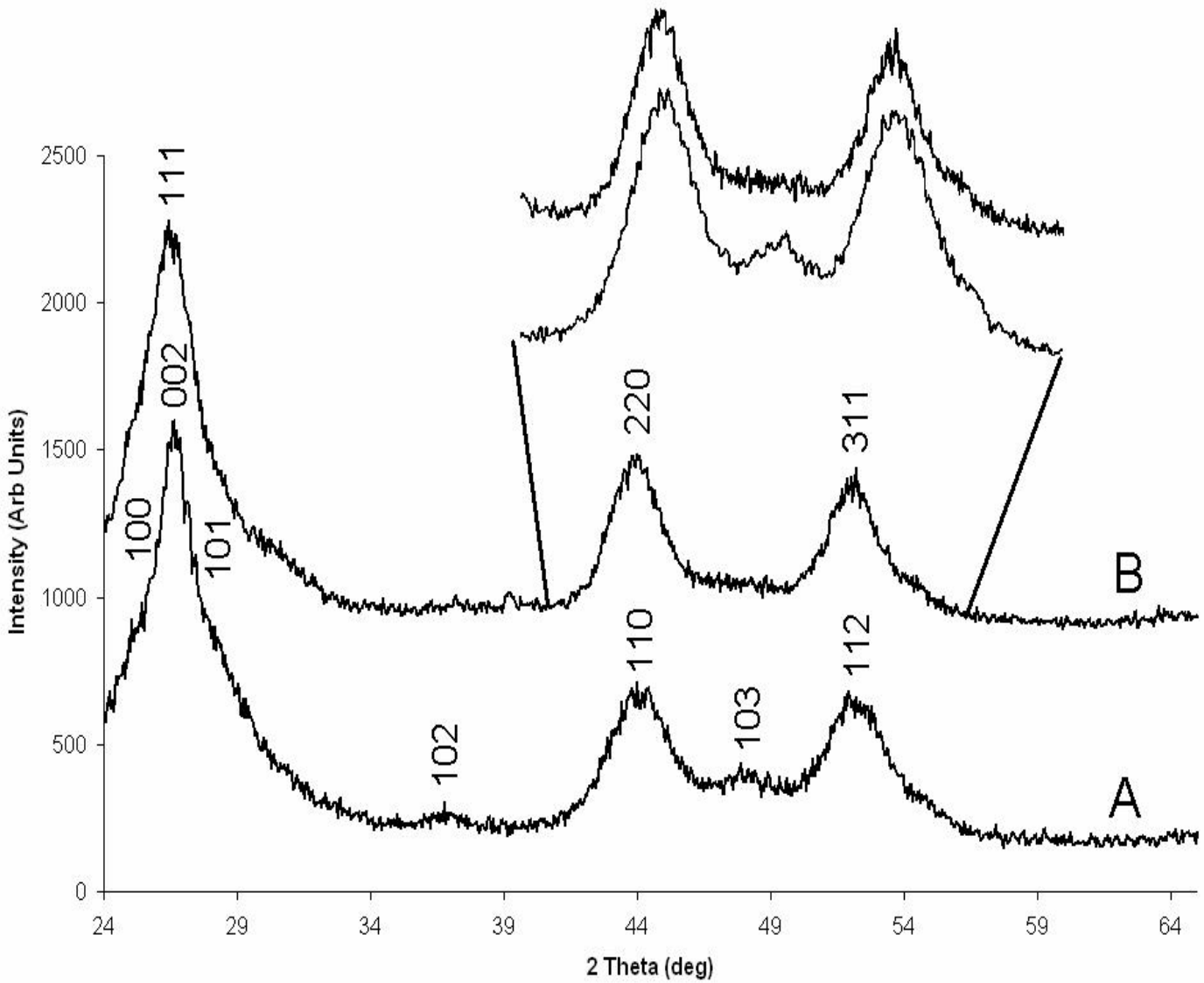


Powder XRD showing hexagonal phase of A and the cubic phase of B. Inset at higher resolution.

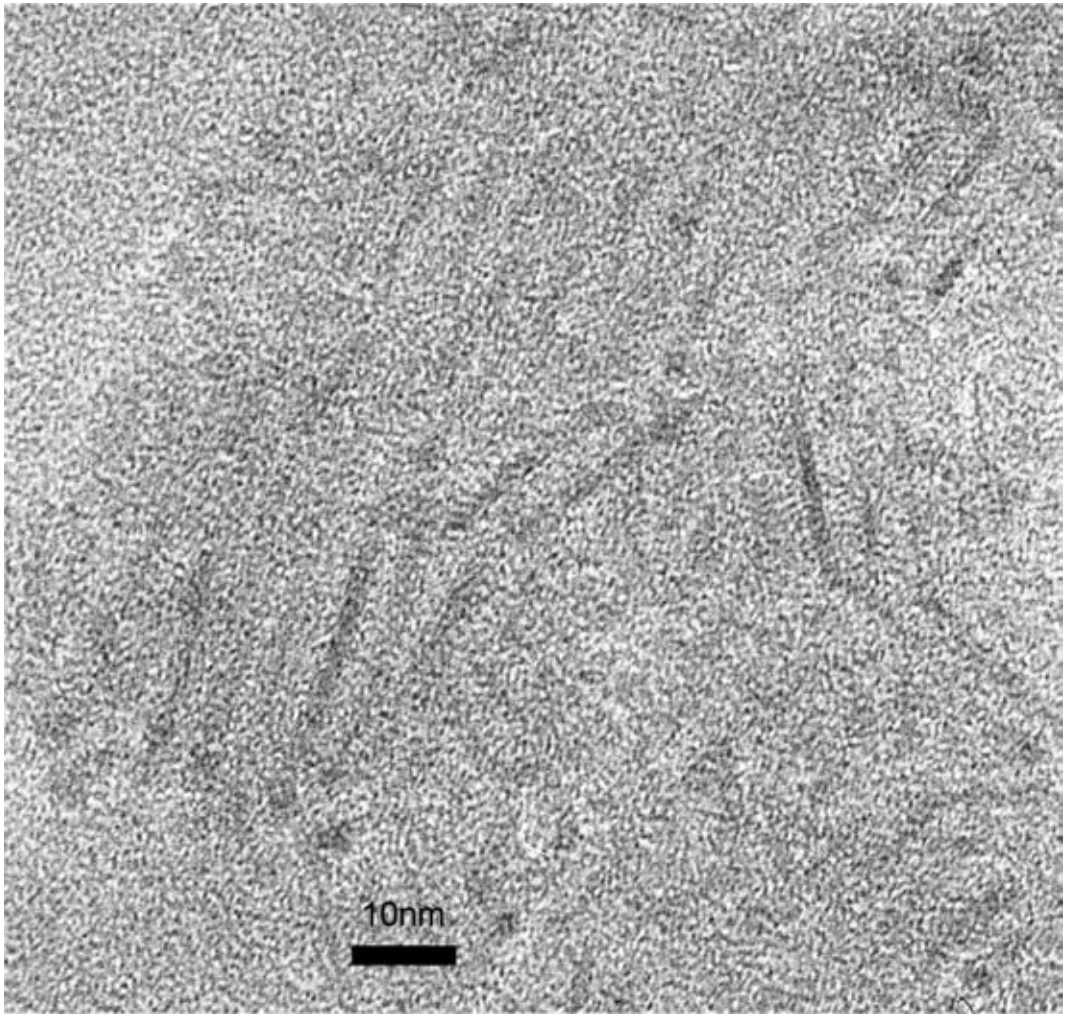


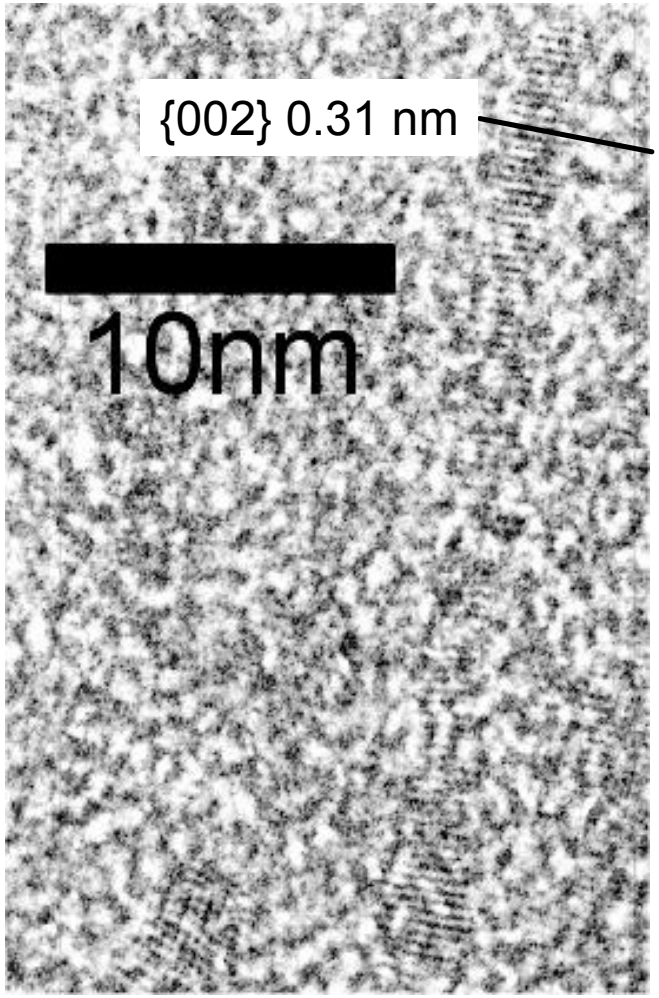


The low temperature (140 ºC) growth of hexagonal ZnS nanorods in a mixture of hexadecylamine and octylamine from sulfur and zinc acetate

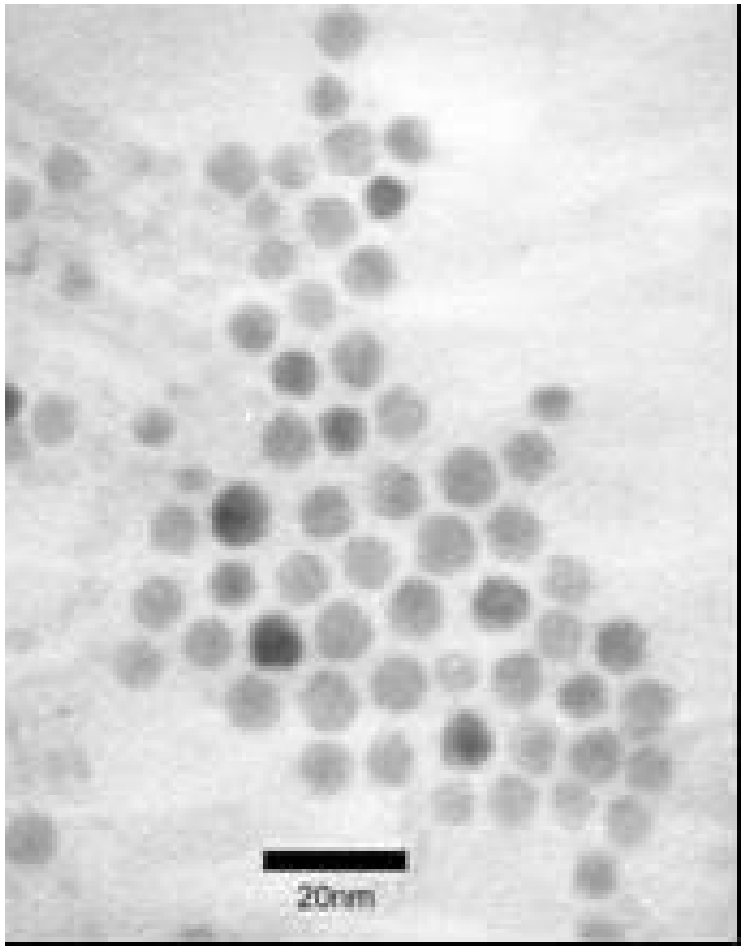


ZnS as before but at 180 º C

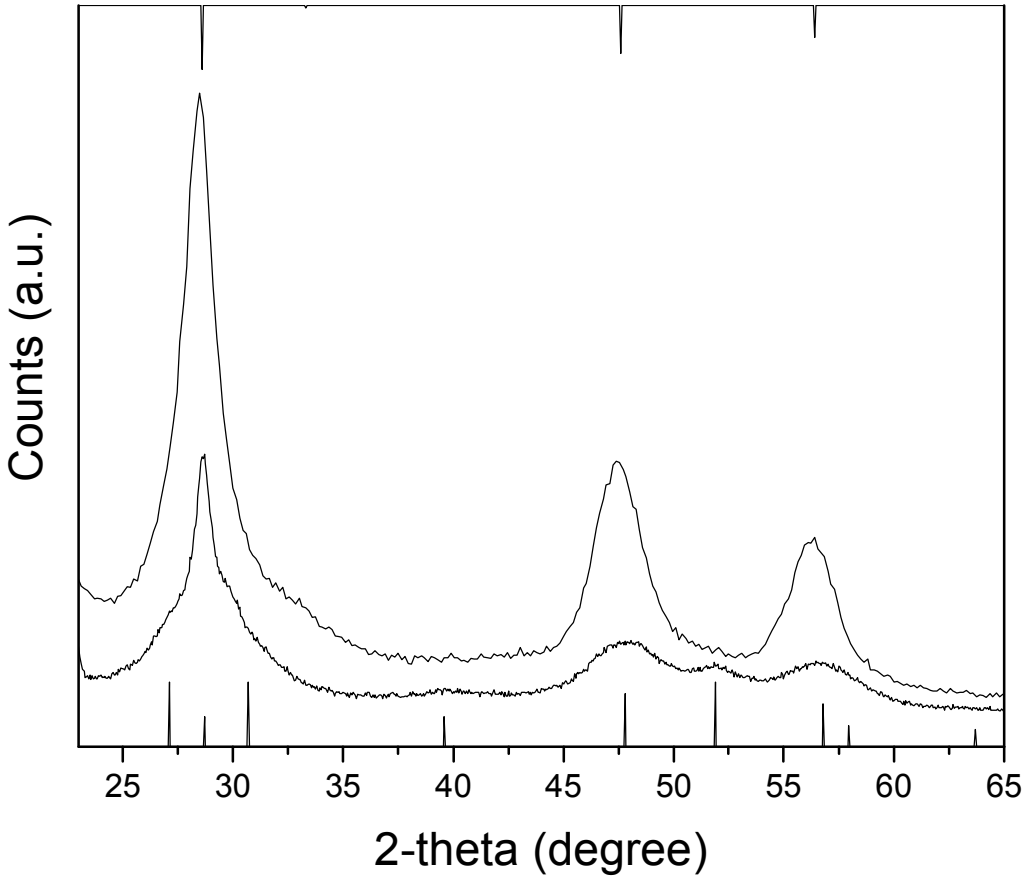


XRPD of ZnS (a) rods grown at 140$^{o}$C and (b)dots grown at 180$^{o}$C. Also shown are the bulk indices for hexagonal (below) and cubic (top).

# Structure of Talk

- Looking at some nanodimensional objects
- Synthetic approaches zinc oxide and doping
- How nanoparticles grow and
- Rods
- **Assemblies of nanoparticles and mesoscopic objects**
- Closing remarks

# *Self Assembly of Inorganic Building Block*

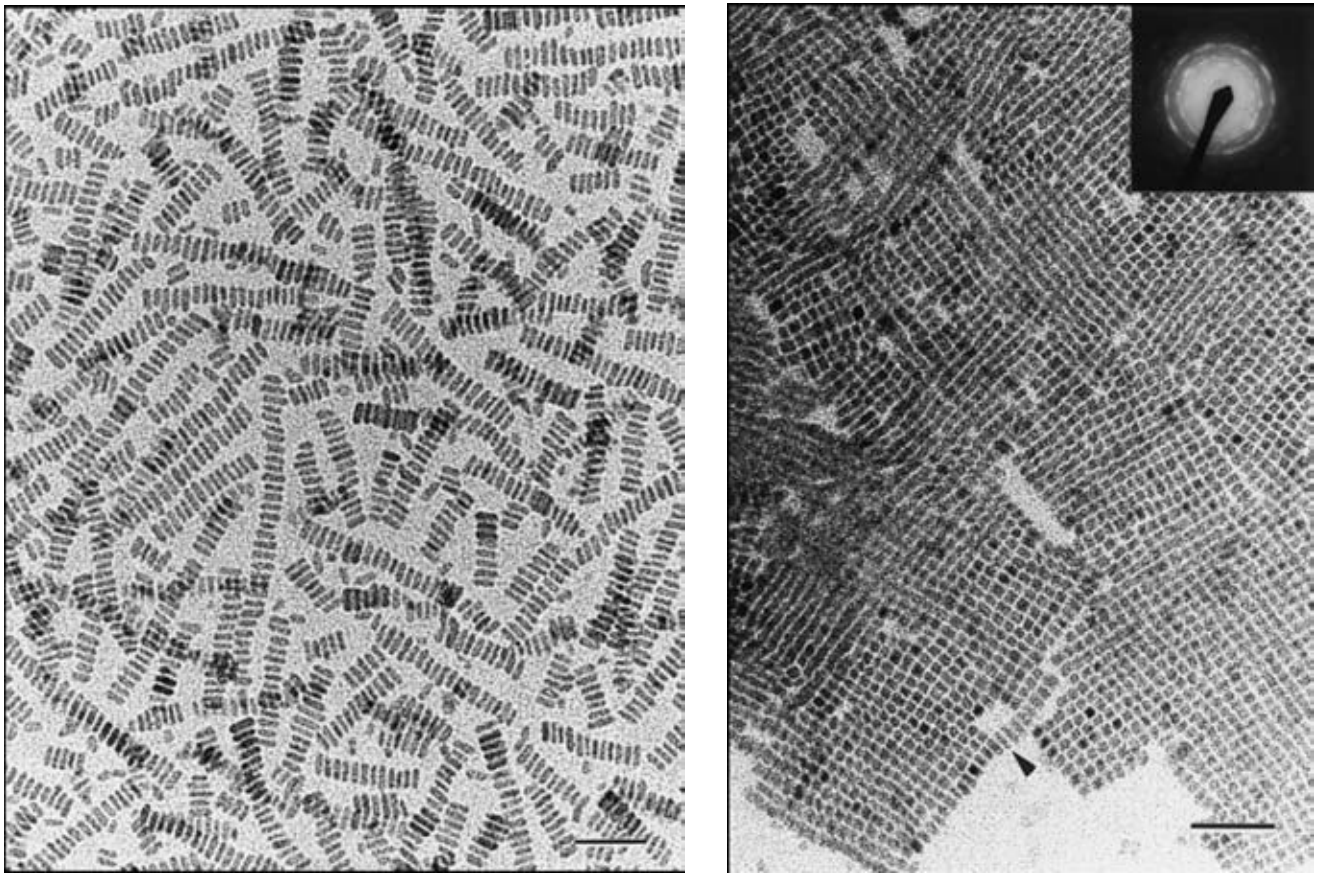

***Left: TEM image showing ordered chains of prismatic BaCrO4 nanoparticles; Right: Rectangular superlattice of BaCrO4 nanoparticles. Scale bar = 50 nm.***

*Mei Li, Heimo Schnablegger and Stephen Mann, Nature, 1999*

# *Self Assembly of Colloidal Spheres*

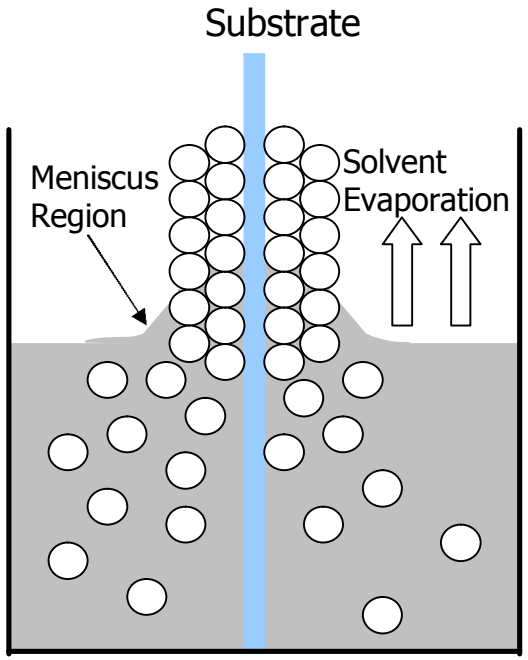


***Schematic of Evaporation-Induced Self-Assembly***

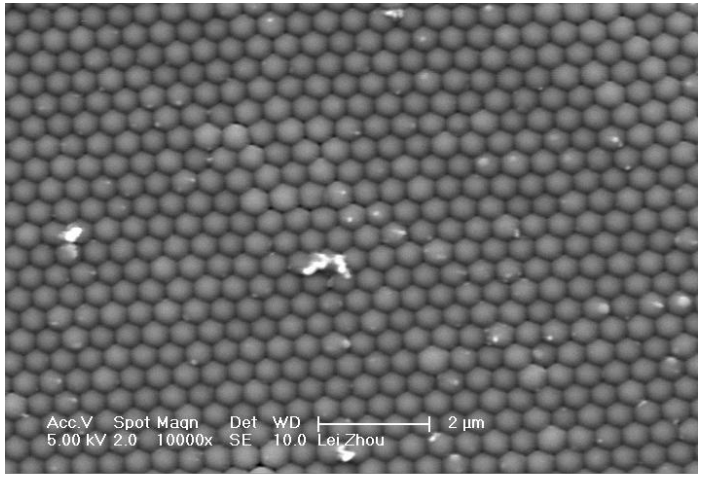


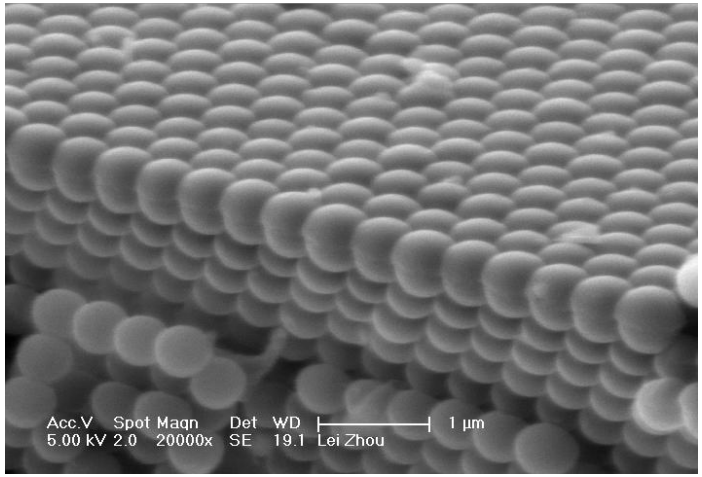


***Colloidal Crystal Templates (Polystyrene) Prepared by Evaporation-Induced Self-Assembly Method***

# *Reaction in Chemical Bath Deposition*

## Chemical bath deposition to prepare CdS films

| | | |
|---|---|---|
| $NH_3$-$H_2O$ equilibrium: | $2NH_3+2H_2O \rightarrow 2NH_4^+ + 2OH^-$ | (1) |
| Dissociation of Cd complex: | $Cd(NH_3)_4^{2+} \rightarrow Cd^{2+}(aq)+4NH_3(aq)$ | (2) |
| Hydrolysis of thiourea: | $S=C(NH_2)_2+2OH^- \rightarrow S^{2-}(aq)+H_2NC\equiv N+2H_2O$ | (3) |
| Formation of CdS: | $Cd^{2+}(aq)+S^{2-}(aq) \rightarrow CdS(s)$ | (4) |

## Chemical bath deposition to prepare $TiO_2$ films

| | | |
|---|---|---|
| Hydrolysis of Ti complex: | $[TiF_6]^{2-} + nH_2O \rightarrow [TiF_{6-n}(OH)_n]^{2-} + nHF$ | (1) |
| Formation of $TiO_2$: | $[Ti(OH)_6]^{2-} + 2H^+ \rightarrow TiO_2 + 4H_2O$ | (2) |
| Removal of HF: | $H_3BO_3 + 4HF \rightarrow HBF_4 + 3H_2O$ | (3) |

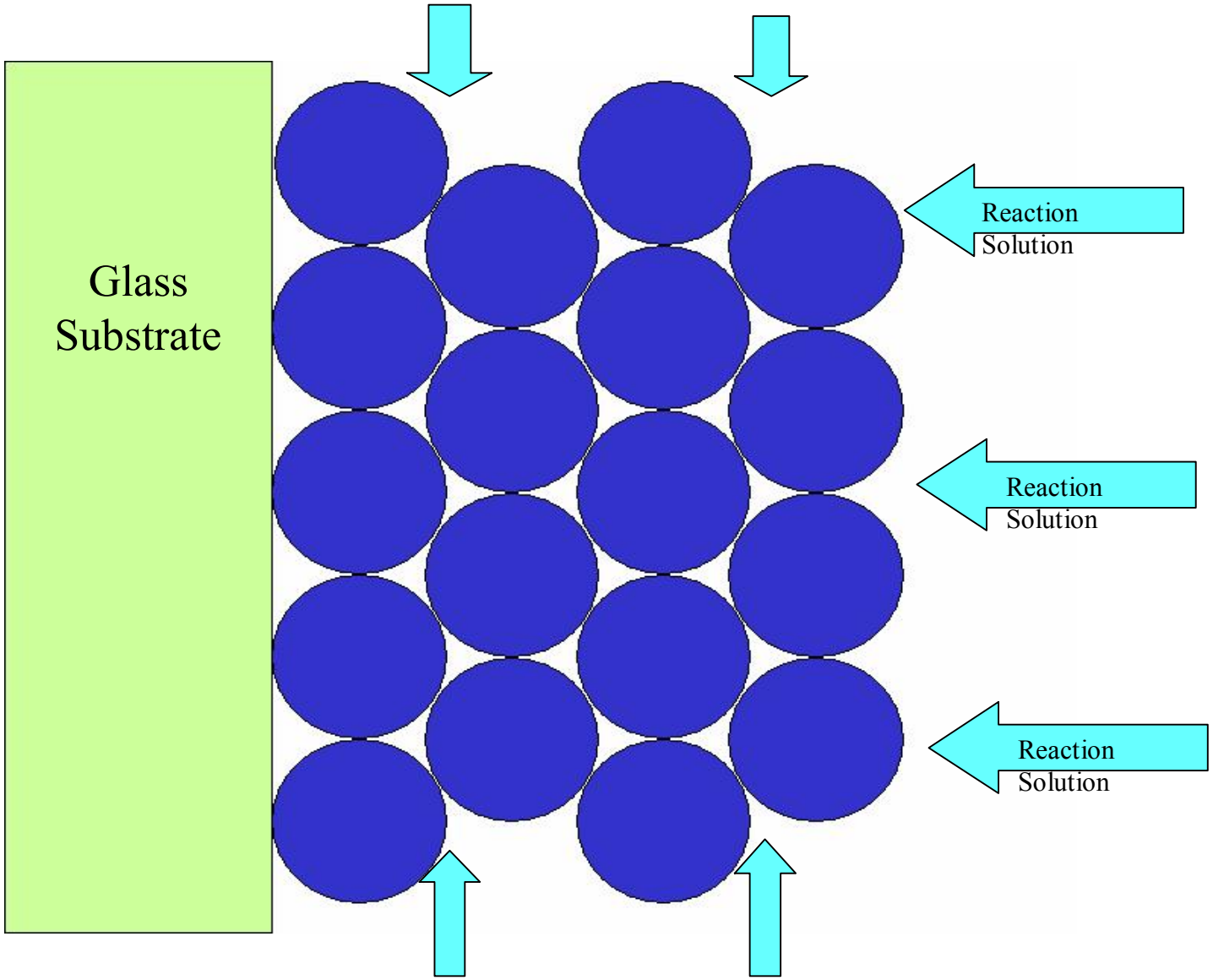
Glass Substrate
Reaction Solution
Reaction Solution
Reaction Solution

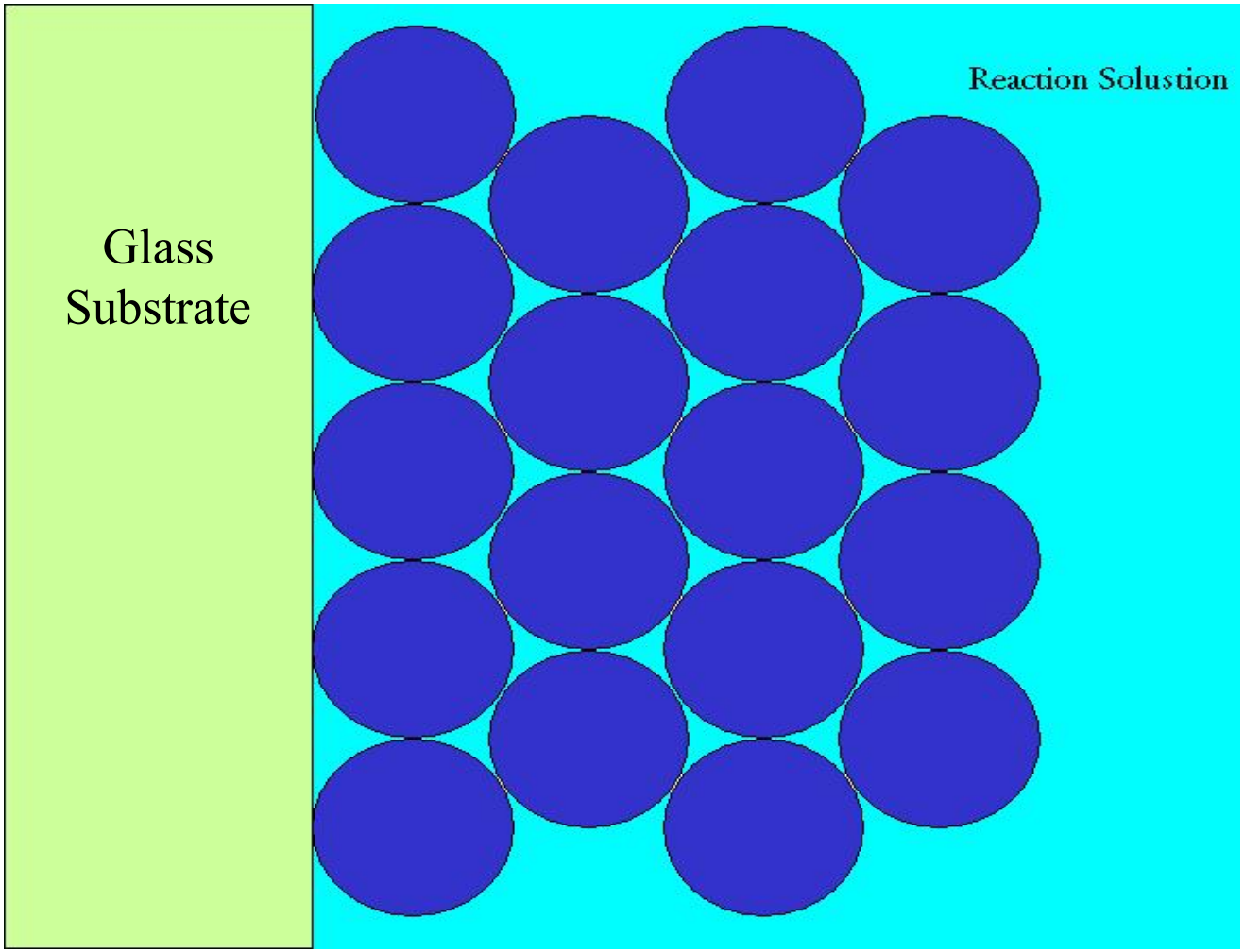


Because of capillary forces, the reaction solution penetrates the voids of the template

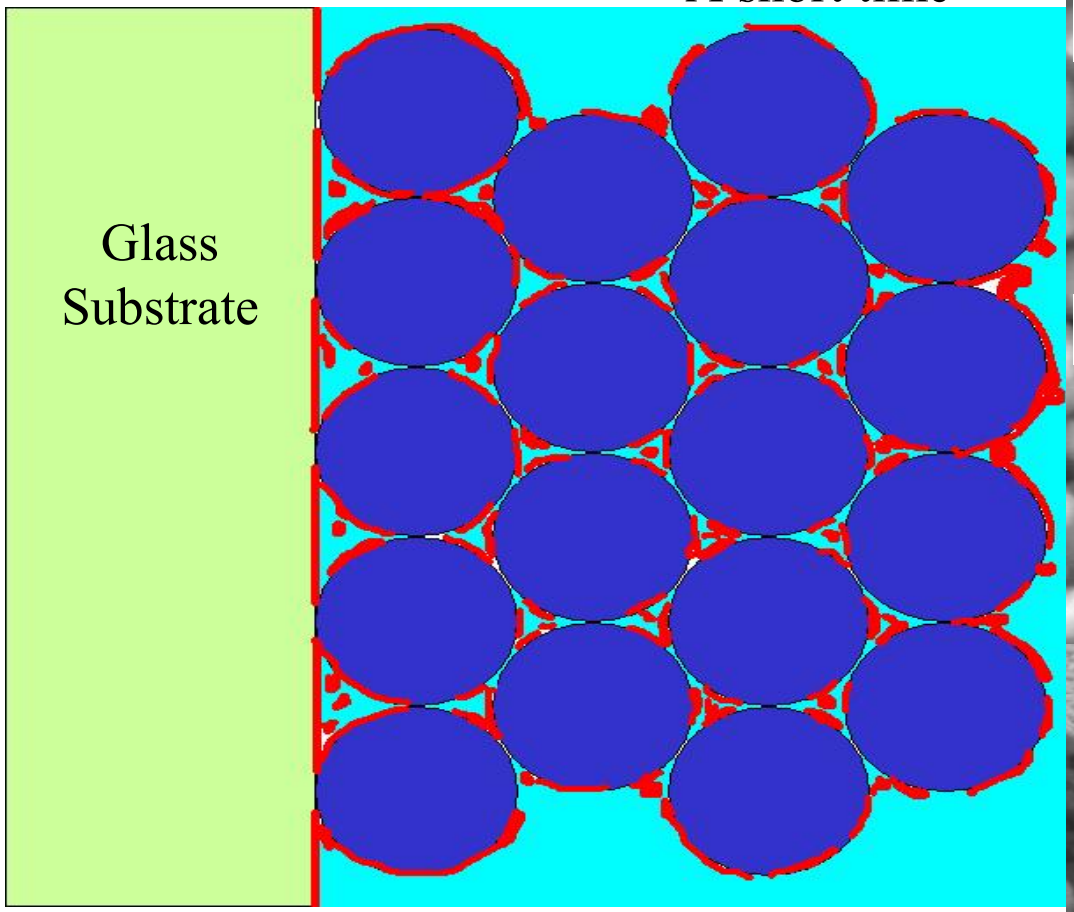



Homogeneous deposition produce the particle in the voids, heterogeneous depositions produce the particles or films on the surface of SiO2 beads.

A long time

Glass Substrate

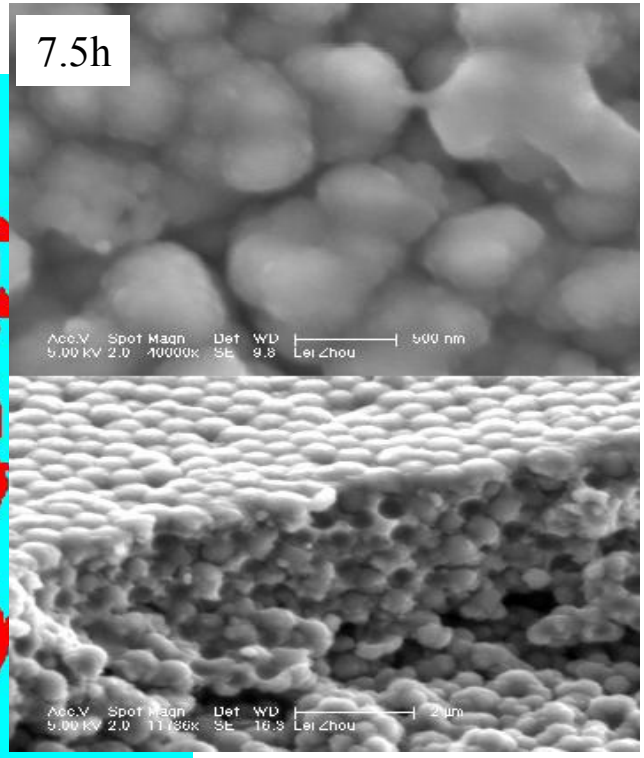

# *Choice of Colloidal Crystal Templates*

**Important Issues:**

- Quality of template
- Interaction between templates and substrate
- Interaction between templates and bath solution

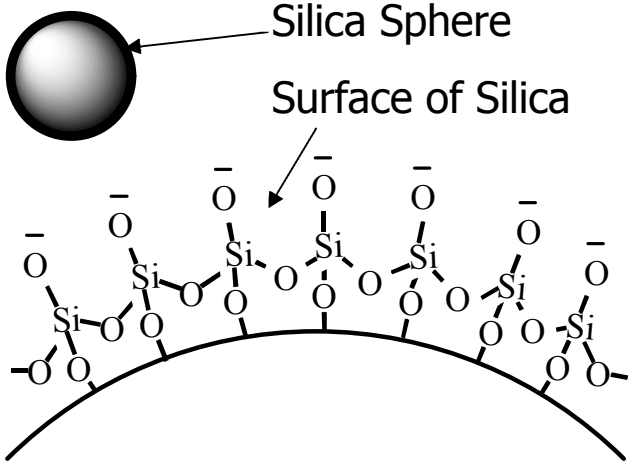


Schematic of hydrophilicity of silica surface

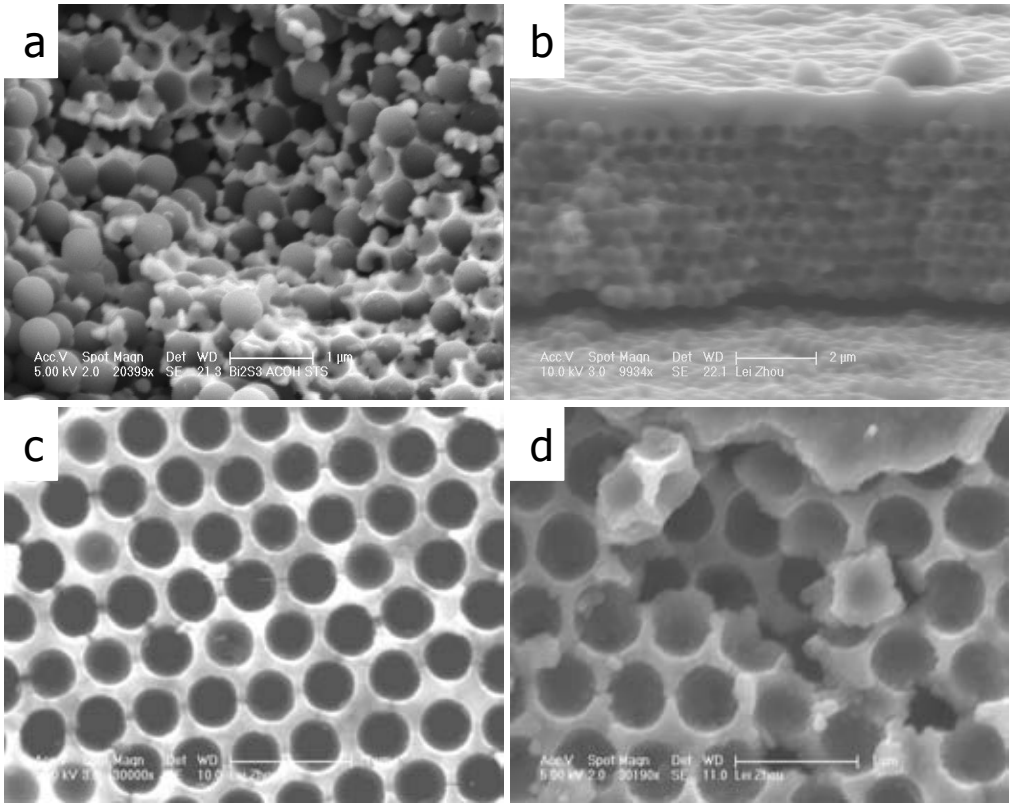


SEM images of composite films after infiltration and growth (8 h) of $TiO_2$ in porous templates *a*) Polystyrene and *b*) $SiO_2$ colloids. Removal of templates shown in c) polystyrene and d) $SiO_2$ leads to formation of macroporous films

# Enhanced Infiltration Using Multi-Cycles

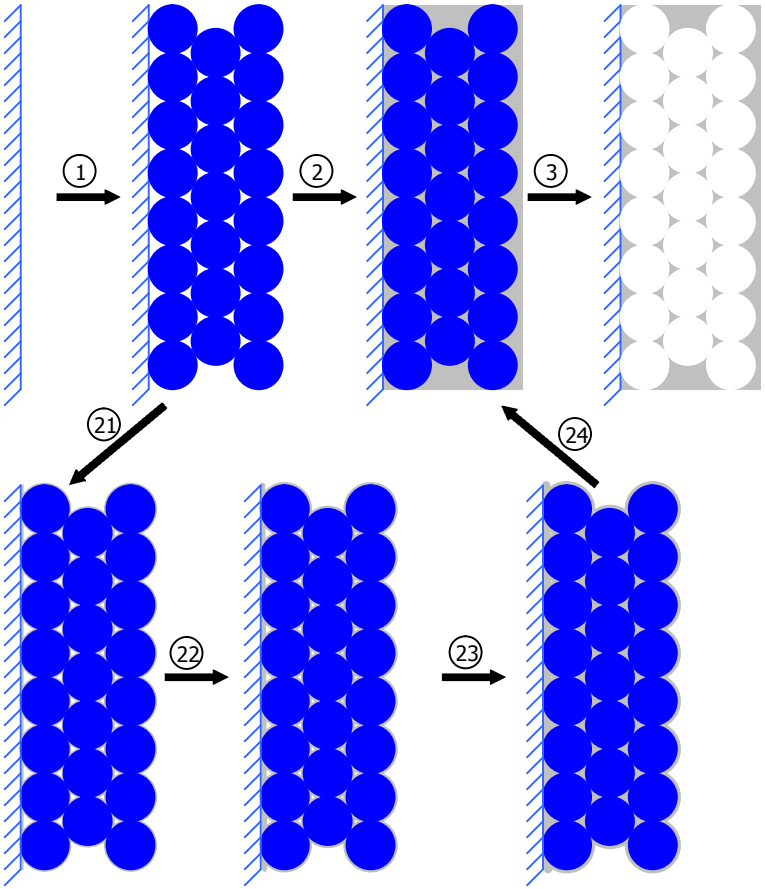


*Schematic of infiltration of multi-step infill-rinse-sinter cycles*

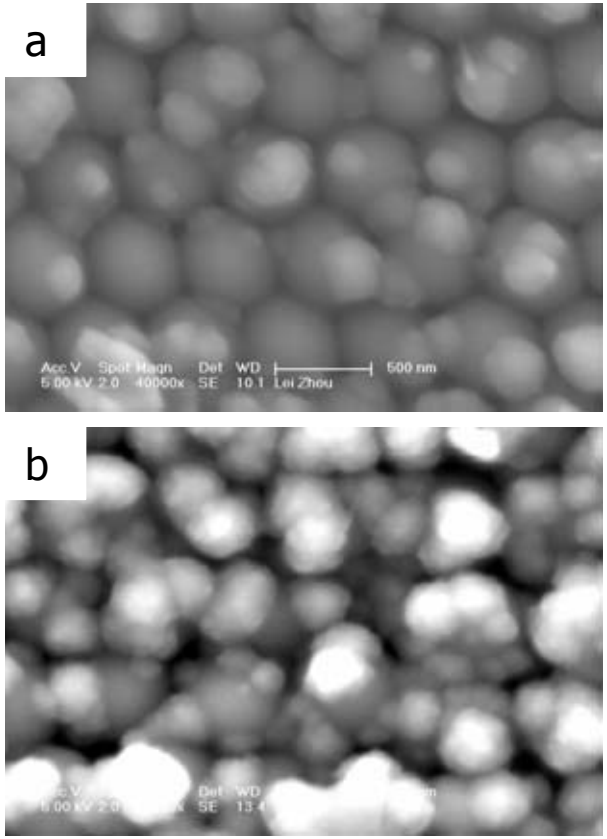


*SEM images of $SiO_2$ templates after infiltration by $TiO_2$. a. two infill-rinse-sinter circles; b.single step infiltration (4 h) and rinse-sinter steps.*

# *Monitor Infiltration Progress Using SEM*

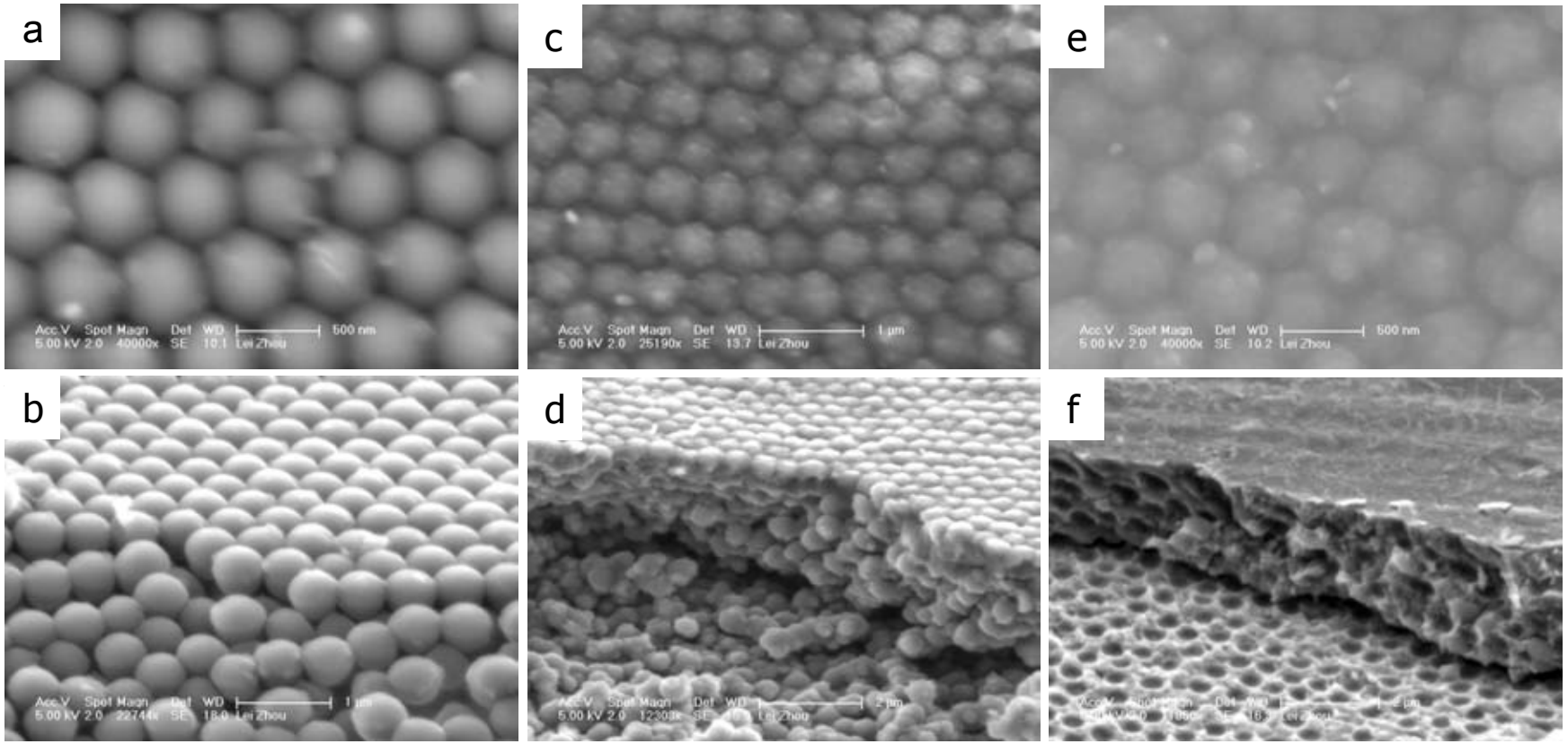


***Evolution of the infiltration process. SEM images (top view and cross section) of template layers after single (a,b), three (c,d) and four (e,f) cycles.***

# Morphology and Crystallinity of Films

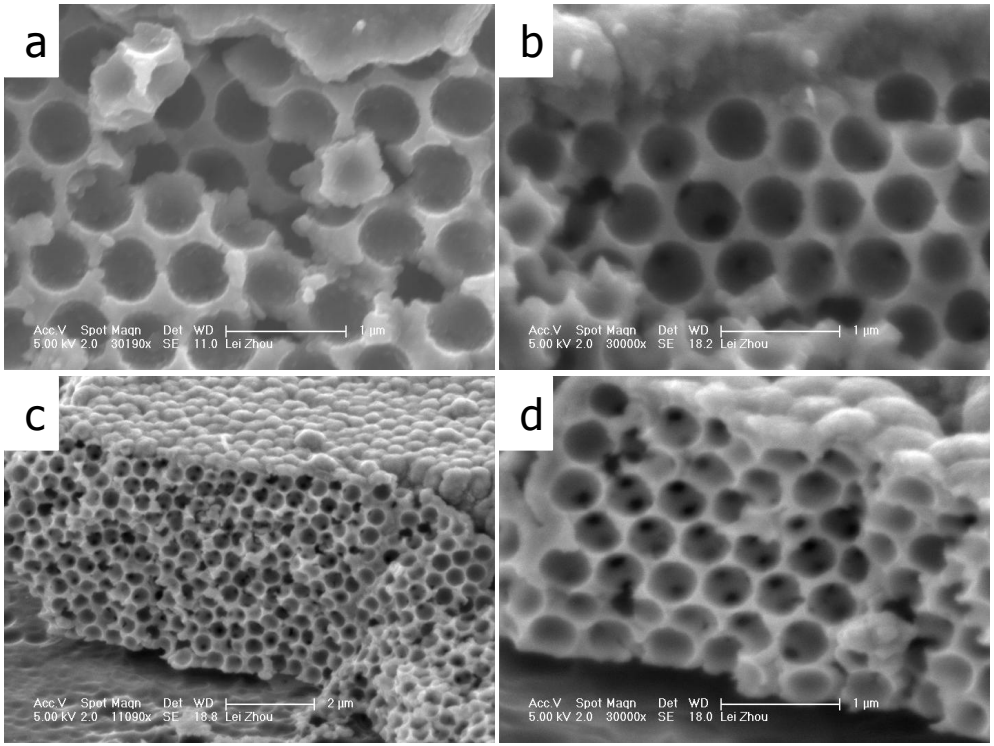


***SEM images of macroporous films. a. Top view. and b. cross section of macroporous $TiO_2$ films (template comprising 523.5 nm $SiO_2$ spheres) and c. low mag. (x 11K) and d. high mag. (x 30K) cross section of macroporous CdS films (template comprising 435.5 nm $SiO_2$ spheres).***

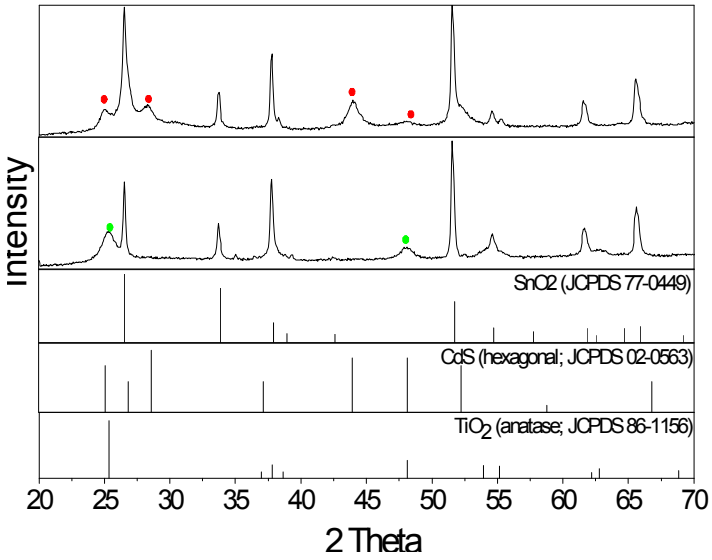


***XRD patterns obtained for macroporous. a) CdS (hexagonal; JCPDS 02-0563); b) $TiO_2$ (anatase; JCPDS 86-1156) films***

# TEM Images of Macroporous Films

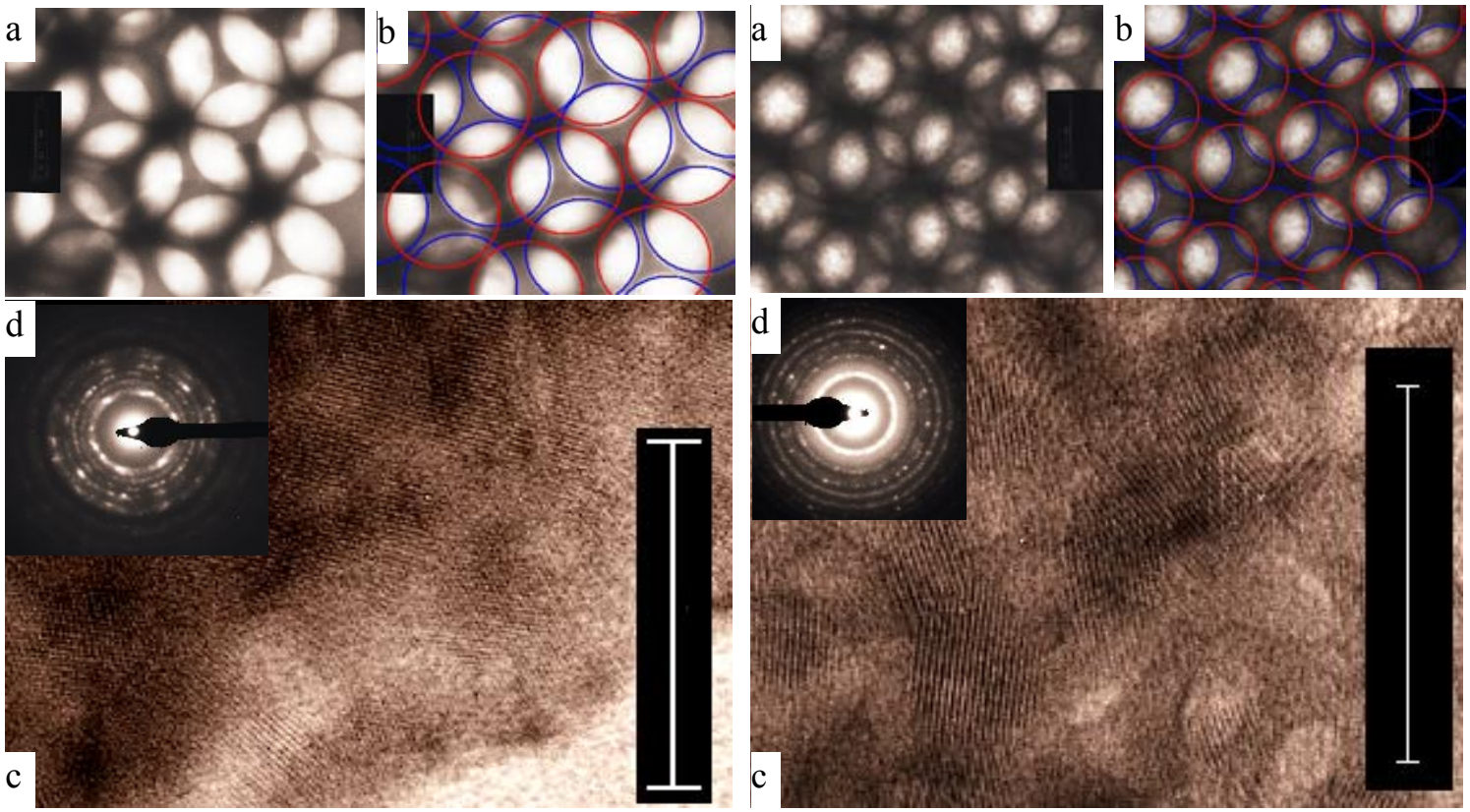


***Left: TEM images obtained from delaminated macroporous CdS films; Right: TEM images obtained from delaminated macroporous $TiO_2$ films.***

# Photonic Properties of Films

## Basic Diffraction: Bragg Equation:

$$\lambda = 2(2/3)^{0.5} D (n_e^2 - \sin^2\theta)^{0.5}$$

*In process of infiltration:* $n_e^2 = (0.26-f)n_{air}^2 + 0.74n_{SiO2}^2 + fn_{CdS}^2$

*After removal of templates:* $n_e^2 = (1-f)n_{air}^2 + fn_{CdS}^2$

*f is filling fraction, varies from 0 to 0.26*

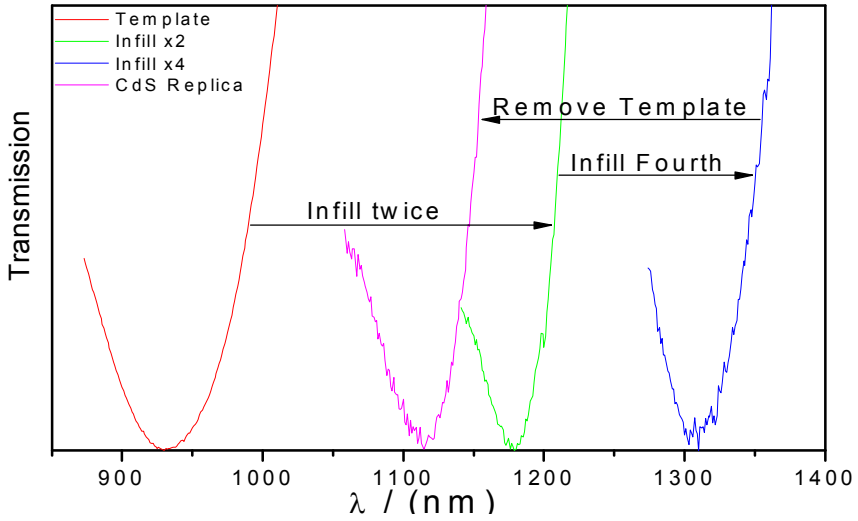


*Optical transmission spectra of films as a function of degree of infiltration.*

| Times of infiltration | Tem plate | Twice | Four times | Inver se opal |
|---|---|---|---|---|
| Real Position of peak | 968 (nm) | 1178 (nm) | 1310 (nm) | 1115 (nm) |
| Filling fraction | 0 | 0.173 | 0.28 | 0.27 |

*Bragg peak position as a function of CdS filling factor (435.5 nm $SiO_2$ spheres)*

Mesoporous uniform mesoscopic objects composed of $NH_4TiOF_3$ or $TiO_2$ particles by self-assembly using solution method at room temperature

# Experiment and Reaction

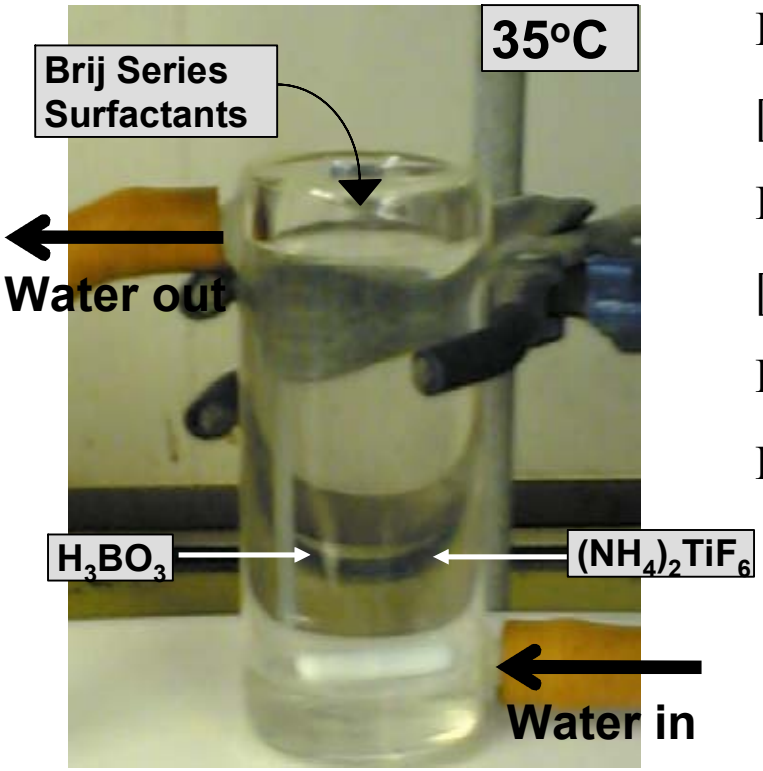


Schematic of Experiment

**Incomplete hydrolysis of Ti complex:**

$$[TiF_6]^{2-} + nH_2O \rightleftarrows [TiF_{6-n}(OH)_n]^{2-} + nHF \ (n \leqq 3)$$

**Formation of $NH_4TiOF_3$:**

$$[TiF_3(OH)_3]^{2-} + H^+ + NH_4^+ \rightarrow NH_4TiOF_3\downarrow + 2H_2O$$

**Removal of HF:**

$$H_3BO_3 + 4HF \rightarrow HBF_4 + 3H_2O$$

e.g. 15 g of Brij 58 is added into the 50 ml bath solution containing $(NH_4)_2TiF_6$ (0.1 mol·dm$^{-3}$) and $H_3BO_3$ (0.2 mol·dm$^{-3}$).

# Uniform particles

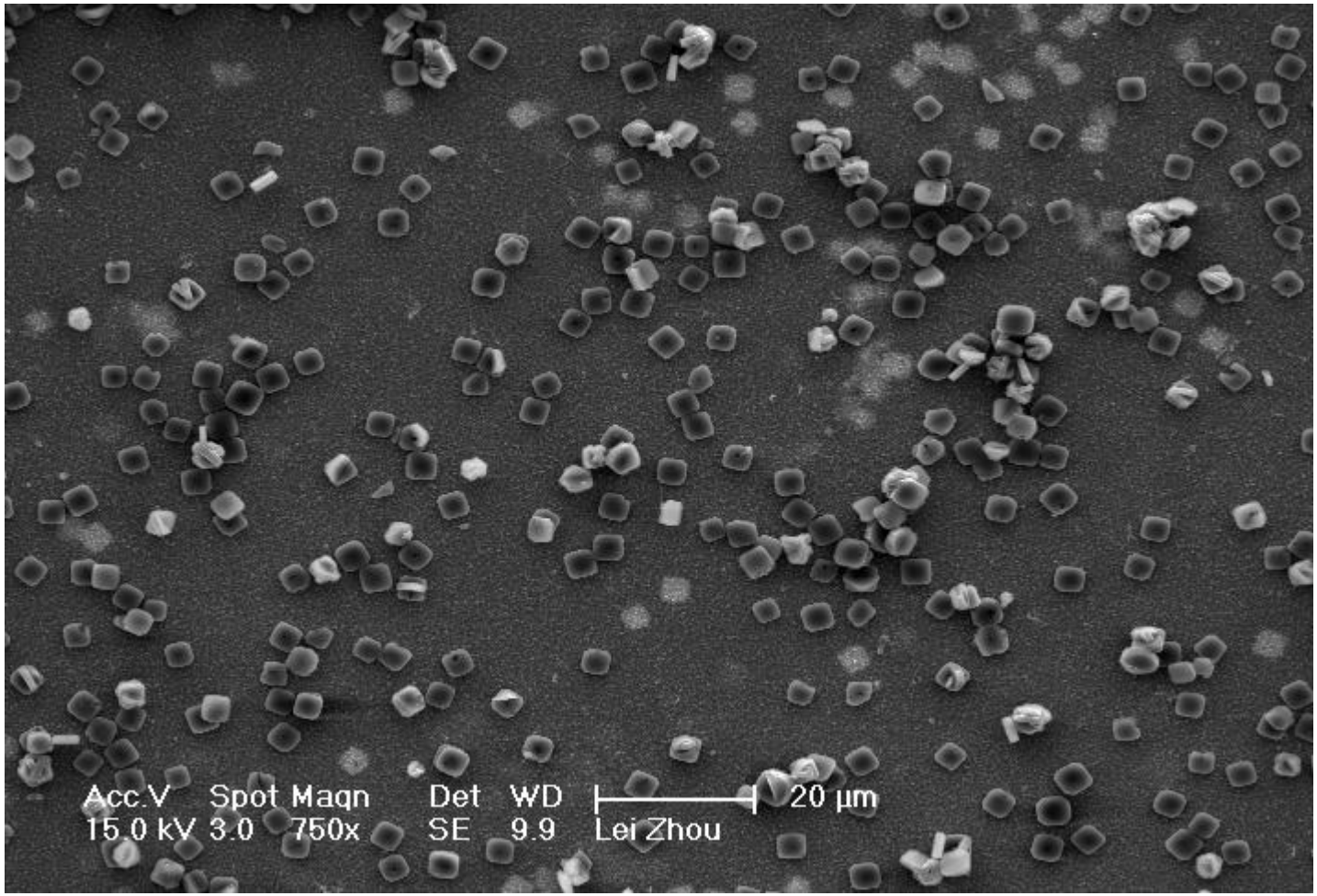


Low magnification SEM image of particles precipitated in presence of Brij 58

# Impact of different surfactants on the shape

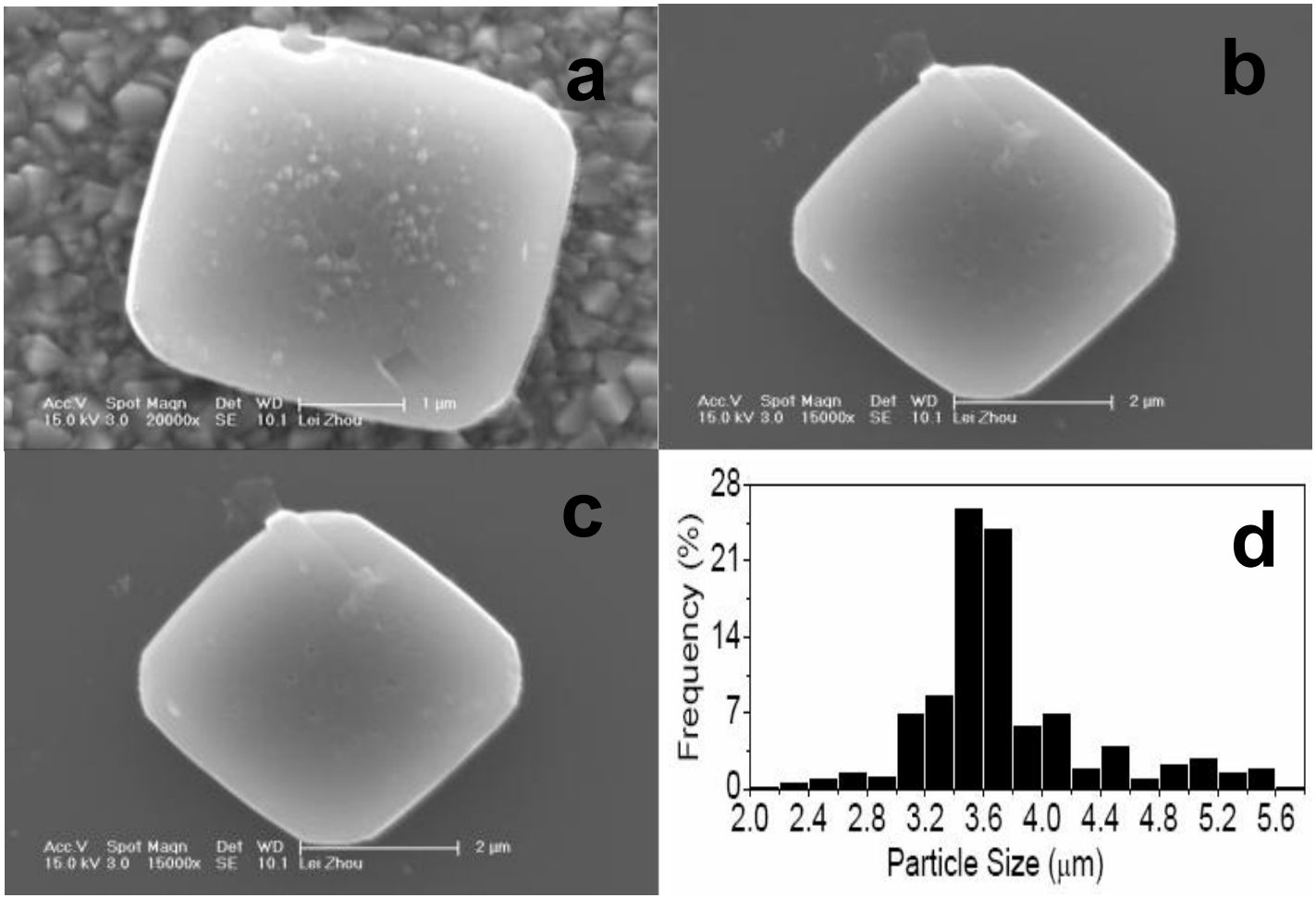


Mesoporous $NH_4TiOF_3$ single crystalline particles with regular shape a. 17.5% Brij 56 ($C_{16}H_{33}(OCH_2CH_2)_{10}OH$), b. 30% Brij 58 ($C_{16}H_{33}(OCH_2CH_2)_{20}OH$) c. 20% Brij 700 ($C_{18}H_{37}(OCH_2CH_2)_{100}OH$), d size distribution of samples prepared in presence of 30% Brij 58 , all at 35 ˚C

# Diagram of Surfactant

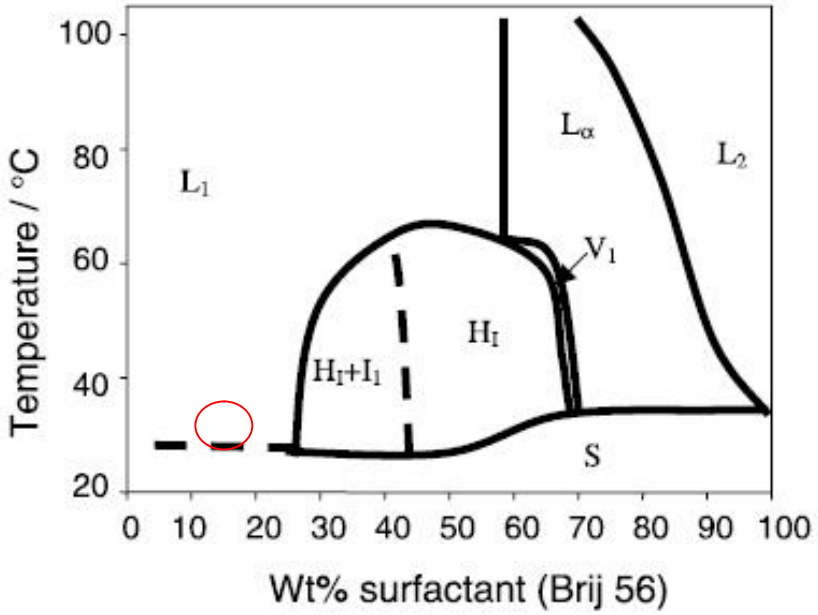


**General Formula of Brij Series Surfactant:**

$C_nH_{2n+1}(OCH_2CH_2)_mOH$

**Brij 56:** $C_{16}H_{33}(OCH_2CH_2)_{10}OH$ (14.9wt%)

**Brij 58:** $C_{16}H_{33}(OCH_2CH_2)_{20}OH$ (23.1wt%)

**Brij 700:** $C_{18}H_{37}(OCH_2CH_2)_{100}OH$ (16.7wt%)

Phase diagram for binary **Brij 56** + $H_2O$ system. Phase notation: S – solid, $L_1$ – micellar solution, $I_1$ – micellar cubic phase, $H_1$ – hexagonal phase, $V_1$ – cubic phase, $L_\alpha$ - lamellar phase and $L_2$ – inverse micellar solution. Ref: Microporous and Mesoporous Materials 44-45 (2001) 73-80

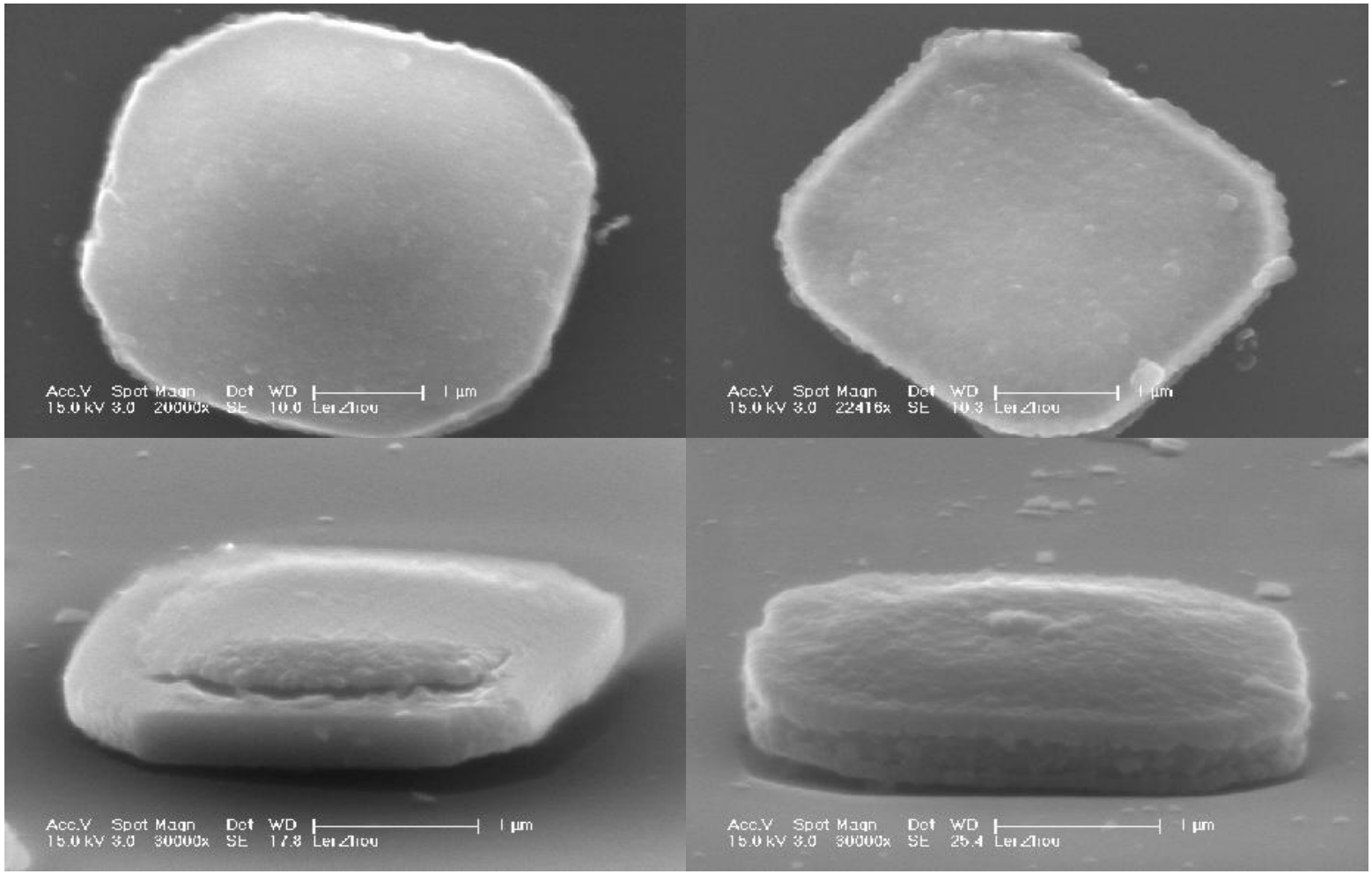


Brij 56 17%, before sintering (left), after sintering (right)

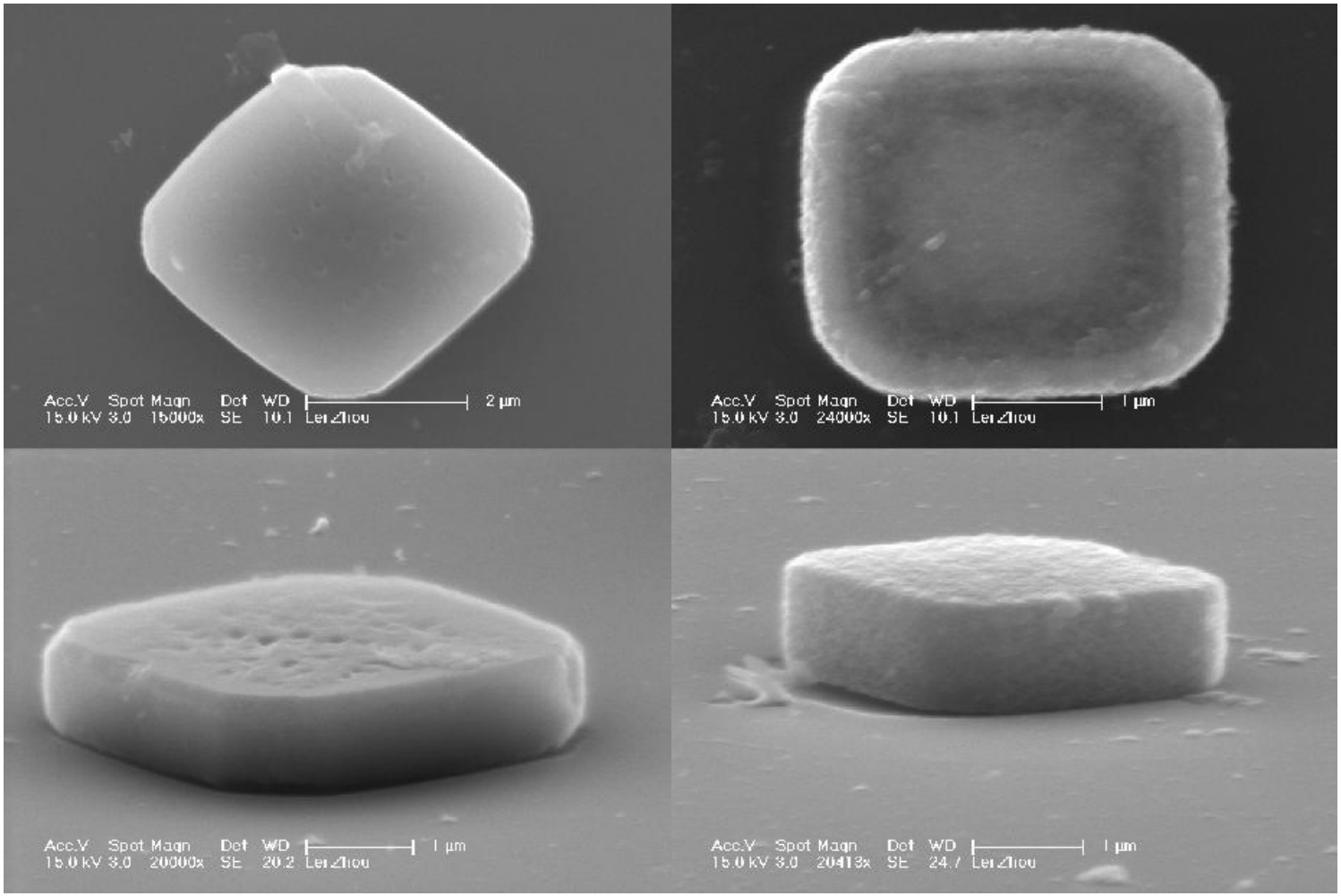


Brij 58 30%, before sintering (left), after sintering (right)

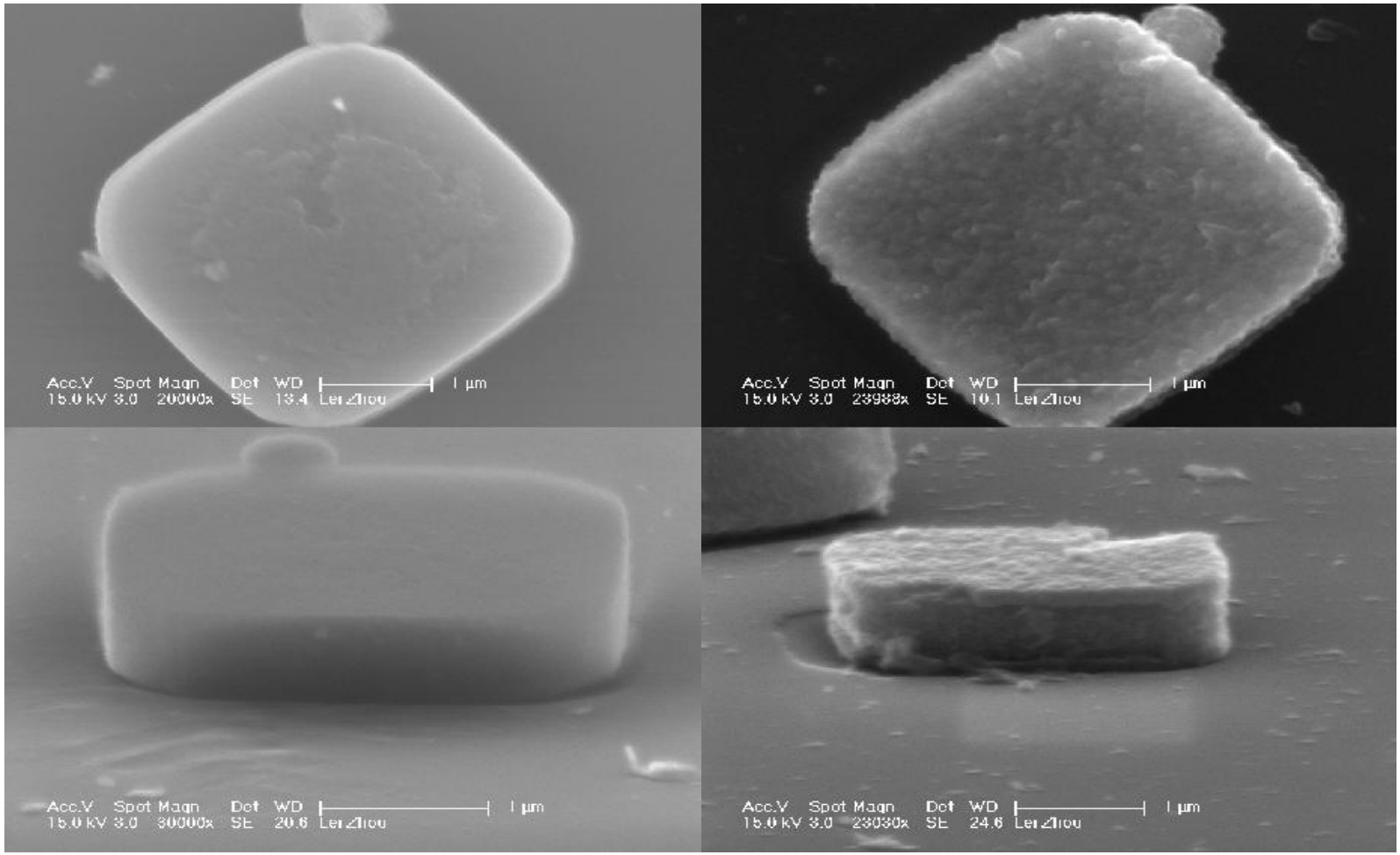


Brij 700 30%, before sintering (left), after sintering (right)

# Impact of sintering on the morphology

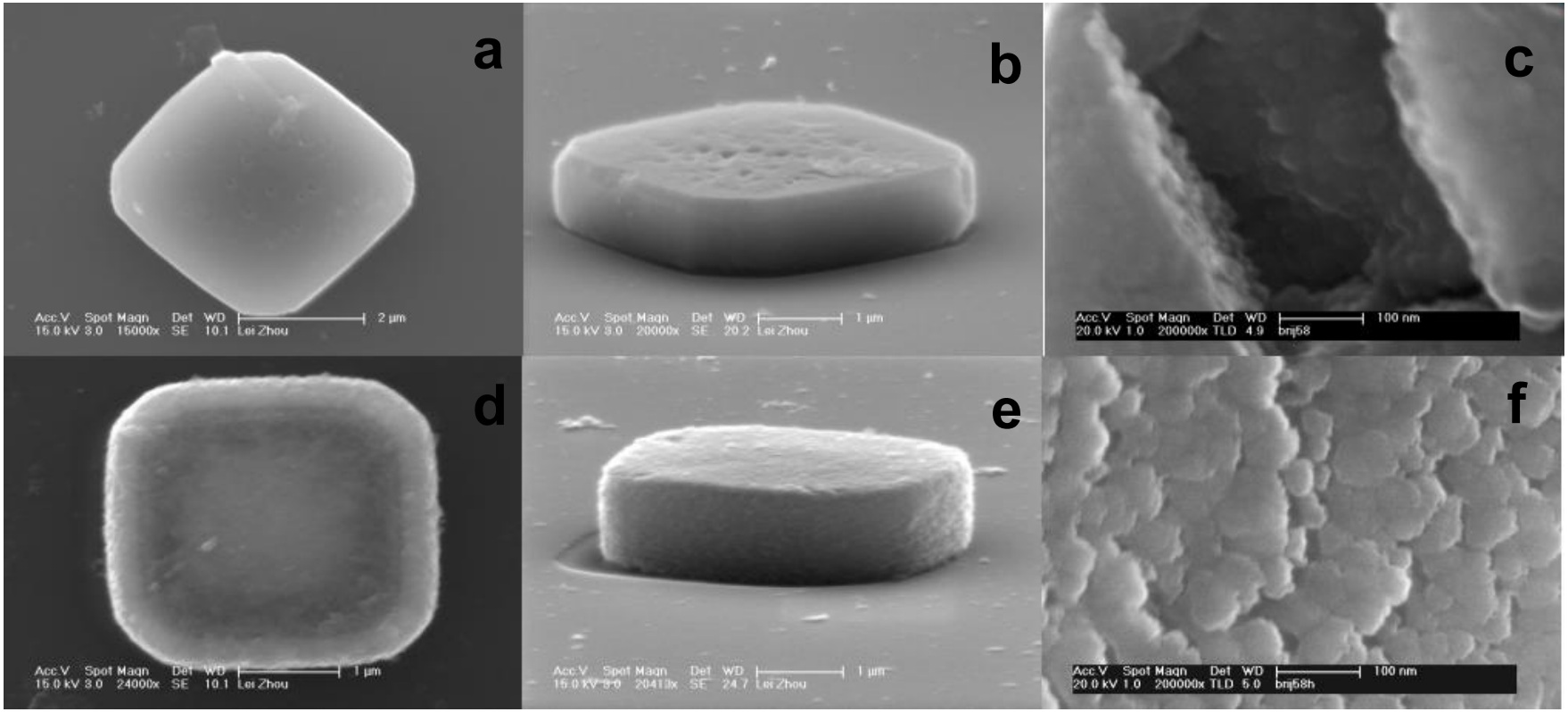


SEM images of samples before and after sintering. a, b, top view and cross-section of an as-prepared sample. c, ultrahigh resolution image of a broken point. d, e, top view and cross-section of after a sintered sample. f, ultrahigh resolution image of surface .

# XRD analysis of as-prepared and sintered samples

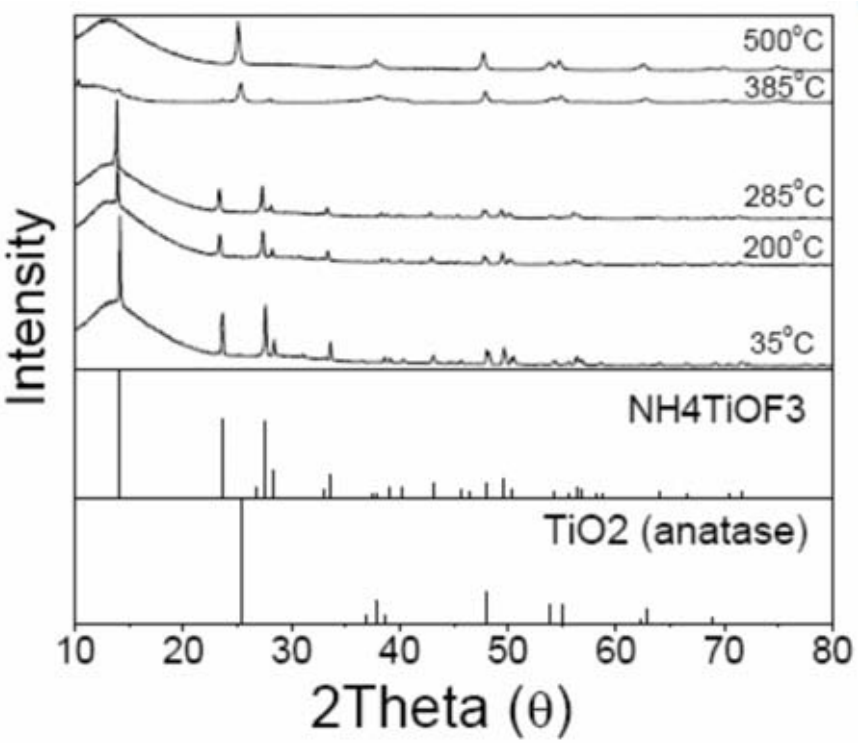


Broad-angle XRD Patterns of as-prepared and sintered samples.

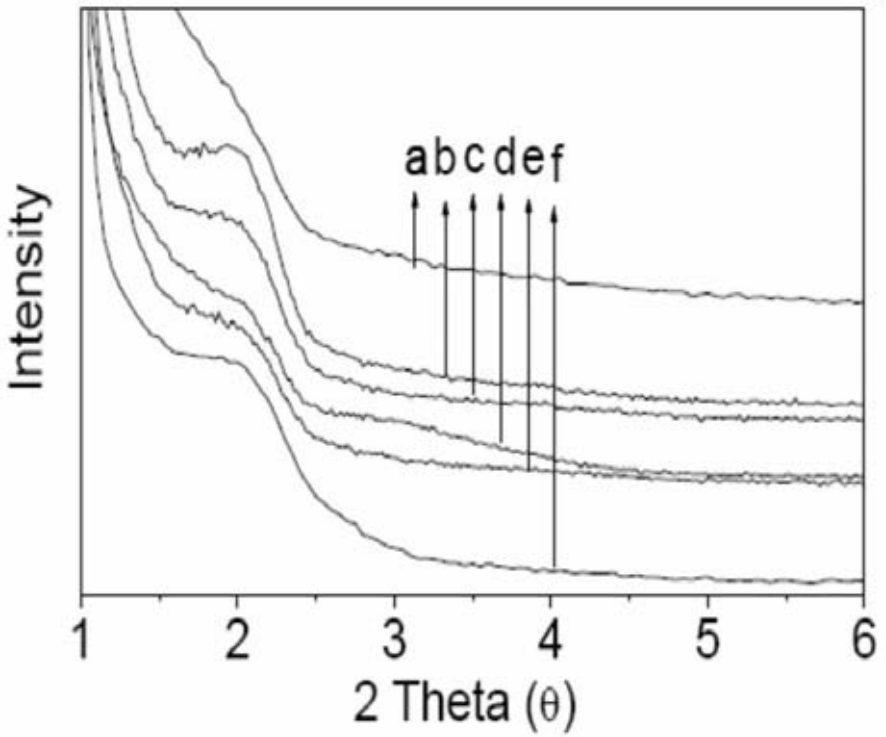


Small-angle XRD patterns of as-prepared and sintered samples. a, no surfactant. b, as-prepared. c, 200°C. d, 285°C. e, 385°C. f, 500°C.

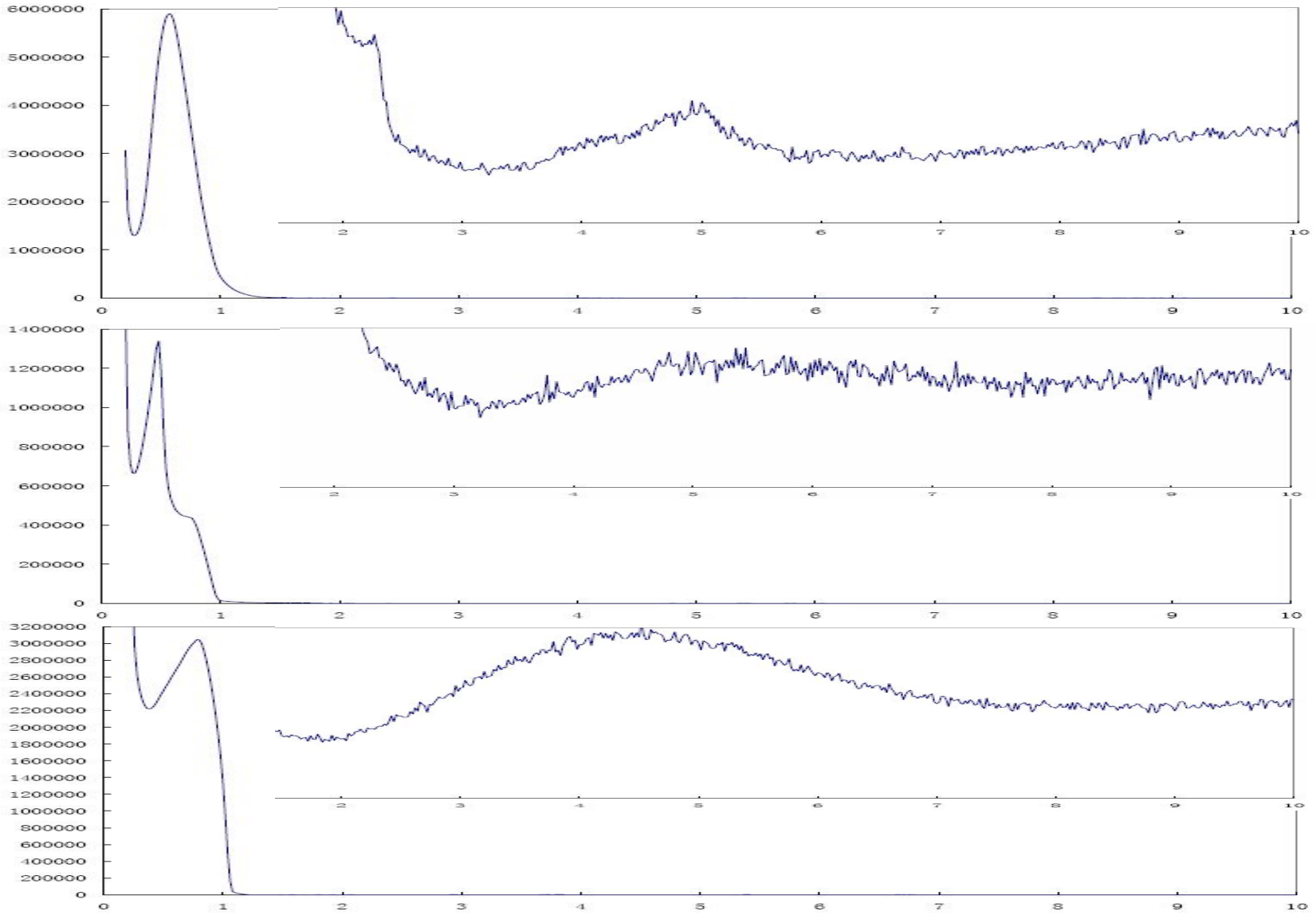


Low angle XRD, from up to down, pure Brij 58, the particles prepared under Brij 58 before sintering, and after sintering.

# TEM analysis of as-prepared samples

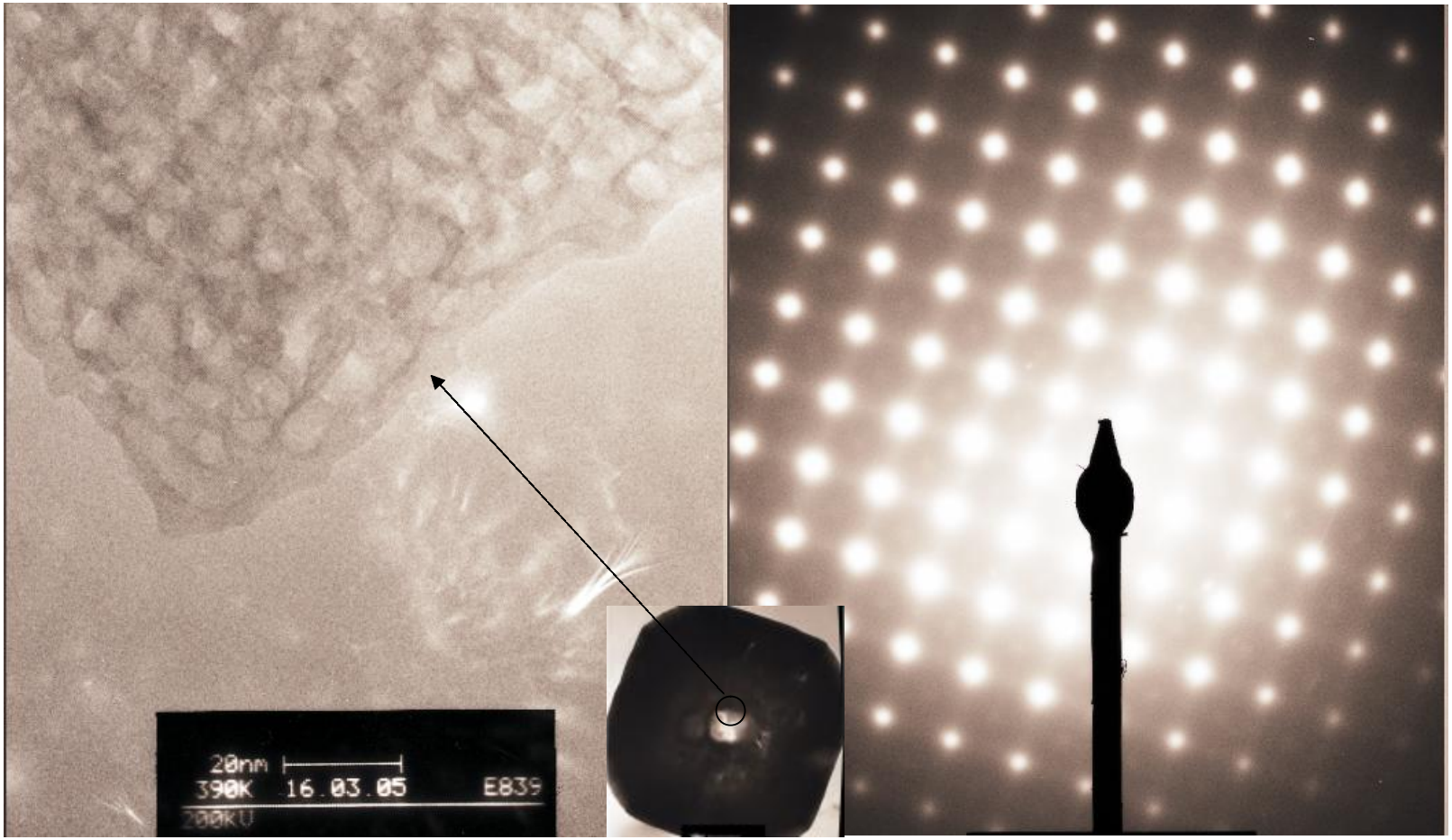


TEM images and SAED Pattern of as-prepared samples.

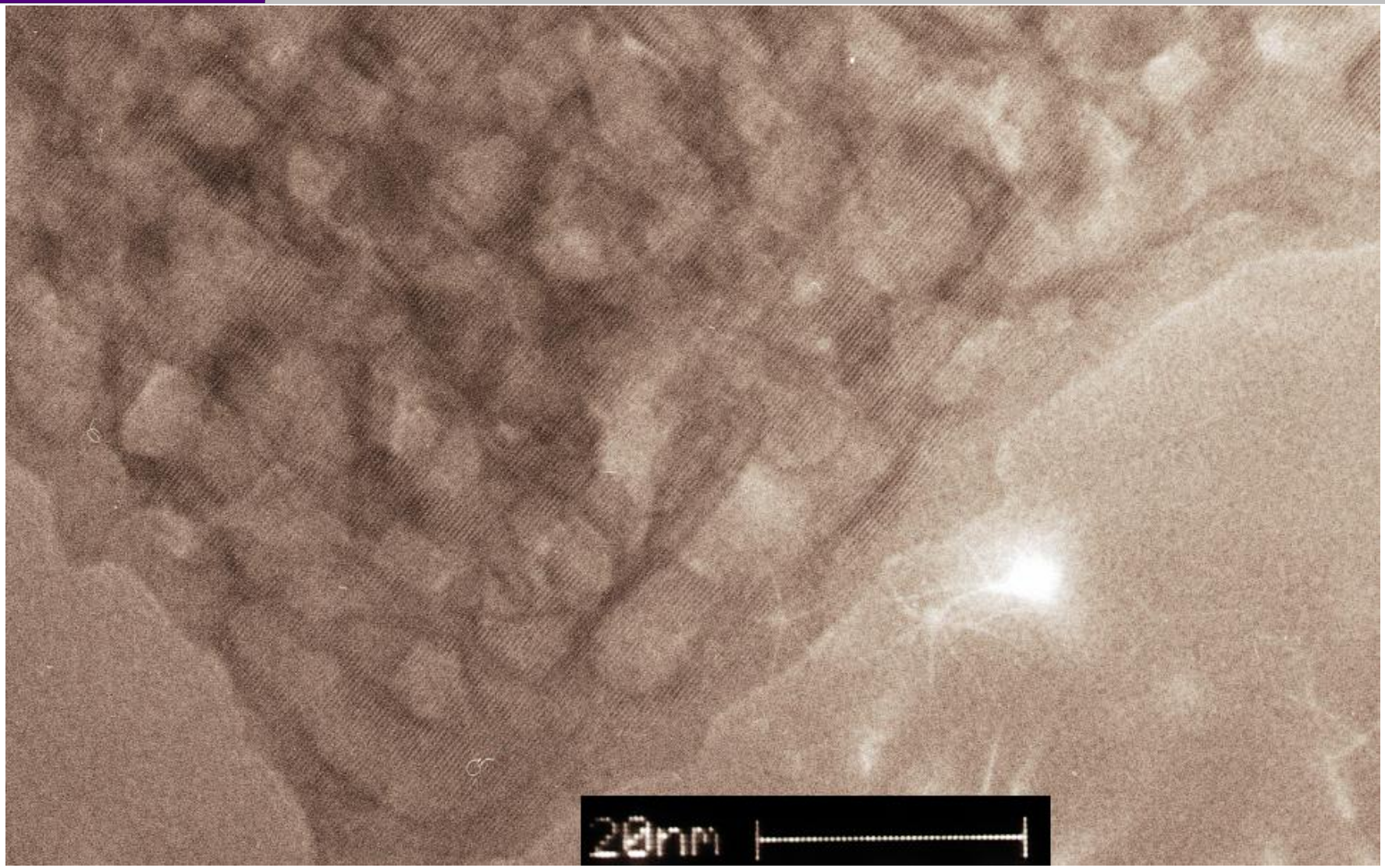


High resolution TEM image of as-prepared samples taken from the broken point in the sample.

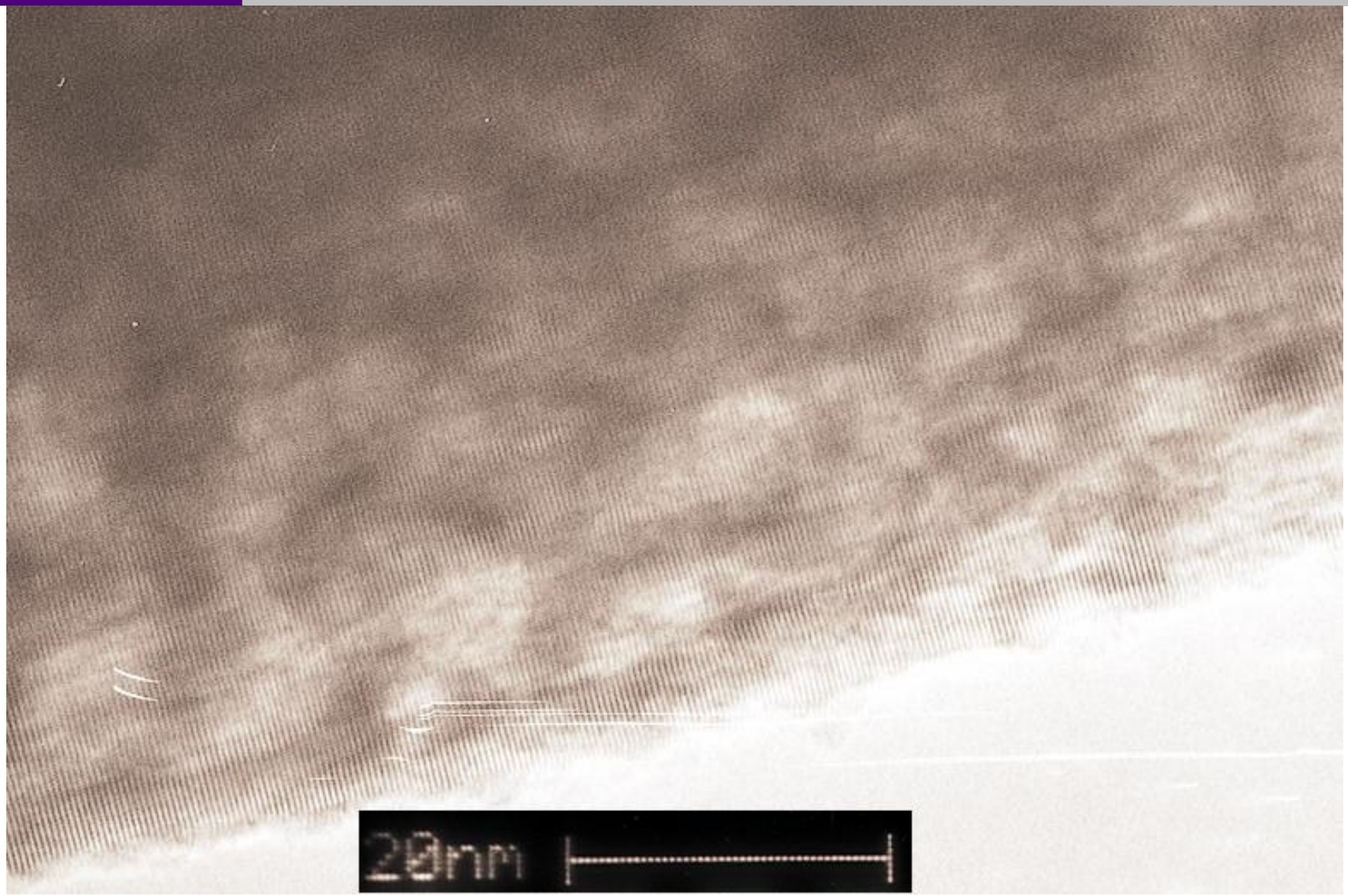


High resolution TEM image of as-prepared samples taken from the edge point in the sample.

Particles Prepared with 30% Brij58, after sintering

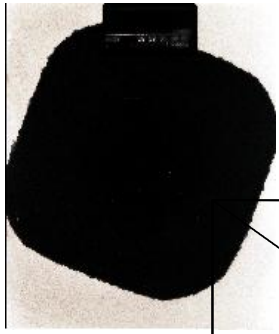

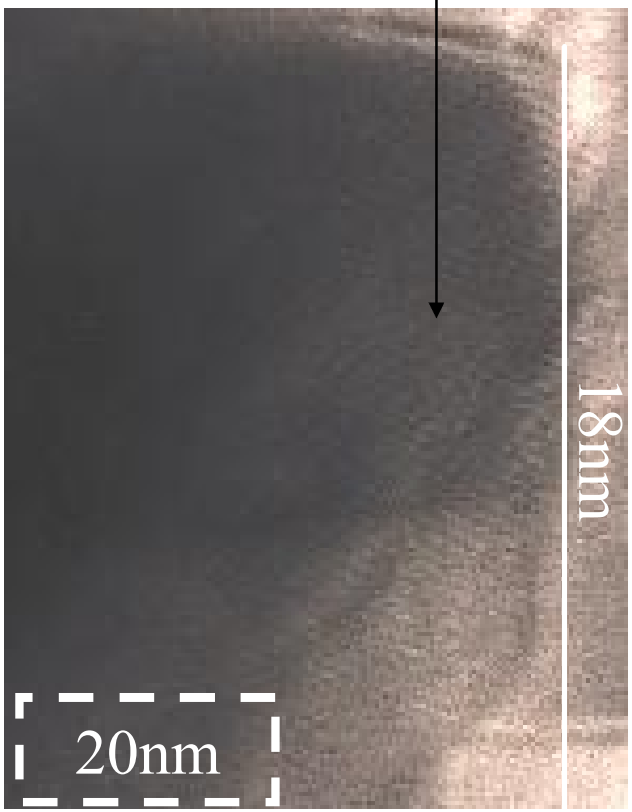


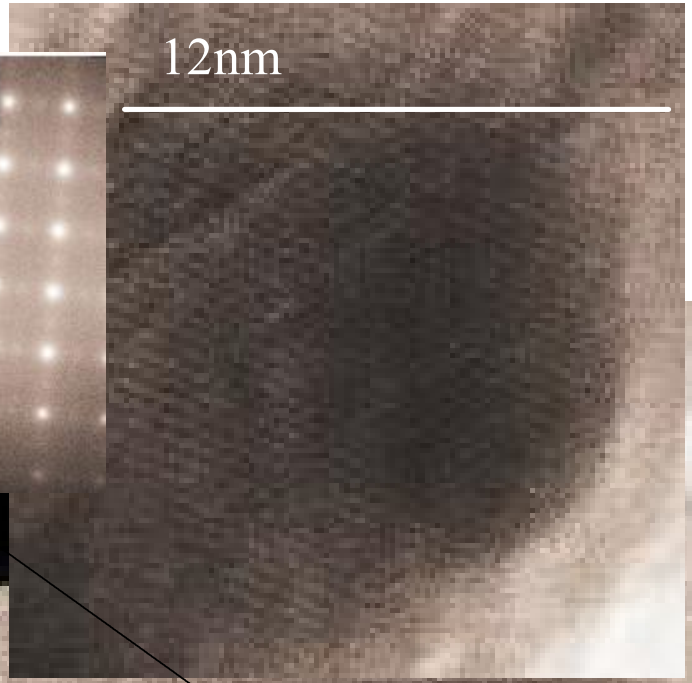


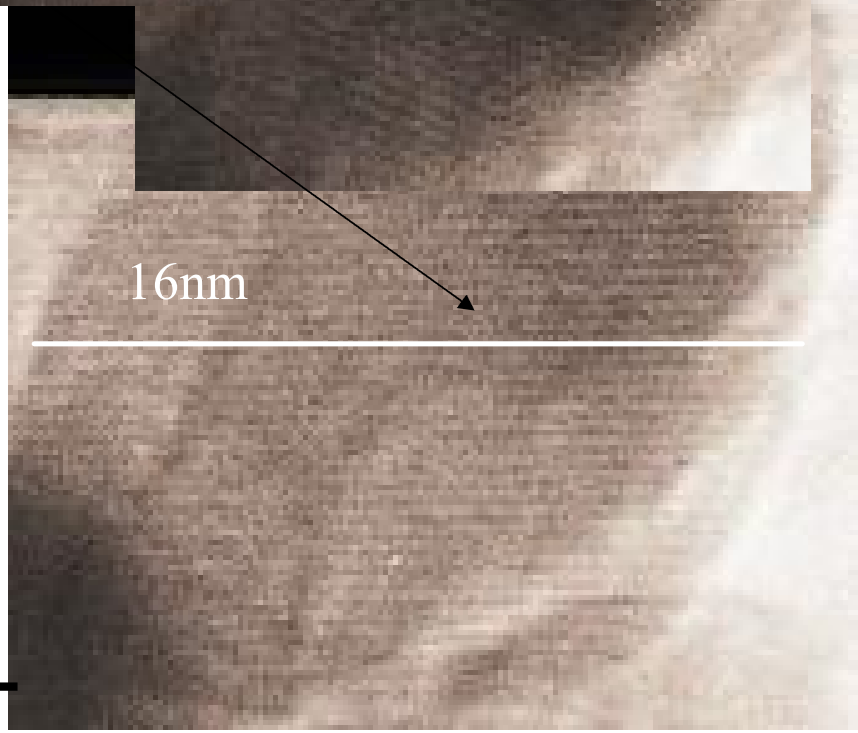

# TEM analysis of sintered samples

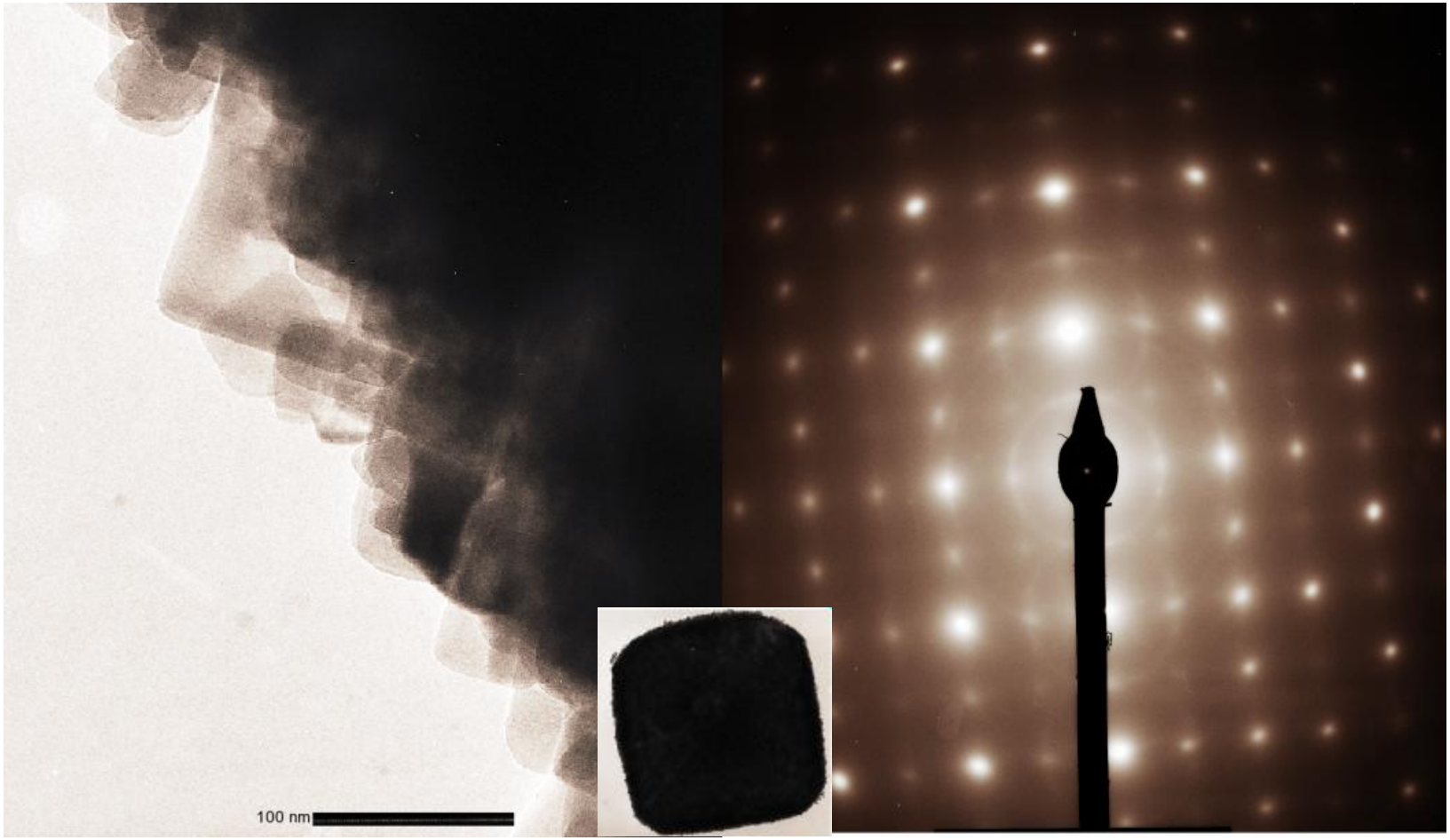


TEM images and SAED Pattern of sintered samples.


High resolution TEM image of sintered samples taken from the edge point in the sample.

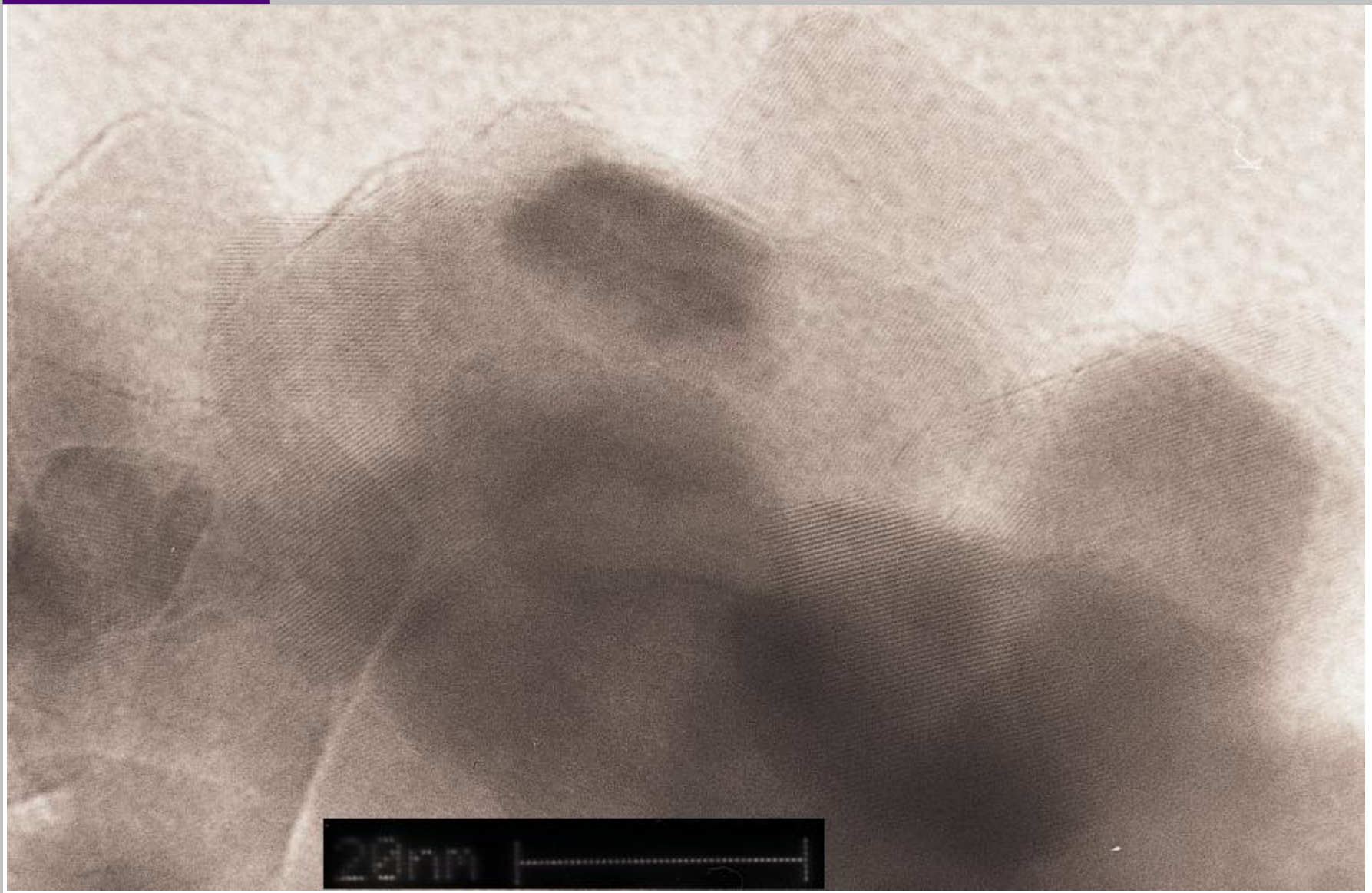


High resolution TEM image of sintered samples taken from the edge point in the sample.

# Impact of reaction time

TEM images of samples taken out at different reaction time. a, 2 hours. b, 8 hours. c, 24 hours. d, plot of particles vs reaction time.

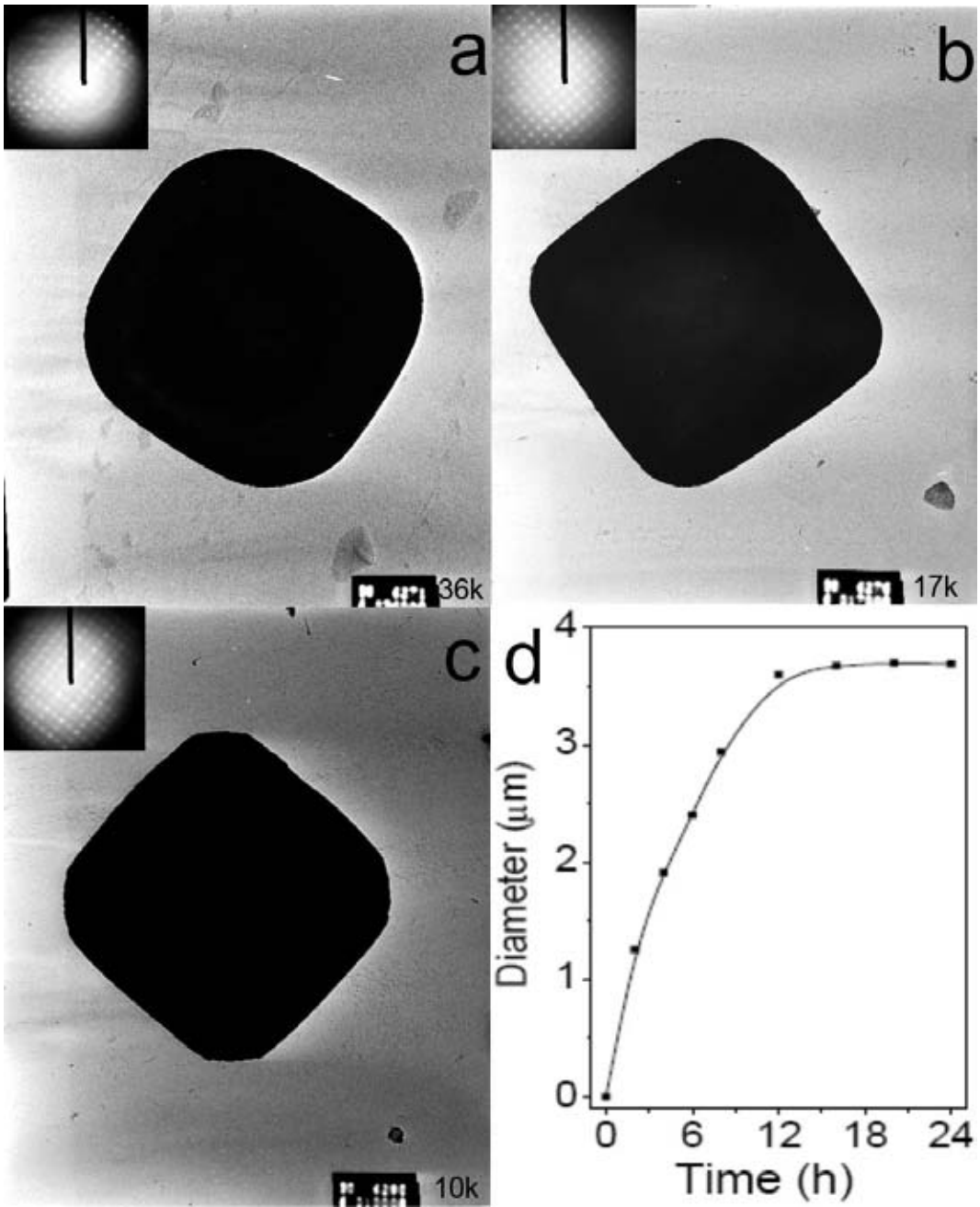

# Impact of temperature on morphology

TEM images of samples prepared at
a) 30°C.
b) 60°C.
c) XRD patterns prepared at different temperature.

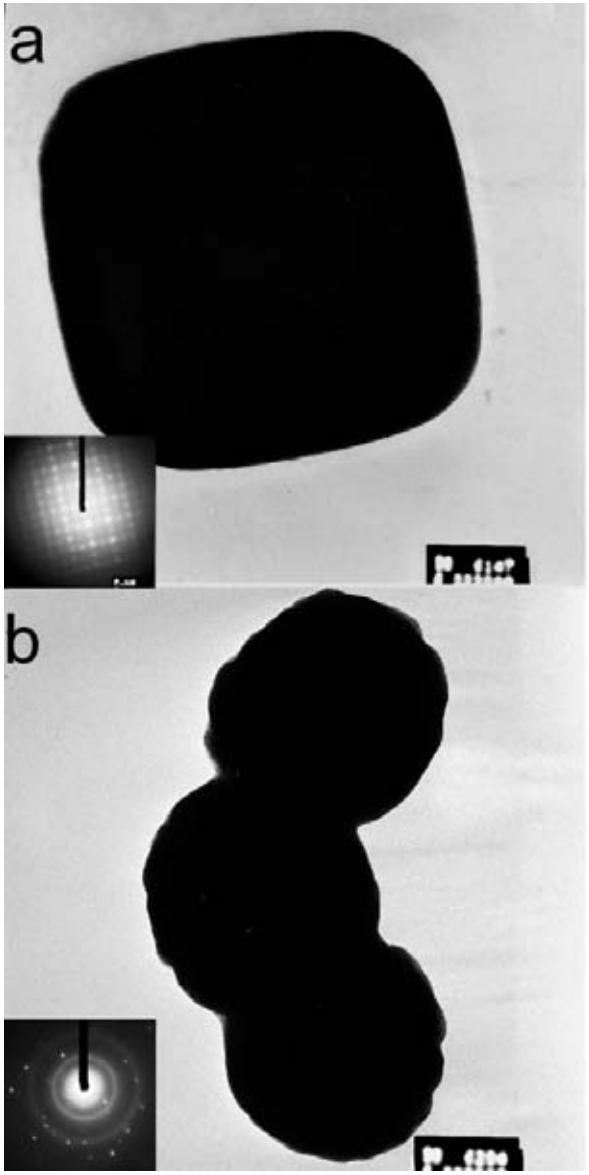


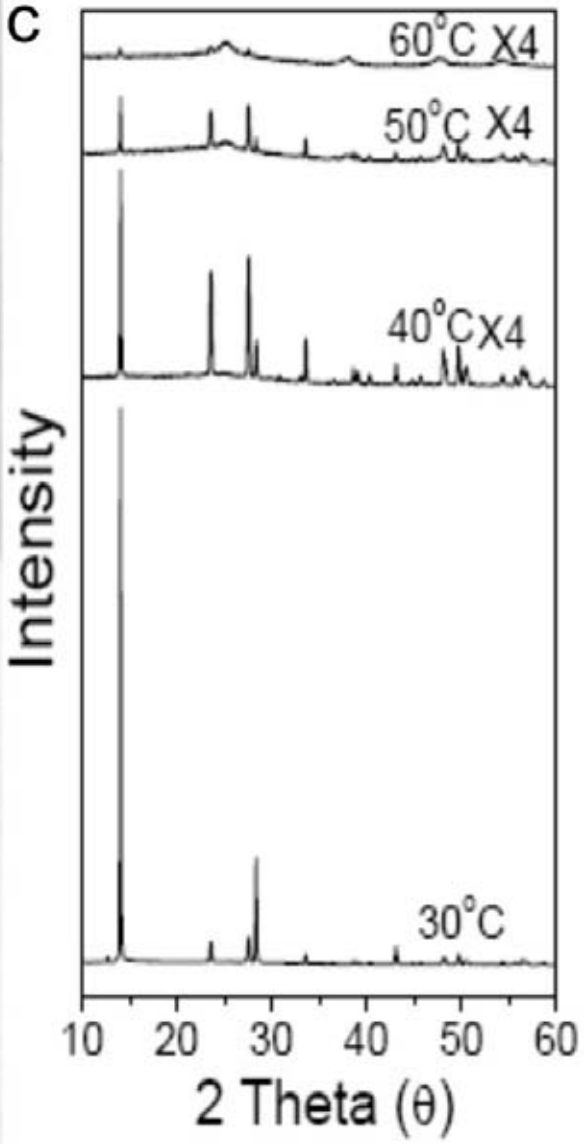

# Impact of reaction time and temperature on morphology

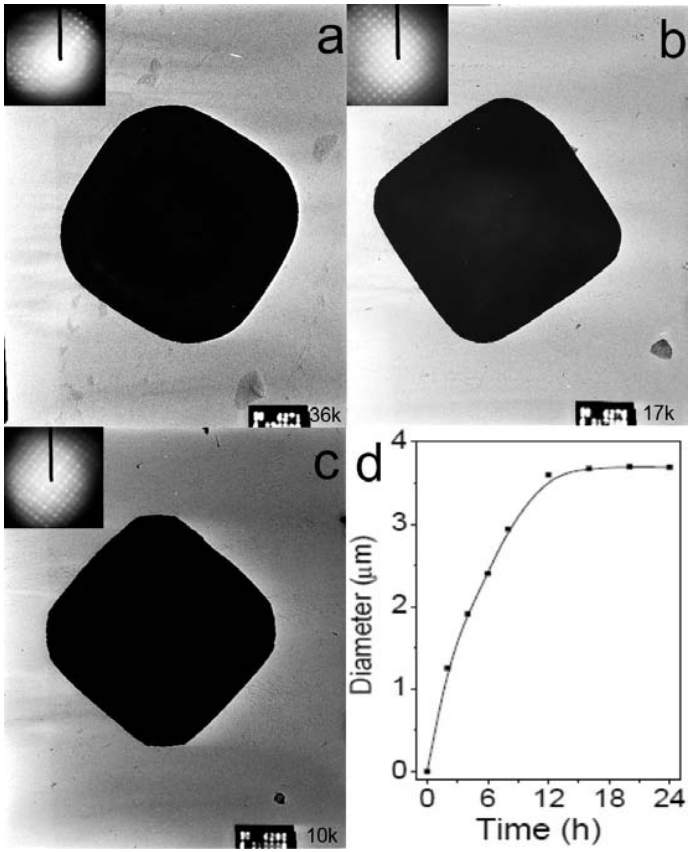


TEM images of samples taken out at different reaction time. a, 2 hours. b, 8 hours. c, 24 hours. d, plot of particles vs reaction time.

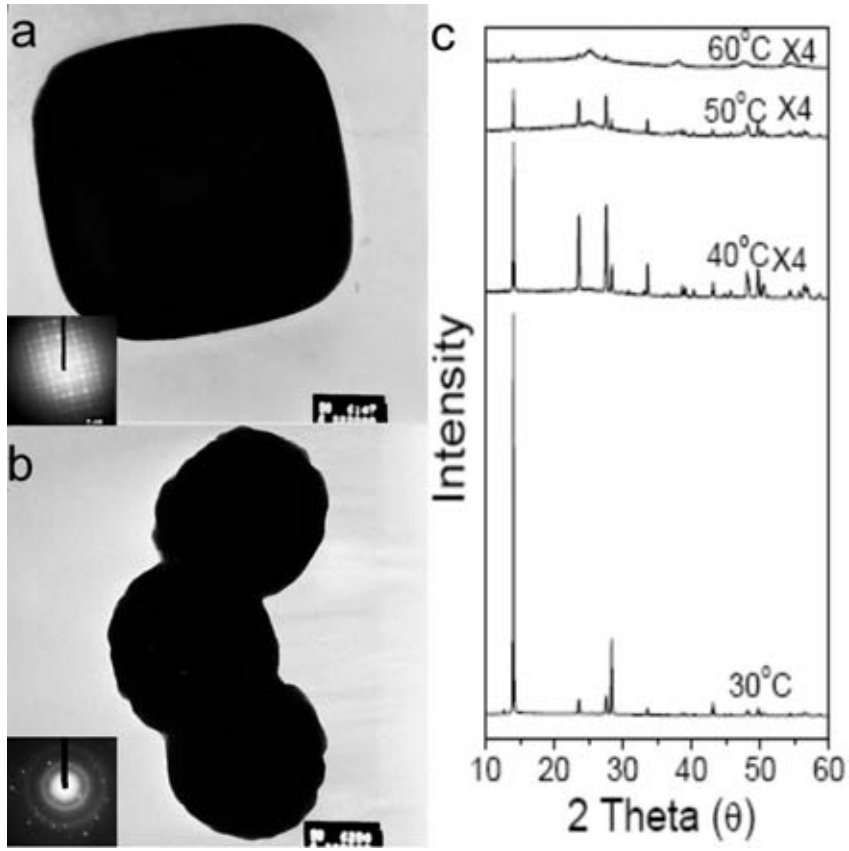


TEM images of samples prepared at a) 30°C. b) 60°C. c, XRD patterns prepared at different temperature.

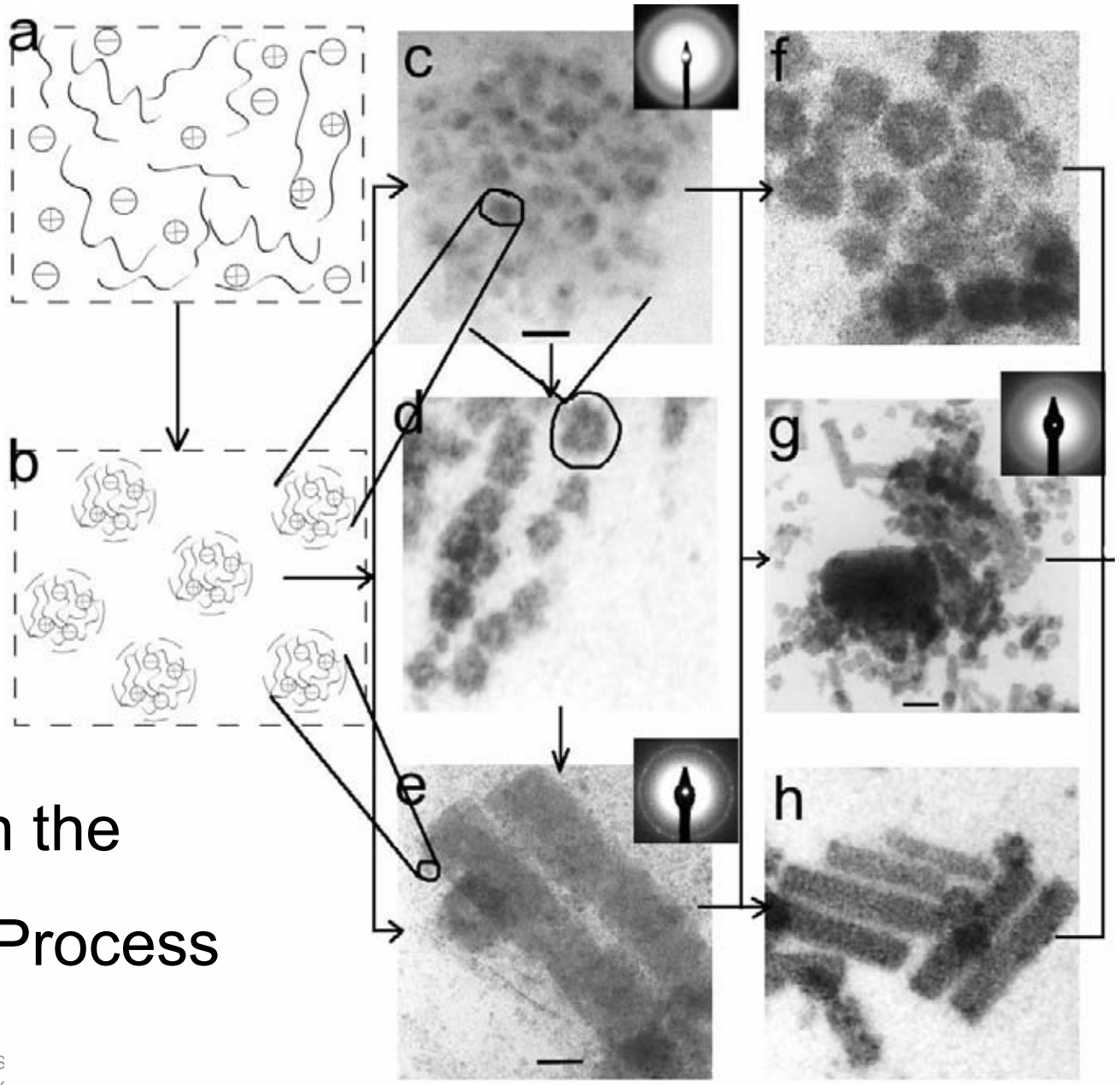


# Ideas on the Overall Process

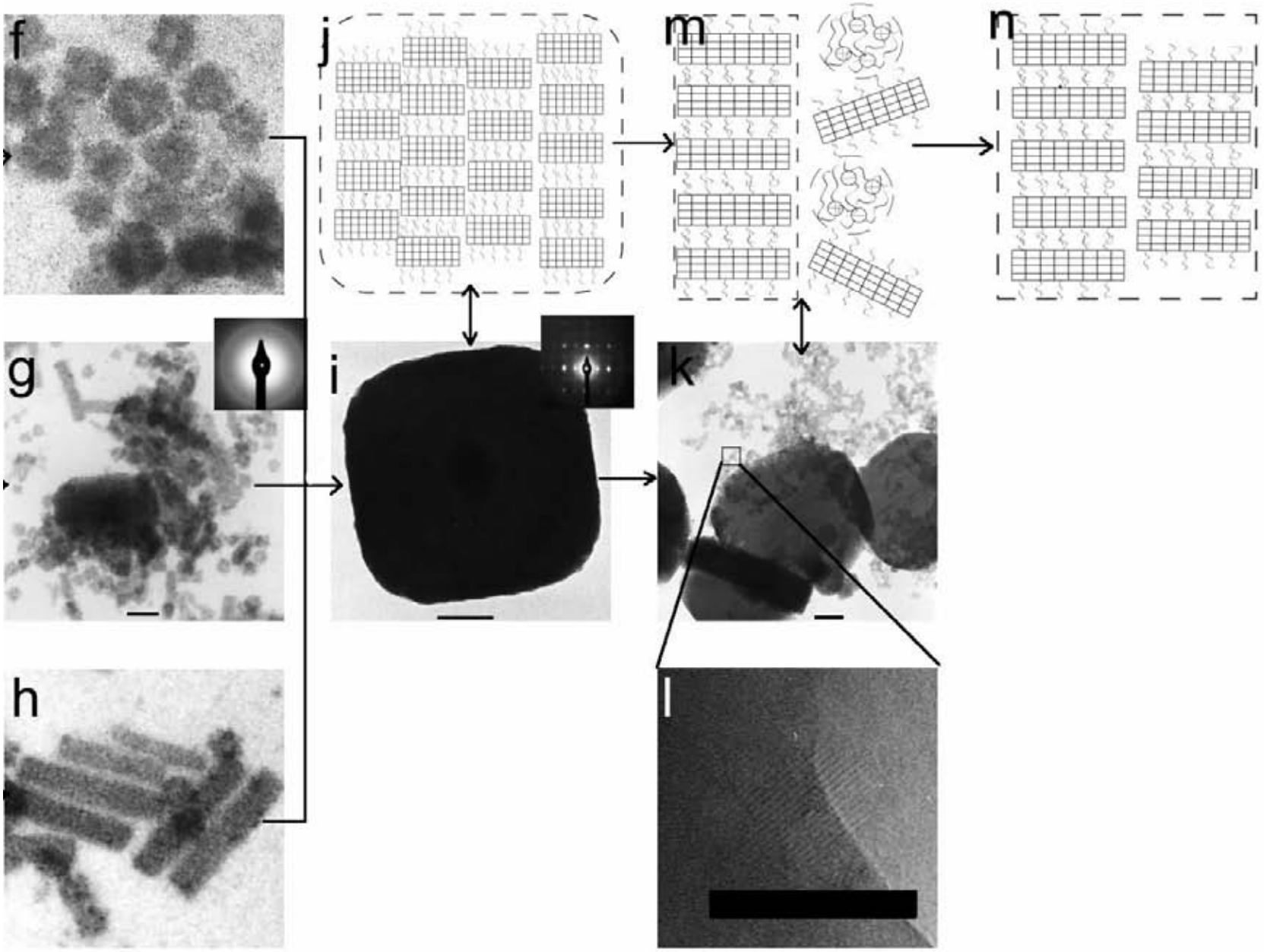
f
j
m
n
g
i
k
h
l

# Schematic of growth mechanism

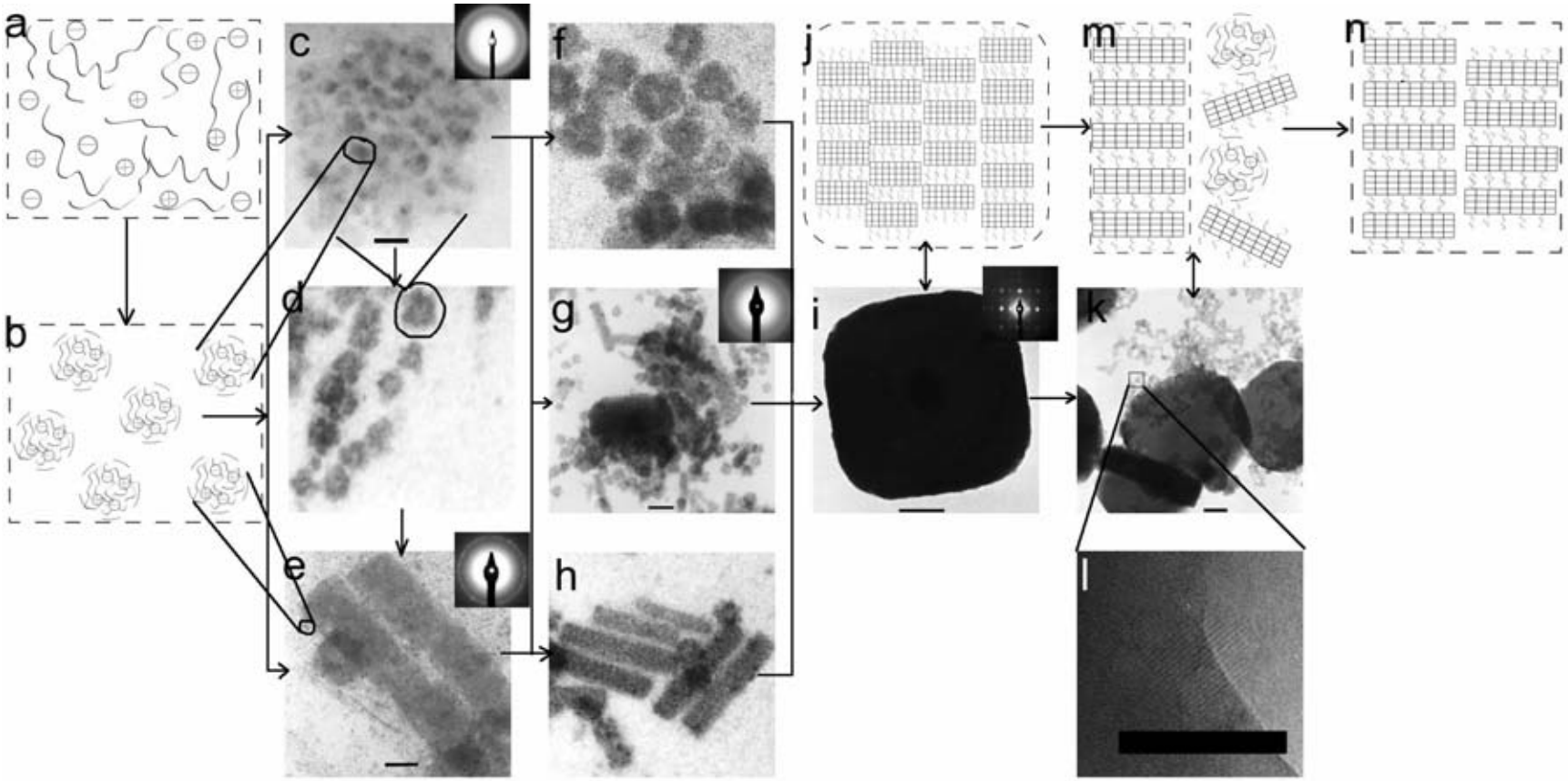


**Stage1**, formation of primary amorphous nanoparticles. **Stage 2**, Mesoscale assembly from amorphous primary particles to amorphous aggregates, i.e. formation of mesoscale building block. **Stage 3**, Self-assembly of mesoscale building block and subsequent crystallization, i.e. formation of seeds. **Stage 4**, The seed grow up to form final product.

**The crystal structures of $NH_4FeF_4$ and anatase $TiO_2$.**

**a,** $TiO_2$ crystal structure projected along y axis.

**b,** $NH_4FeF_4$ crystal structure projected along y axis.

**c,** $TiO_2$crystal structure projected along z axis, the green planes are 020.

**d,** $TiO_2$ crystal structure projected along z axis, the green planes are 101

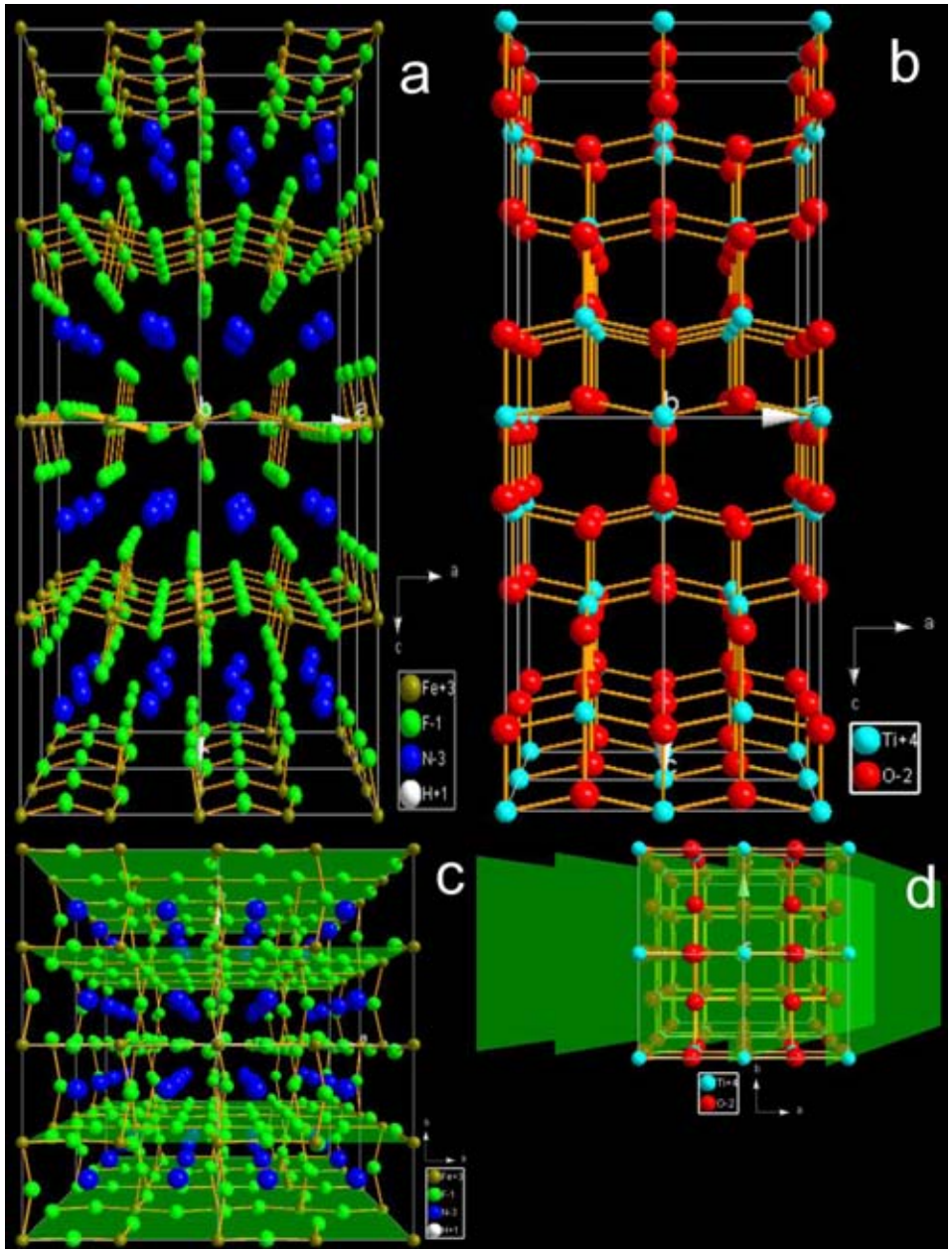


Importance of the lamelar structure of fluoride?

**Schematic of formation of seed**

**a.** low resolution of an unfinished seed.

**b.** medium resolution.

**c.** high resolution.

**d.** possible schematic.

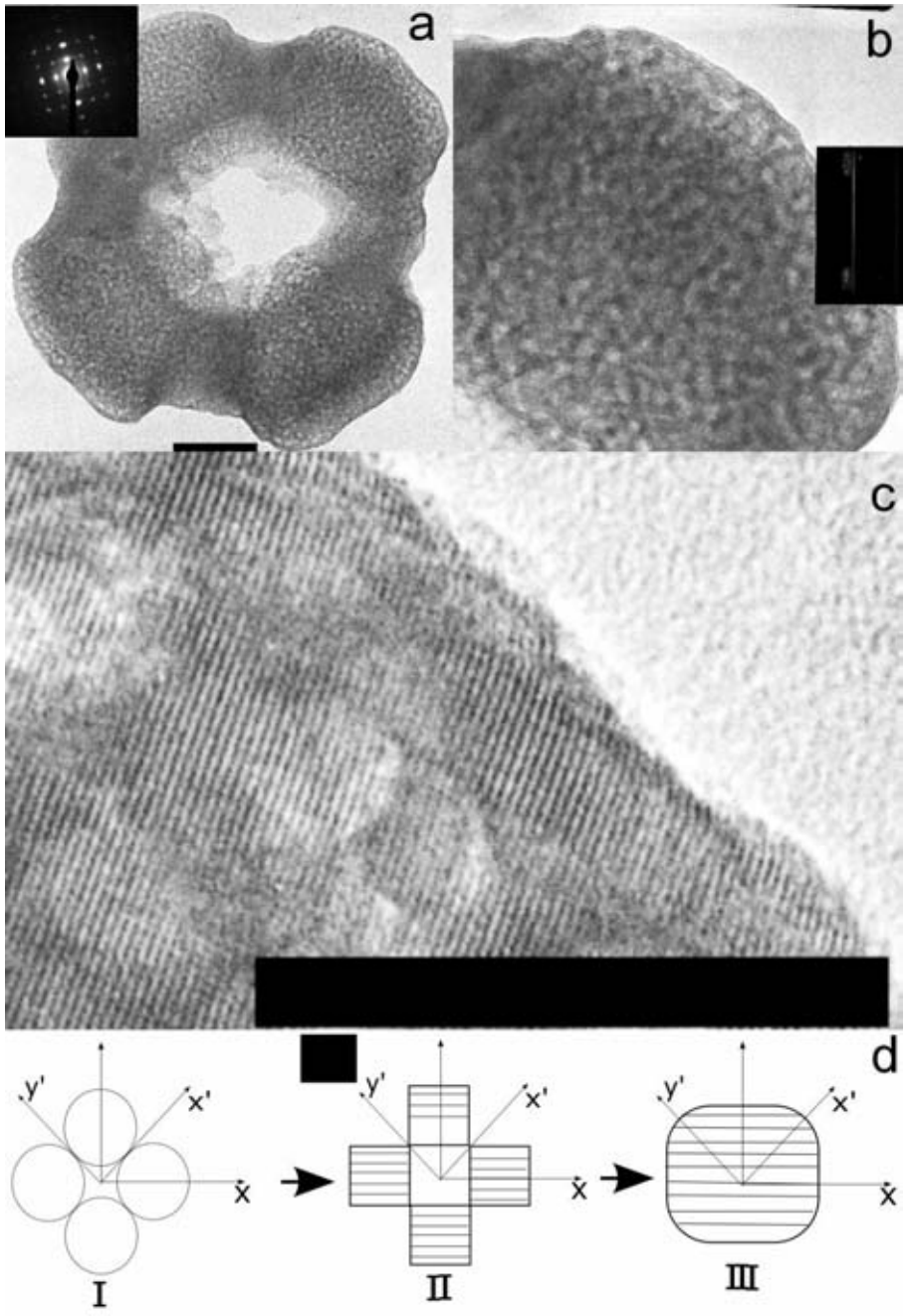

# Structure of Talk

- Looking at some nanodimensional objects
- Synthetic approaches zinc oxide and doping
- How nanoparticles grow and
- Rods
- Assemblies of nanoparticles and mesoscopic objects
- **Closing remarks**


John Prabinder Thomas and Lei Zhou…..Yuishiu Wang

# A New University for the 21st Century

- Established on 1st October 2004
- Royal Charter granted on 22nd October 2004
- 34 000 students from over 150 countries (1/3 postgraduate)
- 2000 academic staff & 1200 research staff
- £504M turnover (2004-5)
- £300M capital investment programme
- Manchester 2015 Agenda launched

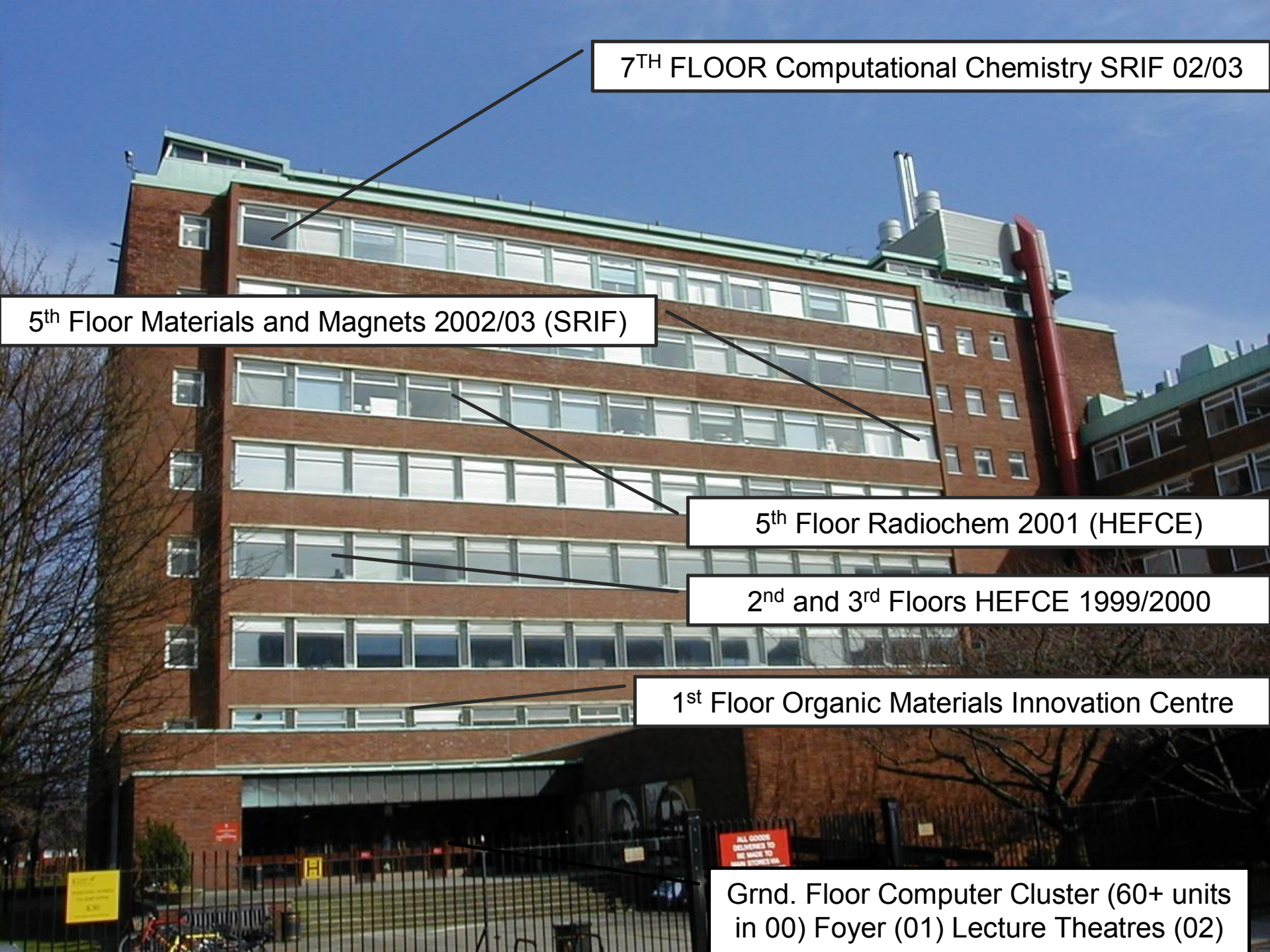
7TH FLOOR Computational Chemistry SRIF 02/03
5th Floor Materials and Magnets 2002/03 (SRIF)
5th Floor Radiochem 2001 (HEFCE)
2nd and 3rd Floors HEFCE 1999/2000
1st Floor Organic Materials Innovation Centre
Grnd. Floor Computer Cluster (60+ units in 00) Foyer (01) Lecture Theatres (02)

MANCHESTER
1824

The University of Manchester

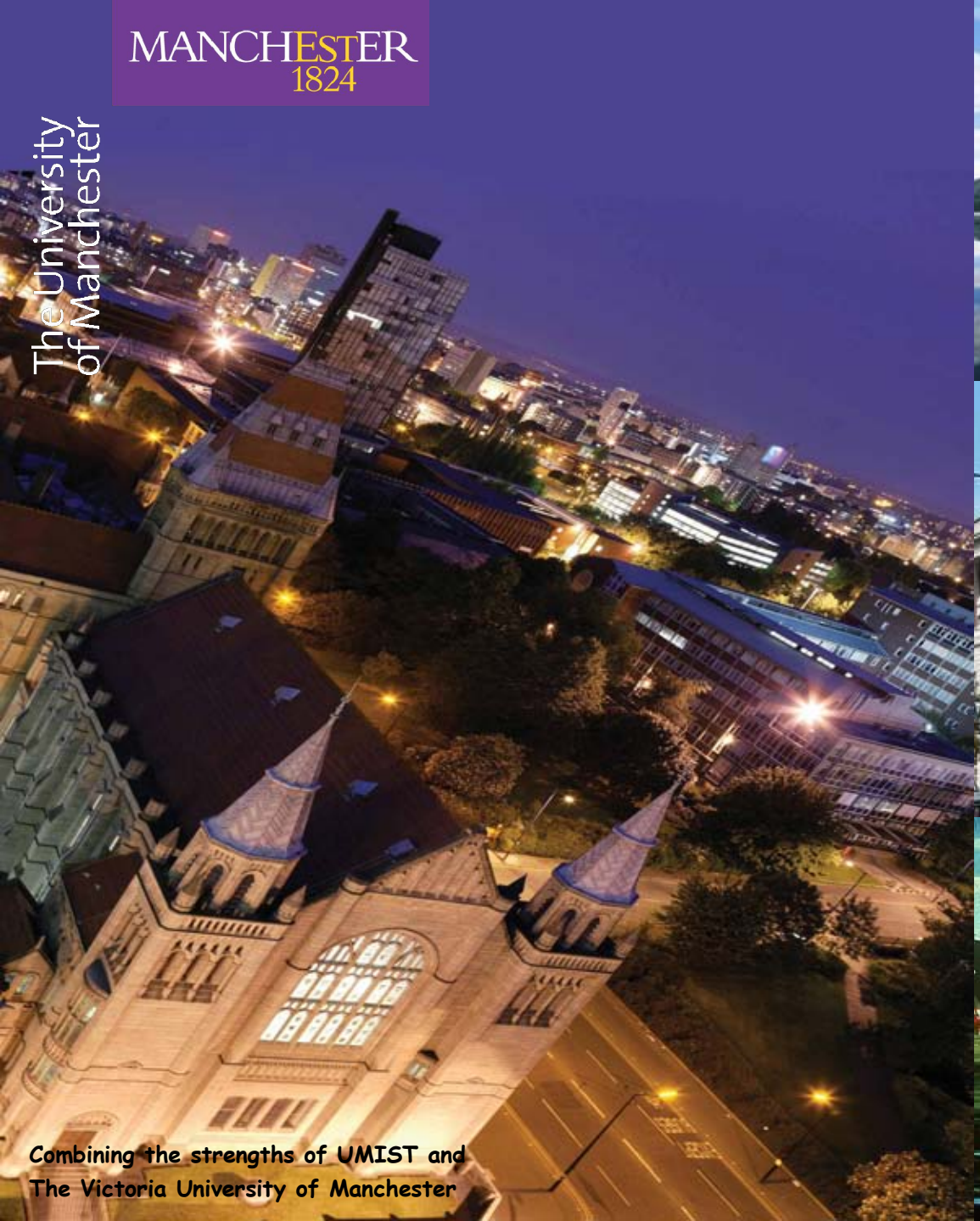

Combining the strengths of UMIST and
The Victoria University of Manchester